The Adaptation of Chinese Hamster Ovary Cells to Hypothermic Temperatures Increases Yields of Monomeric Recombinant Interferon-beta

By

Kevin Michael Sunley

A Thesis submitted to the Faculty of Graduate Studies of
The University of Manitoba
in partial fulfillment of the requirements for the degree of

Doctor of Philosophy

Department of Microbiology
University of Manitoba
Winnipeg, Canada

Thesis Abstract

Mild hypothermic conditions (30ºC to 33ºC) have previously been shown to increase cell specific productivity (Q_P) of recombinant proteins from mammalian cells. However, this is often associated with a lower growth rate which off-sets any potential advantage of higher product titres. This thesis describes the isolation of a novel population of Chinese Hamster Ovary (CHO) cells that have been adapted to low temperature growth by continuous subculture at low temperature for a duration of 400 days.

This adapted cell population achieved a growth rate 2-fold greater than non-adapted cells under low temperature conditions (32ºC) while maintaining an elevated level of cell-specific expression of recombinant beta-interferon. The volumetric titre of beta-interferon was enhanced by 70% in stationary cultures and by more than 2-fold by application of a temperature-shift strategy involving a growth to production phase. However, the low temperature-adapted cells were fragile and demonstrated an increased sensitivity to hydrodynamic stress in agitated cultures. This problem, caused by a weakened vimentin intermediate filament network, was resolved by the use of macroporous microcarriers which were demonstrated to entrap and protect the cold-adapted cells. Cold-adapted microcarrier cultures were able to achieve high cell densities (greater than $5x10^6$ nuclei/mL) cultures under hypothermic conditions. This resulted in a 3-fold enhancement of volumetric titre of monomeric beta-interferon compared to the original control culture at 37ºC.

Acknowledgments

Financial support for this research project has been provided by the Natural Science and Engineering Council of Canada, the CellNet Canadian Research Network, Cangene Corporation and the University of Manitoba.

I would first like to thank my advisor, Dr. Mike Butler, for all of his support, initiative and guidance throughout these last few years. I couldn't have asked for more in an advisor or from the research group he's assembled. I would also like to thank the past and present members of my review committee; Dr. Erwin Huebner, Dr. Brian Mark, and Dr. Kathleen Londry for their invaluable help and feedback.

Thank you to Dr. Brendan McConkey and Andrea Spires at the University of Waterloo for all your expertise and assistance with the proteomic analysis.

Thank you to my family, for their usual and endless support. I hope you all know how much it means to me.

To the students and researchers I've worked with over the last few years: Dr. Tharmala Tharmalingam, Dr. Maureen Spearman, Norm Huzel, Carly Lodewyks, Dr. Jose Rodriguez, Dr. Adam Burgener, Sarah Chan, Vincent Jung, Ben Dionne, Katrin Braasch, and Katie Pundyk; Thank you for all of the help, advice, support and ideas. You've all helped in countless ways, I really appreciate it.

Thank you to the students and staff of the Department of Microbiology, and especially Sharon. I couldn't think of a better department to have worked in, thank you everyone for your help, generosity, and answering my many, many questions. Also, I'd like to especially thank Azizah, Misty, Terry and Veronica and the rest of the Mark lab; you've been like a second lab to me. Thanks for the lunches.

Thanks Zee, for everything.

Table of Contents

List of Tables

List of Figures

List of Acronyms

AIChE	American Institute of Chemical Engineers
ASB	Amidosulfobetaine
ATCC	American Type Culture Collection
ATP	Adenosine triphosphate
Bcl-xL	B-cell lymphoma-extra large
bFGF	Basic Fibroblast Growth Factor
BLV	Bovine leukaemia virus
bp	Base Pairs
BSA	Bovine Serum Albumin
β-ME	beta-Mercaptoethanol
CAATT	Cysteine-Adenosine-Adenosine-Tyrosine-Tyrosine
CAD	Caspase Activated DNAse
CDK	Cyclin-Dependent Kinase
CD-IC	Cytoplasmic Dynein Intermediate Chain
C/EBP	CAATT-Enhancer Binding Protein
CHO	Chinese Hamster Ovary
CIRP	Cold-Inducible RNA-binding Protein
CKI	Cyclin-Dependent Kinase Inhibitor
CO_2	Carbon Dioxide
CSP	Cold-Shock Protein
DAPI	4',6-diamidino-2-phenylindole
DEAE	Diethylaminoethyl
DEVD	Aspartic Acid-Glutamic Acid-Valine-Aspartic Acid
DI	Deformability Index
DIC	Differential Interference Contrast
DIGE	Differential In-Gel Electrophoresis
DMSO	Dimethyl Sulfoxide
DNA	Deoxyribonucleic Acid
DP	Dimerization Partner
EDTA	Ethylenediaminetetraacetic Acid
EIA/RIA	Enzymatic/Radioimmunoassay
eIF	Eukaryotic Initiation Factor
ELISA	Enzyme-Linked Immunosorbent Assay
FBS	Fetal Bovine Serum
FDA	Federal Drug Administration/Fluorescein Diacetate
GE	General Electric
G0	Gap 0
G1	Gap 1
G2	Gap 2

HDAC	Histone Deacetylase
HDI	Histone Deacetylase Inhibitor
HIV	Human Immunodeficiency Virus
hnRNP	Heterogeneous Nuclear Ribonucleoproteins
H_2O_2	Hydrogen Peroxide
IF	Intermediate Filament
IFN	Interferon
IgG	Immunoglobulin G
INT	2-*p*-(iodophenyl)-3-(p-nitrophenyl)-5-phenyltetrazolium chloride
IRES	Internal Ribosome Entry Site
IRF	Interferon Responsive Factor
IVCD	Integral of Viable Cell Density
kDa	kilodalton
LDH	Lactate Dehydrogenase
M	Molar
MAV	Myeloblastosis-Associated Virus
MEF	Mouse Embryonic Fibroblast
MI	Michigan
miRNA	MicroRNA
mIR	MicroRNA
mg	milligram
µg	microgram
mL	milliliter
µL	microlitre
mM	millimolar
µM	micromolar
M-PMV	Mason-Pfizer Monkey Virus
mRNA	Messenger Ribonucleic Acid
MW	Molecular Weight
NAD/NADH	Nicotinamide Adenine Dinucleotide
nM	nanomolar
PAGE	Polyacrylamide Gel Electrophoresis
PBS	Phosphate Buffered Saline
P_{hCMV}	Human Cytomegalovirus Promoter
P_{SV40}	Simian Virus 40 Promoter
$p16^{INK4A}$	Cyclin-Dependent Kinase Inhibitor 2A
$p21^{CIP}$	Cyclin-Dependent Kinase Inhibitor 1A
$p27^{KIP}$	Cyclin-dependent kinase inhibitor 1B
PR	Retroviral Protease

PTFE	Polytetrafluoroethylene
Q_P	Specific Recombinant Protein Production Rate
Rb	Retinoblastoma protein
RBM	RNA-Binding Motif
RNA	Ribonucleic Acid
RPM	Revolutions Per Minute
SDS	Sodium Dodecyl Sulfate
SEAP	Secretory Alkaline Phosphatase
SFM	Serum-Free Media
sICAM	Surface Cellular Adhesion Molecule
TBS	TRIS Buffered Saline
TGF	Transforming Growth Factor
TRIS	Tris(hydroxymethyl)aminomethane
t-PA	Tissue Plasminogen Activator
USA	United States of America
UV	Ultraviolet
3D	Three Dimensional
ºC	Degrees Celsius
λ_{EX}	Excitation Wavelength
λ_{EM}	Emission Wavelength

Chapter 1 – Literature Review and Introduction

Since the first production of recombinant proteins for therapeutic use nearly thirty years ago there have been many significant advances in the processes used for the production of biologics. Although initially produced within bacterial hosts, host cell limitations, particularly in terms of their ability to post-translationally modify the protein product has made mammalian cells the preferred choice for manufacturing of biologics. Chinese hamster ovary (CHO) cells, a eukaryotic cell line originally isolated by Puck et al(1), has become the predominant host for the production of biologics due to their ease of genetic manipulation and the availability of metabolic enzyme deficient mutants to aid in clone selection(4).

The importance of the choice in host cell line has become more critical as the biological importance of post-translational modifications, particularly glycosylation, is better understood(4, 5). Variations in glycan structure are known to play an important role in product quality and pharmacokinetics, affecting the stability of the formulated product and the in vivo half-life of the active molecule(4, 5), and even within mammalian lines some species are more capable of human-like glycosylation than others.

Strategies to increase the overall production from recombinant CHO cells have focused on increasing both the rate of cell growth (μ) and cell-specific heterologous protein production (Q_P). Over the last twenty years improvements in cell lines, process control and media formulations have increased product titres nearly 100-fold(6).

Production process control, which regulates the environment the cells are cultivated within, has undergone continuous improvements since the initial batch cultures of the mid-1980s. Improved environmental control and adoption of fed-batch and perfusion-based culture systems have improved culture densities and durations significantly. In addition, the real-time online monitoring of environmental parameters (pH, dissolved oxygen, cell and product concentrations, and nutrient levels) allows precise regulation, recording and immediate responses to changes within the culture environment.

Traditional culture strategies have attempted to create an environment which encourages unhindered growth of a therapeutic producing cell line. This method does not attempt to maximize the protein production of an individual cell, but instead attempts to create a large biomass of moderately producing cells. Numerous ways have been found to increase the specific productivity (the quantity of protein produced by a single cell over time), however often the increased productivity comes at the cost of greatly reduced cell growth. Alternatively, by purposely maintaining a small population of high producing cells, similar or greater product titres can be achieved with fewer cells and therefore fewer resource requirements. This method of inhibiting growth to increase cell specific productivity is the principle behind controlled proliferation.

Chapter 1.1 - The Cell Cycle

Proliferation in mammalian cells is controlled by a series of checkpoints which are regulated by a complex network of kinases, inhibitors and numerous other signaling

molecules which together form the cell cycle. These checkpoints ensure that events required for proper cell division do not occur prior to the completion of necessary preceding steps(7) and that cellular or genetic damage which could eventually lead to uncontrolled or malignant growth has not occurred(8). The cycle itself is divided into two distinct phases; interphase and M-phase, each with further sub-divisions (Figure 1.1). The transitions between the sub-phases of interphase are tightly controlled. During S-phase, a sub-phase of interphase, the genetic material of the cell is replicated in preparation for cell division. Directly before and after S-phase are the two "gap" phases of interphase, G1 and G2, during which the cell prepares for either the replication of nuclear material (S-phase) or the separation into two progenic cells (M-phase) respectively. M-phase, which consists of mitosis and cytokinesis follows immediately after G2 and marks one complete round of the cell cycle, resulting in daughter cells which begin the cycle again. Cells which no longer need to proliferate can arrest the progression through the cell cycle during the G1 phase, entering the quiescent G0 phase. These cells are maintained in G0 through the phosphorylation of key cell cycle regulators(9), although can re-enter active division if signaled to.

Chapter 1.2 – Controlled Proliferation

Controlled proliferation in the context of biotechnology is the manipulation of the cell cycle of a recombinant cell population to increase heterologous protein expression through a G1/G0 cell cycle arrest(10). While growth arrest can also be induced at the G2/M checkpoint(10), inductions of arrest at G1/S are far more prevalent.

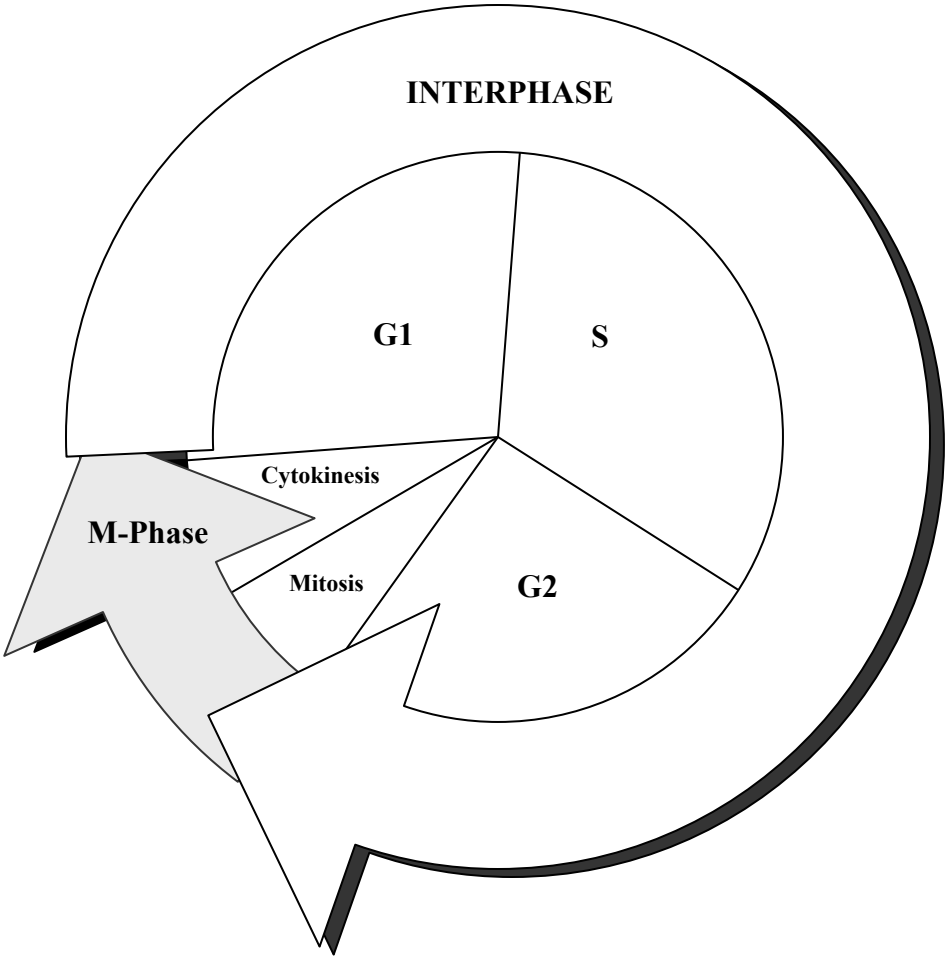

Figure 1.1: The phases of the mammalian cell cycle including sub-divisions of M-Phase and Interphase

Although the relationship between G1 arrest and increased heterologous protein expression has been well documented; the mechanisms responsible for this increase are less clear. It has been observed that cells at the end of G1 are typically more metabolically active, larger in size(11, 12), and are actively expressing many genes responsible for ribosome biosynthesis(13). These traits do not however describe a mechanism, only indicate possible contributing factors.

The key to controlled proliferation strategies is to inhibit the function of the primary regulatory kinase enzymes which allow the transition from the G1 to S-phase. These enzymes, a family of cyclin-dependant kinases (CDKs), are regulated through either positive or negative regulation; requiring the presence of the protein cyclin, or inactivated by members of the family of cyclin-dependent kinase inhibitors (CKI). The downstream target of CDK regulation is the phosphorylation of the retinoblastoma (Rb) protein; a tumor suppressing protein which inhibits the activity the E2F family of transcription factors(14). Entry into the S-phase, and therefore cell proliferation, is inhibited as long as Rb remains unphosphorylated. A complex of CDK 4 and 6, followed by CDK2 phosphorylates two sites on Rb to initiate G1 to S progression. Phosphorylated Rb dissociates from a heterodimeric complex of E2F-DP allowing the transcription of S-phase specific genes(15). Controlled proliferation strategies prevent this from happening through the activation of upstream CKIs. This simplified model of G1 to S progression (Figure 1.2) introduces the regulatory checkpoints which are exploited to introduce growth arrest and increase heterologous protein expression. There are other regulatory channels which regulate cell cycle progression and heterologous protein expression,

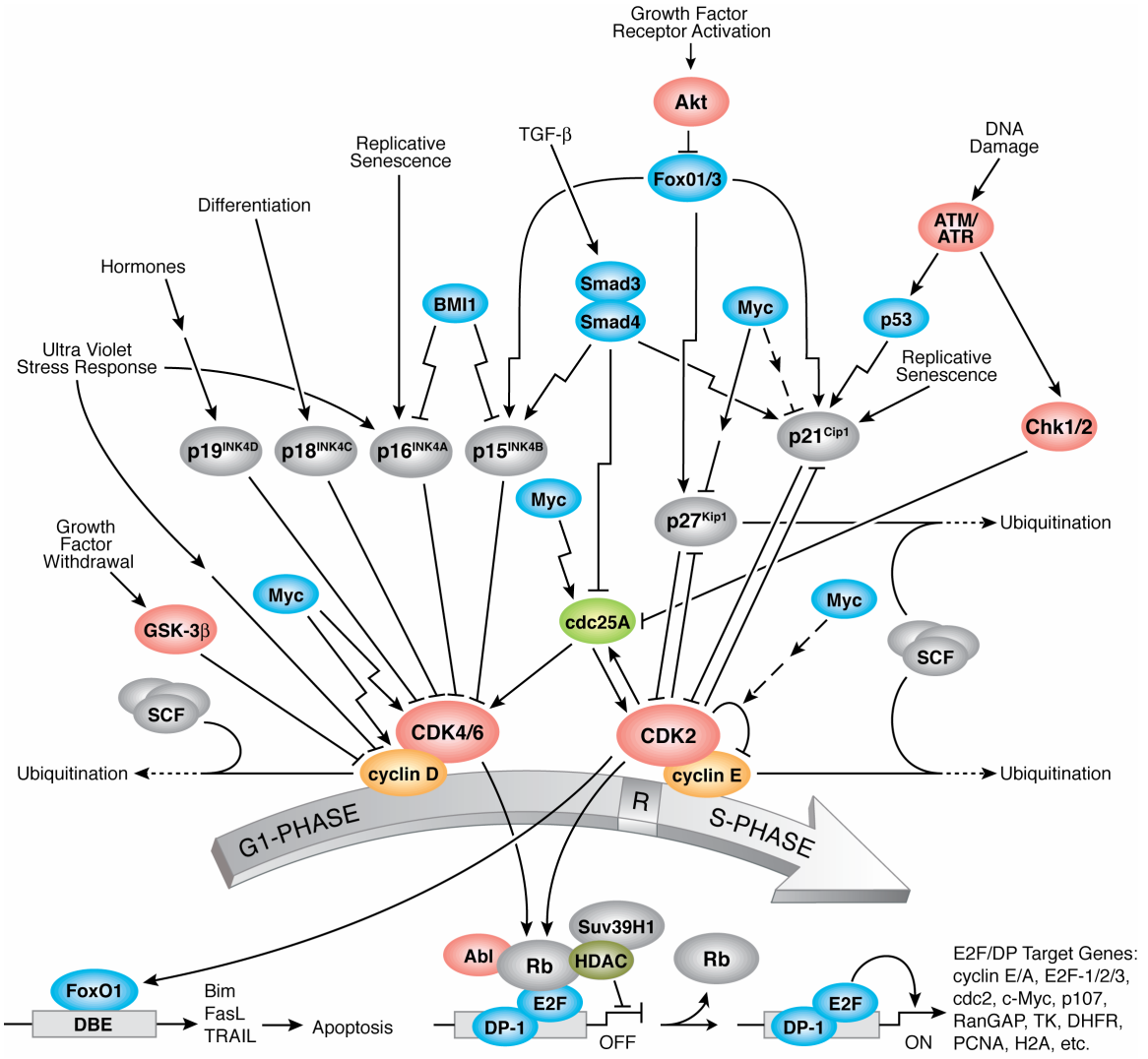

Figure 1.2: Regulation of the G1-phase/S-phase checkpoint in the mammalian cell cycle. Pathway diagram reproduced courtesy of Cell Signaling Technology, Inc. (www.cellsignal.com).

such as histone acetylation through the enzyme histone deacetylase 1 (HDAC1), which is essential for active cell proliferation. Loss of HDAC1 activity has been found to increase expression of CKIs $p21^{CIP1}$ and $p27^{KIP1}$, inhibiting the downstream phosphorylation of Rb and preventing entry into S-phase(16). Intentional activation of CKIs can be achieved in culture through a variety of strategies; including the addition of chemical agents, genetic manipulation of the cell line and environmental changes (specifically mild hypothermic conditions). Each of these strategies, although achieving similar end results, has advantages and disadvantages; however the similarities of between these three approaches are striking. Regardless of whether the cell cycle is arrested through a response to an external environmental stress (low temperature), chemical inhibition of G1/S checkpoint regulators, or genetic manipulation of the regulatory machinery itself, these distinct strategies affect the cell in very similar ways.

Chapter 1.3 – Induction through the Introduction of Chemical Agents

Numerous chemical agents have been found to increase the expression of heterologous proteins while decreasing or arresting cell growth. Sodium butyrate(17-19) (NaBu) and dimethyl sulfoxide(19-21) (DMSO) are two which have been used successfully in existing bioprocesses. Many additional chemical agents with similar effects on proliferation have been identified(22). This review will focus on the inhibitory effects of NaBu as an example of how these chemical agents can affect proliferation and recombinant protein expression.

1.3.1 – Sodium Butyrate Induced Controlled Proliferation

While the growth arresting properties of NaBu were first observed thirty-five years ago(23), its positive effect on recombinant plasmid(24) and protein expression(25) was not recognized for another decade. A product of the microbial fermentation of dietary fiber, NaBu is a non-toxic short chain fatty acid(26) which has been approved by the United States Food and Drug Administration (FDA) for the production of therapeutic proteins(18). Known to induce early G1 growth arrest(27, 28), NaBu is believed to induce cell cycle arrest through the dephosphorylation of Retinoblastoma protein(29, 30) as well as the up-regulation of CKIs $p16^{INK-4A}$ and $p21^{Cip1}$(26, 29, 31). However conflicting reports concerning the involvement of $p21^{Cip1}$(26, 32) seems to indicate that there could possibly be several simultaneous pathways through which NaBu-induced growth arrest can occur.

Sodium butyrate is part of a family of chemical agents known as aliphatic acid-based histone deacetylase (HDAC) inhibitors (HDI). Other members of this family, including phenylbutyrate and valproic acid(33), despite structural differences(34) (Figure 1.3) are believed to induce growth arrest through similar mechanisms; chelating the zinc atom in the active site of class I and/or class II HDACs, inhibiting their activity(35, 36). Inhibition of HDAC affects the transcription of numerous genes(37), inducing growth arrest through the CKIs previously mentioned and the down-regulation of the transcription factor coding gene *c-myc*(38).

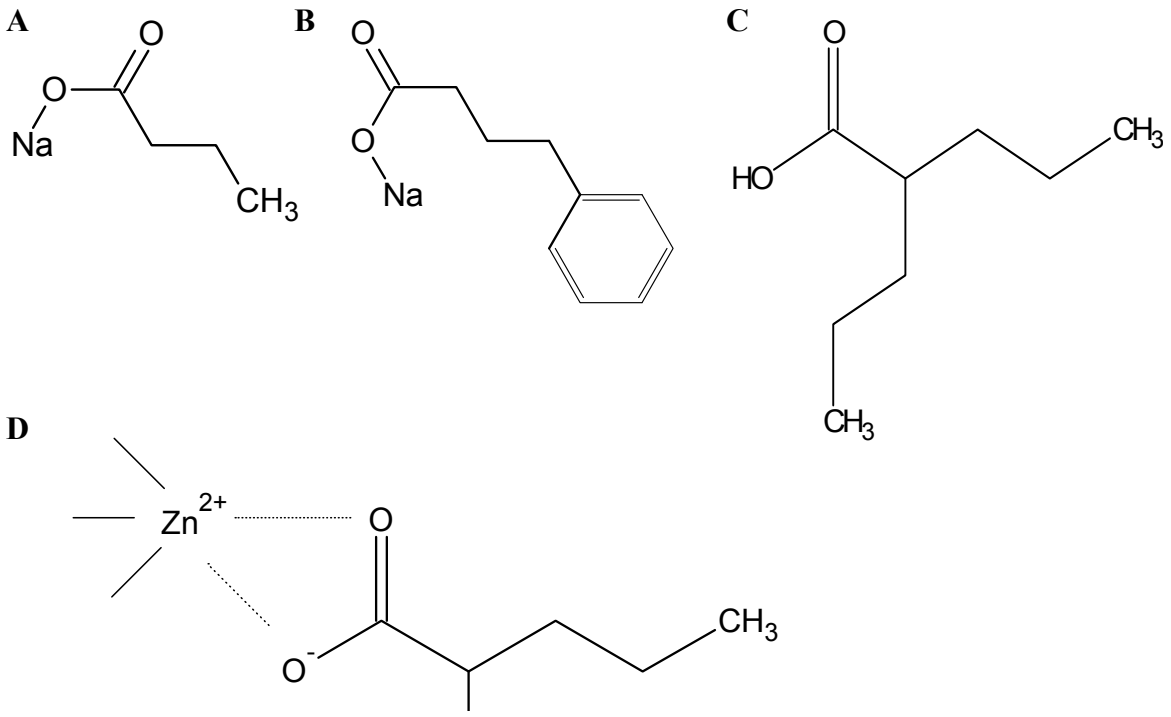

Figure 1.3: Chemical structures of members of the aliphatic acid family of histone deacetylase inhibitors: (A) sodium Butyrate, (B) sodium phenylbutyrate and (C) vaporic acid. A schematic illustration (D) of vaporic acid binding to the zinc atom of a class I/II HDAC active site.

In culture, low concentrations of NaBu (0.1 – 0.5 mM) have been reported to increase production of heterologous protein in CHO cells by 2-4 fold(39-41). The mechanism for the increased heterologous protein expression is less understood than that of the growth arrest. Hyperacetylation of histones through to the inhibition of HDAC has been found to up-regulate transcription by opening up nucleosome structures(42). Such modifications would make a recombinant gene more accessible, and thus increase its transcription rate. However the extent of the increased accessibility does not correlate with the increased rate of protein expression, indicating that there are likely other mechanisms involved as well(38). Additionally the response to NaBu was found to be clone specific(41), and more pronounced in lower producing cell lines(38). As well as growth arrest and an enhanced rate of recombinant protein expression, NaBu also induces apoptosis in a dose-dependent manner(38, 43). This can be alleviated through genetic up-regulation of anti-apoptotic genes(44), or anti-sense RNA-mediated inactivation of the apoptotic executioner enzyme Caspase-3(45). However if genetic manipulation is to occur, other, more direct, strategies can be performed which makes the addition of NaBu unnecessary.

Chapter 1.4 – Induction through Genetic Manipulation

The induction of controlled proliferation through the genetic manipulation of a cell line allows direct control over the expression of anti-proliferative genes. This branch of metabolic engineering has been able to induce reversible growth arrests concurrent with significant increases in heterologous protein expression. Targets which genetically induce growth arrest have included interferon-responsive factor IRF-1(46), and members

of the cyclin-dependent kinase inhibitor family; specifically $p21^{Cip1}$ and $p27^{Kip1}$ (Table 1.1). IRF-1-induced arrest was found to only increase heterologous expression of genes under the control of IRF-1 responsive promoters, additionally cell mortality was high in induced cells. Over-expression of the *c-jun* oncogene has been found to result in G0 arrest, however under this phase heterologous protein expression is typically reduced rather than elevated(46).

The up-regulation of the CKIs $p21^{Cip1}$ or $p27^{Kip1}$ is in principle similar to the use of cytostatic compounds such as NaBu. Both induce growth arrest through the inhibiting of cyclin-dependent kinase activity, halting downstream phosphorylation of the Rb protein and arresting the cell cycle in G1. However engineering growth arrest allows only for the up-regulation of a few targeted genes, while chemical agents can affect numerous genes, many likely still uncharacterized despite proteomic and genomic studies(37). Attempts to induce growth arrests were initially through single gene modulation, up-regulating the production of p53, $p21^{Cip1}$ or $p27^{Kip1}$(47). These approaches demonstrated the initial limitations of metabolic engineering. A transiently transfected CHO cell line engineered to co-express secreted alkaline phosphatase (SEAP) and $p21^{Cip1}$ exhibited productivity 5-fold greater than an unmodified cell line(47). However when selected as a stable transfectant the productivity reverted to that of a proliferative line(48).

A successful $p21^{Cip1}$ line was produced in which production was increased 10 to 15-fold. However this required the simultaneous over-expression of two additional gene products; the differentiation factor CAATT/enhancer binding protein α (C/EBPα; which induces

Table 1.1: Effect of CKI up-regulation on recombinant protein expression in CHO cells

Contributor	Inhibitor	Recombinant Product	Increased Specific Productivity	Host	Expression System
Bi et al. (11)	$p21^{CIP1}$	IgG4	4-fold	CHO	Stable
Carvalhal et al. (12)	$p27^{KIP1}$	SEAP	2-fold	CHO	Stable
Fussenegger et al. (47)	$p21^{CIP1}$	SEAP	4.6-fold	CHO	Transient
	$p27^{KIP1}$	SEAP	3.9-fold		
	p53	SEAP	3.9-fold		
Mazur et al. (48)	$p21^{CIP1}$	SEAP	No Increase	CHO	Stable
	$p21^{CIP1}$†	SEAP	10 to 15-fold		
	$p27^{KIP1}$†	SEAP	30-fold		
Meents et al. (49)	$p27^{KIP1}$	sICAM	5-fold	CHO	Stable

† Indicates mutli-cistronic co-expression with C/EBPα and Bcl-xL

and stabilizes $p21^{Cip1}$) and the anti-apoptotic protein Bcl-xL(50). Up-regulating $p27^{Kip1}$ in tandem with C/EBPα and Bcl-xL increased SEAP expression up to 30-fold over unmodified, proliferative controls(50).

The selection of CKI targets highlights the inherent complexity of attempting to over-express key regulatory molecules. The pathways involved in CDK-mediated cellular proliferation are highly redundant, interconnected and regulated by many intrinsic and external signals(51-53). Increased p53 expression leads to increased $p21^{Cip1}$ expression, however elevated p53 level also induce apoptosis(54). $p27^{Kip1}$ is produced under the control of the anti-mitogenic cytokine transforming growth factor β (TGF-β)(52), which also can induce $p21^{Cip1}$ in a p53-independent manner. $p21^{Cip1}$ can be over-expressed directly, but as already discussed, the effectiveness of this is dependent on the inherent variability of mammalian transfection methods and as recently described by Khoo et al., the internal physiological state of the cell during production(55). Accessibility of the gene to transcription machinery is dependent on the site of integration within the genome, which greatly affects transcription levels(56). Multi-cistronic expression vectors(46) simply this process considerably by expressing several genes off of a single promoter (through the use of internal ribosome entry sites), however this results in a cell line specific for controlled proliferation strategies, unable to also be used in traditional bioprocesses.

Chapter 1.5 – Induction through Hypothermic Conditions

The culturing of cells at temperatures below their physiological ideal induces numerous changes at the genetic, molecular and phenotypic level. Traditional mammalian cell culture has overwhelmingly adopted the mammalian physiological body temperature of 37°C as it results in cultures of highly proliferative, highly viable cells(57). Deviation from that temperature, under hyper- or hypothermic conditions, significantly reduces cell proliferation. Growth under hyperthermic conditions have been extensively characterized in both prokaryotic and eukaryotic species(58-60), yet aside from a few specific research areas, hypothermic growth, particularly in mammalian species, has received very little attention(61-64).

From a biotechnological perspective, culturing cells under mild hypothermic conditions (30°C to 35°C) has been found to induce an actively regulated growth reduction in cells within S or G1 phase of the cell cycle(62). Actively metabolizing cells induce growth arrest though the induction of growth repressing mechanisms. This differs remarkably from more extreme hypothermic conditions (4°C) where cellular metabolism and ATP synthesis is not observed(63). Although the mechanism of this response is not completely understood, two molecules believed to play key roles are p53 and $p21^{Cip1}$(61). Through numerous proteomic(65), miRNA(66) and genomic(67, 68) expression studies additional low temperature-induced cellular effects have been observed. These can be categorized into effects on cellular metabolism (increase in phosphoglycerate kinase expression), protein expression and folding (increased protein disulfide isomerase, ERp57, and heat shock cognate 71 kDa; decreased heat shock protein 90-β and

elongation factor-2), RNA chaperones (increased cold-inducible RNA binding protein and RNA-binding motif protein 3) and cell cycle arrest (increased nucleoside diphosphate kinase B, p53, $p21^{Cip1}$ and microRNAs miR-21 and miR-24)(61, 66, 68-71).

In addition to a growth arrest-induced increase in specific productivity, the cultivation of cells under mild hypothermic conditions offers other relevant advantages: extended culture durations (lower cell populations reduce overall nutrient uptake and waste production)(72), decreased O_2 demand(73), reduced intermolecular product aggregation (74), increased sensitivity to deviations in culture pH(75, 76) and a decreased sensitivity to pro-apoptotic agents(77, 78). Product quality (in terms of protein sialylation) is also improved under hypothermic conditions over physiological cultures(72), and genetically ($p27^{Kip1}$) induced controlled proliferation strategies(79).

Low temperature enhanced therapeutic production has been observed for numerous heterologous products (Table 1.2) and under the control of both of the two most common genetic promoters; the human cytomegalovirus promoter (P_{hCMV}) and the simian virus 40 promoter (P_{SV40})(79). However despite being product and promoter independent, enhanced hypothermic heterologous protein expression has been found to be cell line(80) and even clone specific(81). In a pool of 12 methotrexate-amplified clones derived from a low temperature-responsive CHO cell line, two of the newly derived clones showed no enhanced low temperature expression(81). Indicating that the phenomena of G1-growth arrest and elevated Q_P, despite concurrent induction under lower temperature conditions, are not inherently linked and can occur independently of each other.

Table 1.2: Effect of low temperature growth on recombinant protein expression in CHO cells

Contributor	Temp.	Recombinant Product	Host	Increased Specific Productivity	Increased Volumetric Productivity
Nam et al. (82) †	33°C †	SEAP	CHO	1.3-fold	3-fold
Tharmalingam et al. (83)	32°C †‡	Interferon-β	CHO	N/A	4.2-fold
Fox et al. (84)	32°C	Interferon-γ	CHO	4.9-fold	2-fold
Rodriguez et al. (74)	30°C	Interferon-β	CHO	N/A	2-fold
	30°C †			N/A	5-fold
Yoon et al. (72)	30°C †	Erythropoietin	CHO	4-fold	No Increase
	33°C †			5.4-fold	2.5-fold
Schatz et al. (85)	28°C †	Fab Antibody	CHO	6.8-fold	14-fold
Chen et al. (86)	34°C †	Pro-urokinase	CHO	1.7-fold	1.5-fold
Yoon et al. (80)	30°C †	Anti-4-1BB	CHO	No Increase	-3.9-fold
	33°C †			0.16-fold	No Increase

† Indicates use of a temperature shift culture strategy
‡ Indicates the use of macroporous microcarriers as an extra-cellular support structure
N/A = Information Not Available

1.5.1 – The Molecular Mechanism of Low Temperature Response

The two key elements of the mammalian low temperature response are the arrested progression of the cell cycle and the elevated transcription of recombinant genes. Although the mechanism which initiates and coordinates these events is still poorly understood, a model was proposed by Al-Fageeh and Smales(64) which encompasses the five aspects of the low temperature gene response: (i) generalized reduction in transcription and translation, (ii) inhibited RNA degradation, (iii) increased transcription of cold-specific genes (through a promoter-encoded cold response element), (iv) alternative pre-mRNA splicing, and (v) increased translation of cold-specific genes (through internal ribosome entry sites within the 5'-leader sequences)(2).

1.5.2 – Increased Production under Hypothermic Conditions

Cold stress is believed to be initially communicated to the cell through a generalized down-regulation of translation. In both eukaryotes(87) and prokaryotes(88) the ribosome itself functions as a biosensor which detects environmental thermal changes. Cold-induced reduced ribosome activity(2, 89), likely in combination with other yet to be identified signals, triggers a cell-wide stress response which culminates in $p53/p21^{Cip1}$ mediated G1-growth arrest(2). Although there are likely numerous molecules involved in the transduction of the cold-shock response, only two have been well characterized to date: cold-inducible RNA binding protein (CIRP)(69, 90), alternatively known as hetero-nuclear ribonucleoprotein A18 (A18 hnRNP)(91) and RNA-binding motif protein 3 (RBM3)(70, 92). CIRP and RBM3 both belong to the family of glycine-rich RNA binding proteins(70), a group of highly conversed proteins which have been speculated to

facilitate low temperature translation as RNA chaperones(93, 94). These two proteins have received particular interested due to their elevated expression under mild hypothermic conditions(2), and as potential mediators of low temperature growth arrest and elevated heterologous protein expression. Despite their structural similarities(69), CIRP and RBM3 have remarkably different functions under hypothermic conditions. Additionally, within cell culture models, those roles also vary among different mammalian cell lines.

The majority of eukaryotic protein translation (predicted to be 95-97% of mRNAs) occurs through the cap-dependent translation pathway(95). In prokaryotes, under hypothermic conditions, cap-dependent translation is inhibited through the formation of secondary structures in the 5'-untranslated region of mRNAs blocking ribosome access to the Shine-Dalgarno sequence(96). However in eukaryotes under mild hypothermic stress, inhibition occurs through a different mechanism; the de/phosphorylation of initiation and elongation factors(97, 98). Repression of cap-dependent translation does not inhibit IRES-mediated translation, allowing the expression of genes including internal ribosome entry sites.

Transcription of cold-inducible genes continues (or up-regulates) under hypothermic conditions through the binding of cold-shock proteins (CSPs) to *cis*-elements within their promoters(64). Concurrent with the inhibition of cap-dependent translation, phosphorylation of eukaryotic initiation factor 2α (eIF2α) activates IRES-mediated translation(99). The transcripts of certain cold-shock proteins, including RBM3, are

enhanced further through the recruitment of ribosomes to an IRES within the mRNA(93). Increased expression of RBM3 has been found to increase protein translation at both mild-hypothermic and physiological temperatures(70), likely preventing even further down-regulation of protein synthesis under cold-shock conditions. It has been postulated that RBM3 is affecting overall protein expression post-translationally by altering microRNA levels(70).

It remains unclear how this low temperature response is capable of specifically increasing the production of heterologous proteins while the primary mechanisms of transcription and translation are repressed. Even as the mechanisms of low temperature transcription and translation are better understood, how these interact specifically to benefit recombinant protein expression is still unknown. There is likely a combined effect of cold-temperature RNA stabilization, up-regulation of RNA chaperones, CSPs functioning as cold-specific transcription factors, alternative pre-mRNA splicing, altered phosphorylation of initiation and elongation factors and the up-regulation of RBM3-like proteins.

1.5.3 – Low Temperature Growth Arrest

As previously discussed, the basis of controlled proliferation strategies is to inhibit cell growth as a mechanism to increase specific heterologous protein production. Although the molecular mechanism of cold-enhanced Q_P is still not clear, as of yet there does not seem to be any significant overlap between the mechanisms of enhanced productivity and

growth arrest other than the initial detection of thermal stress (reduced ribosome function). RBM3, a CSP involved in elevated protein expression has not been observed to induce growth arrest under hypothermic conditions. Despite its elevated hypothermic expression, the over-expression of RBM3 induces a proliferative effect at physiological temperatures(100).

Cold-induced growth arrest, similar to chemical and genetically-induced growth arrest, is achieved through the activation of cyclin-dependent kinase inhibitors (Figure 1.2). However in the previously described strategies the growth limiting mechanisms were induced directly (engineered up-regulation of relevant genes or chemical agents which affected the G1/S checkpoint itself). Cold-inducible RNA-binding protein (CIRP), the second of the two identified CSPs, is involved in this role. The induction of CIRP occurs through two distinct pathways, both initiating with exposure to sub-physiological temperatures (Figure 1.4). The mechanisms under which the induction occurs is still poorly understood, however at least one of the known cold-induced stimuli is an overall inhibition of protein synthesis(2). This is supported by the observations of Danno et al.(101) and Tokuchi and Fujita(2), who observed that exposure to cycloheximide or puromycin simultaneously induced CIRP and RBM3 while generally inhibiting protein translation. Subsequent addition of the protein kinase A activator forskolin reverses cycloheximide/puromycin-mediated CIRP induction. However, forskolin has no effect on CIRP expression when induced through low temperature exposure(2). This is relevant as it indicates that while cold-shock and chemical translation inhibitors both result in the repression of cap-dependent translation and increased CIRP expression, their mechanism

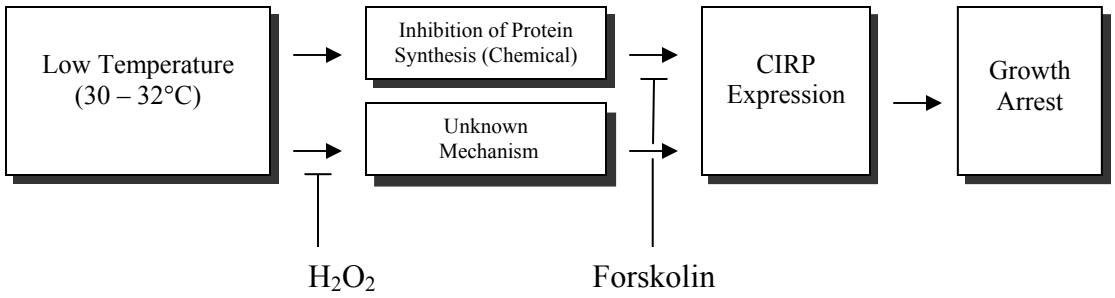

Figure 1.4: Low Temperature induction of Cold-inducible RNA-binding protein (CIRP). Schematic illustration of the two distinct induction pathways and the inhibitory effects of H_2O_2 and Forskolin (a protein kinase A activator). Figure adapted from Fujita. 1999(2).

of induction differs.

Hydrogen peroxide (H_2O_2), a strong chemical oxidizer, has a similar dose-dependent inhibitory effect on cold-induced CIRP expression(102), but no effect when induction is caused by chemical inhibitors (cycloheximide or puromycin). From this, two different induction pathways can be inferred; both likely using the inhibition of protein synthesis as a regulatory signal, yet the method of inhibition differing sufficiently that separate down-stream regulators (H_2O_2 and forskolin) have developed(2).

The role of CIRP in cold-induced growth arrest and cold-shock has been primarily based upon two observations: the up-regulation of CIRP under hypothermic conditions and the alleviation of cold-induced growth arrest through anti-sense oligonuclecotide CIRP suppression. Anti-sense inhibition reduced CIRP expression significantly (although not entirely) and increased hypothermic growth nearly 2-fold in mouse embryonic fibroblasts (MEFs)(69). As CIRP suppression was incomplete, it is unclear whether it is the sole mediator of growth arrest, or if there still are other unidentified members involved. Numerous mRNA transcripts have been found to selectively bind to CIRP, indicating possible regulatory targets; these are primarily UV- or stress-responsive genes, ribosomal genes, and transcriptional elongation factors(103).

Further complicating the model of CIRP-induced growth arrest is the work of Hong et al. who observed that small interfering RNA-based CIRP suppression had no alleviating effect on low temperature growth arrest of recombinant CHO cells. Significant down-

regulation of CIRP caused no statistically significant ($P < 0.18$) effect on hypothermic growth compared with CIRP-producing populations. Recombinant protein expression was also not affected in CIRP-repressed cultures(104). Neither at physiological temperatures did the over-expression of CIRP in CHO cultures induce hypothermic-like growth arrest as was observed in MEFs(69). Increased CIRP expression did not significantly diminish μ in erythropoietin or γ-interferon producing CHO populations (104, 105), however γ-interferon production was increased significantly resulting from increased product transcript levels(105).

Both severe (4°C) and mild (28°C) hypothermic arrest is produced through a p53-dependent $p21^{Cip1}$ mediated mechanism(71, 106). Populations of human glioblastoma and mouse embryonic fibroblasts demonstrated elevated $p21^{Cip1}$ expression when exposed to a hypothermic environment. p53, a $p21^{Cip1}$ inducing transcription factor was also post-translationally up-regulated under these conditions(106). In p53-null populations there was no evidence of elevated $p21^{Cip1}$ expression or subsequent growth arrest, indicating its central role in the induction of cold-mediated growth arrest(71, 106). These findings clearly indicate that despite the progress made in the understanding of the mammalian cold response, much more study is need to further our understanding of its regulation, even in the limited context of the production of biologics.

1.5.4 – Bi-phasic (Temperature-shift) Strategies to Increase Hypothermic Response

While attempting to exploit the numerous advantages of low temperature growth, cellular proliferation is reduced, limiting the overall population available for protein expression. Total protein production is measured as the product of cell specific productivity (Q_P) (units of product/cell·day) and the integral of the concentration of viable cell density (IVCD) (cells/day per mL)(107).

As growth is limited, the IVCD is concurrently reduced, affecting the total protein yield. Hypothermic growth therefore is a balance between increased specific productivity and reduced IVCD. Manipulating this balance can be achieved by partitioning a culture into two distinct phases differentiated by temperature. After initiating a culture with a small inoculum at physiological temperatures (37°C), cells actively proliferate creating a biomass suitable for maintaining a large IVCD. After this initial phase, the culture is subjected to sub-physiological temperatures (typically 30 – 33°C) inducing growth arrest and elevated protein expression. This two phase system; an initial growth phase and a subsequent production phase harnesses aspects of both physiological and hypothermic growth within a tunable system. This allows for biasing the culture towards enhanced Q_P or cellular growth (μ), controlling the system through the manipulation of two variables: the time and degree of the temperature shift. An earlier shift alters the culture towards a more hypothermic growth profile, while later shifts produce a more physiological culture (Figure 1.5). Modifying the temperature of the production phase (between 30°C and 33°C) induces a direct effect on the specific productivity and growth rate of the culture; with lower temperatures increasing Q_P and decreasing μ, and higher temperatures

producing the opposite effect(72, 108). The Q_P of low temperature cells has also been found to be significantly affected by small changes (pH of ±0.2) in environmental pH(75). This sensitivity has been found to affect cell viability during the production phase of a bi-phasic culture(76). Proper pH control increases the proportion of viable cells within a culture significantly (at pH 6.8) over a control culture at pH 7.0.

Simultaneous manipulation of these variables yields a complex culture system from which maximum protein yields can be achieved in the context of reduced nutrient use and product aggregation.

Fox et al. have produced and validated a model which can balance the variables of Q_P, μ, and nutrient utilization within a bi-phasic temperature-shift culture(109). Through such simulations, hypothermic bioprocesses can be predicted and developed for the production of therapeutics, circumventing many of the limitations of low temperature growth.

1.5.5 – Decoupling the Hypothermic Response

Despite their simultaneous induction under hypothermic conditions (or other CKI-inducing stimuli), no evidence has been found to directly link the mechanisms of cell cycle arrest with enhanced heterologous protein expression. This suggests the possibility of a bioprocess which could decouple these two phenomena; allowing the induction of enhanced Q_P during periods of active proliferation.

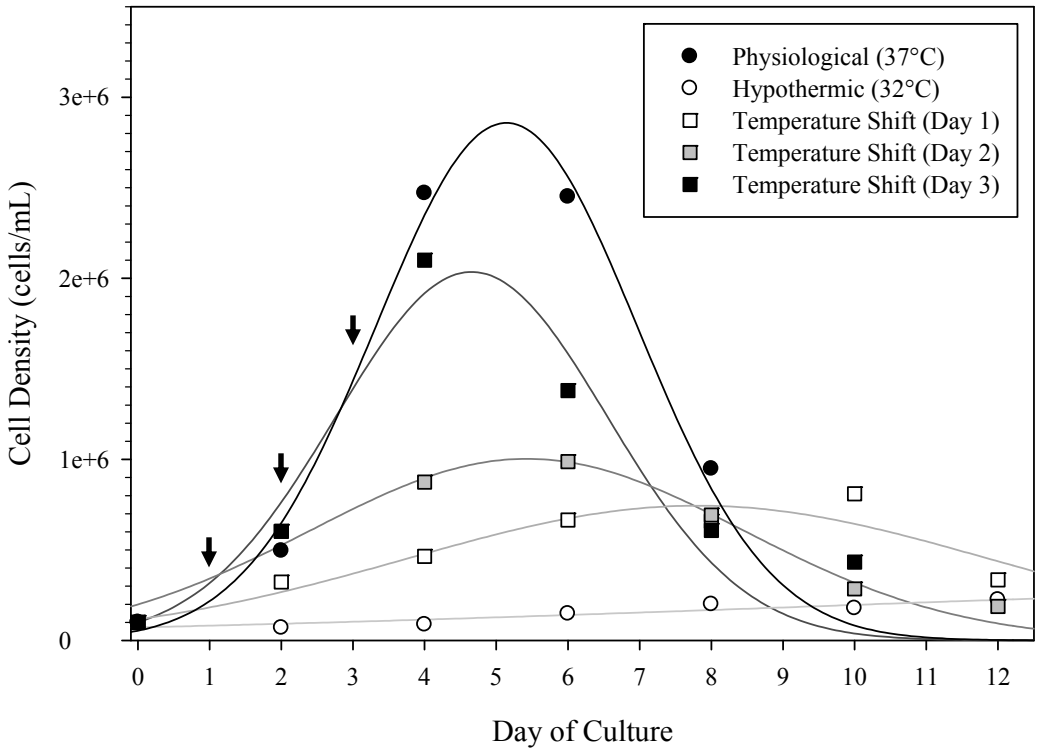

Figure 1.5: Manipulation of the bi-phasic low temperature response of a β-interferon producing CHO cell line through the modification of the time of temperature shift. Arrows indicate time of temperature shift. (Sunley et al., unpublished)

Genetic up-regulation of the relevant genes would provide the most direct approach, however our understanding of the involved pathways is not nearly sufficient to predict which genes to target. Approaches need to either induce cold-like elevated protein expression under physiological conditions or inhibit the manifestation of cold-induced growth arrest within a hypothermic environment. Alleviating growth arrest under hypothermic conditions provides a more favourable strategy due to the greater understanding of the underlying mechanism of the G1/S cell cycle checkpoint.

Cold-induced growth arrest was circumvented at 32°C by Fox et al. through the addition of mitogens to hypothermic cultures of CHO cells. High concentrations of insulin (5-25μg/mL), basic fibroblast growth factor (bFGF; 13-45ng/mL), and fetal bovine serum (FBS; 10-25%) were added to γ-interferon producing CHO cells. bFGF addition resulted in a dose-dependent increase in hypothermic growth, achieving nearly 70% of that of a physiological culture. Cultures supplemented with insulin responded similarly, although to a lesser extent. The addition of 25% FBS resulted in near physiological growth. All the mitogens resulted in significant increases in γ-interferon yields, however different factors prevent the use of each in industrial bioprocesses; high concentrations of insulin induce apoptosis(110), bFGF is prohibitively expensive as a media supplement, and current regulations prohibit the use of serum in current bioprocesses(84). This work demonstrated that active hypothermic growth could be achieved with a biotechnologically relevant cell line without the compromising cold-enhanced productivity gained under hypothermic conditions. However the authors acknowledged

that this finding was only a proof of concept, and that more cost-effective strategy would be needed to benefit from these findings.

1.5.6 – Low Temperature Adaptation

As the mechanism of cold-induced growth arrest is not sufficiently understood to target at the molecular level, the application of selective pressure could be used to isolate a population of cells capable of low temperature growth. The methodology of this is simple; continuously subculture a population under hypothermic conditions. At each passage the most proliferative cells will be selected for, generating a population capable of enhanced hypothermic growth.

This strategy was employed by Yoon et al. with two recombinant CHO cell lines. Throughout the adaptation process μ gradually increased by 73% and 20%, however the specific productivities were concurrently reduced by similar proportions. The mechanisms of adaptation were not immediately apparent. No significant changes in CIRP mRNA levels were observed despite increased hypothermic growth. Reduced Q_P was not associated with loss of foreign gene copies, indicating expression was down-regulated at the transcriptional or translations level. However the increased μ was not sufficient to counter the reduction of Q_P which occurred during the adaptation process and resulted in no net increase in production(111). Cold-adapted populations have been described previously to the work of Yoon et al., however not involving therapeutic protein production. Therefore no comparable effects on Q_P could be reported(112).

Chapter 1.6 – Objectives of Research

This thesis describes how hypothermic cell culture can be applied to the production of the hydrophobic cytokine β-interferon. Low temperature strategies were employed with the aim of increasing cell specific productivity, product quality and product yield.

Further enhancement of hypothermic culture processes were attempted through the successful isolation of a CHO population capable of active growth under hypothermic conditions. This resulted in the first successful isolation of a recombinant CHO cell population capable of enhanced growth simultaneous with elevated heterologous protein expression under mild hypothermic conditions.

Chapter 2 - Materials and Methods

2.1 – Cell Lines and Culturing

Throughout this thesis cell populations were maintained in both stationary and agitated cell cultures. Unless otherwise mentioned, routine culturing was carried out in 75 cm^2 T-flasks (Corning Inc., New York, USA) at 37°C in an atmosphere of 10% CO_2 within CHO-SFM serum-free media (Biogro Technologies Inc., Winnipeg, Canada). Subculturing was performed every four days (corresponding to mid-exponential growth) and seeded at a concentration of $1x10^5$ cells/mL.

Low temperature culturing (30°C to 33°C) conditions were otherwise identical to those at a physiological temperature, however subculturing was only performed every eight days.

2.1.1 – Cell Lines

A recombinant Chinese hamster ovary (CHO-K1; ATCC CCL 61) cell line transfected with the gene for human Interferon-beta (β-IFN) was provided by Cangene Corporation (Winnipeg, Canada). From this line, numerous serum-free adapted clones were isolated. Clone CHO-674, a highly proliferative clone capable of producing high titres of recombinant protein is referred to in this work as either the non-adapted or parental population and was the source of the low temperature-adapted population. A tissue plasminogen activator (t-PA) producing CHO cell line (ATCC CRL-9606) was also utilized for cold-adaptation, however no successful isolation occurred and use of this line was discontinued.

2.1.2 – Cell Line Maintenance and Subculturing Procedures

As previously described, stationary cell cultures were typically maintained in 75 cm^2 T-flasks (although 25 and 150 cm^2 flasks were also employed depending on cell titres required). When cultured in serum-free media the CHO-674 clone displays a non-adherent phenotype, growing as spherical cells suspended within the culture media. Subculturing was performed by resuspending the cells within a solution of phosphate buffered saline (pH 7.1) supplemented with 5 mM ethylenediaminetetraacetic acid (EDTA) through centrifugation (approx. 430x*g*) for 5 minutes. Cell-free spent media samples were stored at -80°C for further analysis.

Cell enumeration was performed through manual counting using a hemocytometer and an optical bright-field microscope (total magnification 100x). Viable cells were differentiated from non-viable by mixing a 200 µL aliquot of the resuspended cell population 1:1 with a solution of trypan blue (0.2% w/v) in phosphate-buffered saline (PBS) following the trypan blue dye exclusion method(113). Cells were seeded to a concentration of $1x10^5$ viable cells per mL in 12 mL of serum-free media (for a 75 cm^2 T-flask).

Viable cell concentrations were determined using the following formula:

$$\textit{viable cell concentration} = \frac{\textit{total viable count x } 10^4 \textit{ (conversion to mL) x 2 (trypan blue dilution factor)}}{\textit{4 (number of hemocytometer squares observed)}}$$

Cell viability was determined by multiplying the ratio of the viable cells over the total population counted and multiplied by 100. All cell culture manipulations were performed under aseptic conditions in a NuAire Laminar Flow Hood. All media, trypsin, trypsin inhibitor, and other reagents used for cell culture were sterilized by 0.2 μm membrane filtration (Pall, Ann Arbor, MI).

All growth profiles except for the adaptation process were performed in duplicate and reported ± standard error.

2.1.3 – Hypothermic Culturing

Hypothermic, or low-temperature culturing was carried out following the previously described protocols, only at a reduced incubation temperature. Temperature control was maintained using a NuAire water-jacketed incubator (Temperature ± 0.2°C) in an atmosphere of 10% CO_2. Temperature shifts were performed through transporting the culture vessels (T-flasks or spinner flasks) from a 37°C incubator to a second incubator pre-set at the hypothermic temperature. The time of this shift (abbreviated as T_{shift}) varied and is described with the experimental details described further in this thesis.

2.1.3 – Suspension and Microcarrier Cultures

Populations of adapted or non-adapted cells were inoculated into autoclaved 100 mL glass spinner flask vessels (Bellco Biotechnology Inc.) to a final concentration of $1x10^5$ viable cells/mL in CHO-SFM serum-free media. The cultures were stirred at 45

revolutions per minute (RPM) at 37°C or 32ºC in an atmosphere of 10% CO_2 to allow for cell entrapment and proliferation. Temperature-shifted cultures were incubated at 37ºC for 48 hours prior to incubation at 32ºC. Microcarrier cultures were supplemented with a solution of Cytopore 2 microcarriers (GE Healthcare) suspended in CHO-SFM media according to the manufacturer's instructions at a final concentration of 1 mg/mL prior to inoculation.

2.1.4 – Preparation of Cytopore™ 2 Microcarriers

Cytopore 2 beads were initially hydrated at a concentration of 1g/100mL in PBS. The solution was autoclaved for 20 minutes at 121ºC in accordance with manufacturer's instructions. The microcarrier preparation was then washed twice in fresh PBS, followed by three washings in CHO-SFM serum-free media.

2.1.5 – Nuclei Enumeration of Microcarrier Cultures

The growth within microcarrier cultures was determined through the lysis of entrapped cells and the enumeration of released stained nuclei. Suspension cultures which were directly compared to microcarrier cultures were enumerated using the same method.

Each culture sample (0.5 mL) was mixed with an equal volume of crystal violet reagent (0.2M citric acid, 0.2% w/v crystal violet and 2% w/v Triton X-100) for up to 3 hours at 37ºC (114). Nuclei were released from the carriers by repeated aspiration (25 times) through a 25 gauge needle. Nuclei were counted with the aid of a hemocytometer and reported as nuclei/mL of culture volume. All growth profiles were performed in

duplicate and reported ± standard error. Nuclei release from microcarriers has been determined to be in excess of 90% by Spearman *et al*.(114) using this method for Cytopore concentrations between 0.25 mg/mL and 2.0 mg/mL.

2.1.6 – Specific Growth Rate (μ) and Specific Productivity (Q_P)

The apparent specific growth rate (μ_{app}; h^{-1}), referred to simply as μ, is described by the following equation:

$$\ln N = \ln N_0 + \mu \cdot t$$

where N represents the maximum cell yield achieved by the culture, N_0 is the initial cell concentration at time of inoculation, t is the duration of the culture at time of sampling (hours) and μ is the growth rate. Growth rate values were reported ± standard error. The specific productivity of the culture (units/cells per day) was determined from a plot of the product concentration (units/mL) against the integral of the concentration of viable cells over time (cells or nuclei/day per mL). The slope of the relationship was calculated as the specific productivity.

2.1.7 –Solutions and Chemicals

Unless otherwise mentioned, all standard laboratory chemicals were purchased from Sigma-Aldrich Canada (Oakville, Ontario).

2.2 – Recombinant Protein Production and Quality

Quantification of the β-IFN recombinant product was performed using an enzyme-linked immunosorbent assay (ELISA). This method was also utilized to differentiate between monomeric and aggregated β-IFN.

2.2.1 – Interferon-beta Quantification

The concentration of β-IFN was determined using an enzyme-linked immunosorbent assay. Media samples from cultures were cleared of cell debris and/or microcarriers through centrifugation (approximately 300x*g*) and stored at -80ºC for later analysis. EIA/RIA 96-well polystyrene plates (Corning Inc.) were coated with a 0.2 μg/mL solution of polyclonal rabbit anti-human β-IFN antibody (Biogenesis Ltd.) in 0.1M pH 9.6 carbonate buffer and incubated overnight.

Plates were washed (3x) with 50mM Tris-buffered saline (TBS) and 0.1% Tween 20 between all additions. After blocking with BSA to prevent non-specific binding, pre-diluted media samples were added and incubated at room temperature. The secondary antibody, mouse monoclonal anti-human β-IFN (Chemicon International), was diluted to 1:1000 in 50mM TBS with 0.1% Tween 20 and 3% w/v BSA and incubated. The conjugate detector antibody, goat anti-mouse IgG alkaline phosphatase (Sigma-Aldrich), was added and developed with *p*-nitrophenyl phosphate (Sigma-Aldrich). The plate was read photometrically at 405nm. Sample values were determined with the aid of a

standard curve of known β-IFN concentrations (United States Biological Inc.) and reported as relative units of β-IFN/mL.

2.2.2 – Interferon-beta Aggregation

The relative proportion of aggregated interferon-beta monomers was determined through a modified ELISA assay. Samples of culture supernatant (containing β-IFN) were subjected to an aggressive denaturing treatment. This involved the addition of sodium lauryl sulfate (SDS) and β-mercaptoethanol (β-ME) to final concentrations of 0.1% and 1% respectively. This was then incubated at 100°C for 5 min in a sealed polypropylene 1.5 mL microcentrifuge tube.

This treatment dissociated interferon aggregates through two distinct methods; minimizing hydrophobic intermolecular attraction through the addition of the SDS detergent, and reducing any inter- or intramolecular disulfide bonds which may have formed between cysteine residues.

The ELISA assay was then performed as described (section 2.2.1), simultaneously quantifying the native (or non-denatured) and denatured samples. By pre-treating the samples and dissociating the aggregates, all epitopes are exposed and available to be bound by the detecting antibody. In the non-treated samples, only epitopes on the non-aggregated monomers are available to the antibodies, therefore the ELISA signal is reduced. The proportion of the non-aggregated monomers was determined by dividing the non-treated ELISA response by the denatured response.

2.3 – Western Blotting of Vimentin Intermediate Filament

2.3.1 – Sample Preparation

Populations of cells ($1x10^7$ cells) were ultrasonically lysed through four cycles of 30 seconds (50% power) using a Branson Sonifer 450 and a model 102 converter (Branson Ultrasonics Inc.) in a 2x sample buffer solution.

2.3.2 – SDS-PAGE Separation

SDS-PAGE (sodium dodecyl sulfate polyacrylamide gel electrophoresis) was performed according to the discontinuous buffer system described by Laemmeli(115). The gels were prepared using 10% polyacrylamide gels to allow for accurate separation of the protein molecules. The SDS gel preparation and protein separation was performed using the Bio-Rad Mini-PROTEAN 3 electrophoresis apparatus following the manufacture's instructions. Electrophoresis was run at 200 volts for 45 min (allowing for the dye front to travel the length of the gel). Electrical current was supplied by a Bio-Rad electrophoresis power supply (Model 1000/500).

Pre-stained protein ladder was purchased from Bio-Rad with a molecular weight range of 10 to 250 kDa, 5 μL of standard was loaded onto each SDS-PAGE gel.

2.3.3 – Immunodetection of Vimentin Protein Molecule

The electrophoretically separated proteins (Section 2.2.3.1) were then transferred to a nitrocellulose membrane following the procedure provided by Bio-Rad. After transferring the gel to nitrocellulose the membrane was treated overnight with blocking buffer (3% BSA-Tween 20) at 4°C. The membrane was then incubated with the mouse anti-human vimentin monoclonal antibody (Clone V9 from Sigma Aldrich) at a concentration of 0.5 µg/mL for 3 hours. The blot was then washed (3x 5 minutes in PBS-Tween 20) and incubated with alkaline phosphatase conjugated goat anti-mouse IgG (Sigma Aldrich) for 2 hours. The substrate, nitroblue tetrazolium (0.3 mg/mL) and 5-bromo-4-chloro-3-indolyl phosphate (0.15 mg/mL) in 5 mM $MgCl_2$ was then applied for up to 15 minutes to allow for colour formation. The reaction was stopped by addition of PBS-EDTA, and the blots were rinsed thoroughly with distilled water.

2.4 – Characterization of Cell Size and Fragility

Overall cell strength was determined through a number of physical and biochemical methods. The following were used to demonstrate the adaptation-induced changes relevant to cellular fragility.

2.4.1 – Determination of Cell Size

Samples of adapted and non-adapted cultures were centrifuged (approximately 300x*g*) to remove supernatant and resuspended in 3% w/v paraformaldehyde in phosphate buffered saline. Samples were stored at 4ºC for later analysis. Microscope slides were coated

with a 0.1 mg/mL solution of MW 300,000 Poly-L-lysine (Sigma-Aldrich) according to manufacturer's instructions. Fixed cell samples were then applied to slides, mounted in 10% phosphate buffered saline in glycerol under a coverglass and observed microscopically.

Cells were imaged using a Zeiss AxioImager Z1 with a Plan-Apochromat 20x/0.8 objective and their areas determined using AxioVision 4.5 LE software (Carl Zeiss, Inc.). A minimum of 650 cells per population were measured.

2.4.2 – Nucleation / Nuclear Fragmentation Profile

Samples of adapted and non-adapted cultures were prepared as indicated above for cell size determination, except that prior to mounting the cells were stained with a 0.3μM solution of 4',6-diamidino-2-phenylindole (DAPI) (Invitrogen Corp.) in phosphate buffered saline. *n*-Propyl gallate (Sigma-Aldrich) was added to the mountant at a concentration of 1 mg/mL to reduce photobleaching. Cells were imaged using a Zeiss AxioImager Z1 and a Plan-Apochromat 100x/1.4 objective. The nuclei of at least 400 cells per population were counted manually.

3D reconstructions were produced through capturing a Z-stack of fluorescence images using a Zeiss AxioImager Z1 with a Plan-Apochromat 100x/1.4 objective. Images were captured every 0.22 μm along the Z-axis using a 16-bit AxioCam MRm. Image stacks were developed using the iterative deconvolution module of Zeiss AxioVision 4.5 (Carl Zeiss, Inc.). Contrast was adjusted to show 3D structure using Adobe Photoshop CS

(Adobe Systems Inc.); ensuring manipulations were linear and did not affect the data within the image.

2.4.3 – Mechanical Stress Sensitivity and LDH Release

Cells at a concentration of $1x10^6$ cells/mL were added to a 10mL glass beaker containing an 8 mm diameter cross-shaped magnetic stir bar. Cells were stirred at rates of 0, 300 or 500 rpm for 120 minutes at 32ºC with supernatant samples collected every 30 minutes. Microcarrier samples were assayed following the same methods, except that microcarriers were inoculated with cells at $1x10^5$ cells/mL four days prior to the trial, incubated at either 32ºC (adapted cells) or 37ºC (non-adapted cells), and added in equal volumes to the suspension cell samples.

The activity of the endogenous lactate dehydrogenase (LDH) enzyme released into the media was assayed using the CytoTox 96 Non-radioactive Cytotoxicity assay kit (Promega Corp.) as described in the manufacturer's instructions. The values were normalized against the total LDH activity per vessel by lysing a population equal to the initial concentration using a freeze/thaw cycle at -80ºC. Released values were calculated as a percent of the total cellular LDH. Each trial was performed in triplicate and reported ± standard error.

2.5 – Immunofluorescence and Lectin-based Imaging of Cellular Structures

Fluorescent dye conjugates were utilized throughout different aspects of this thesis as a method to visualize intracellular structure (vimentin and p53 localization) and cellular morphologies (centrifugation-induced deformation). These methods followed standard protocols as suggested by their manufacturer (Invitrogen Corp.)

2.5.1 – Immunofluorescence Staining

Cells taken from actively growing (viability > 90%) were allowed to settle on poly-L-lysine (MW > 300,000; Sigma Aldrich) pre-coated (0.5 mg/mL) microscope cover slips (thickness 0.15 - 0.19 mm; Corning Inc.). After incubation for 30 minutes in a humidified environment (37°C) cells were fixed with 4% paraformaldehyde in phosphate buffered saline (PBS) and subsequently permeabilized with 0.1% v/v Triton X-100 in PBS. Cells were washed twice in PBS between all steps.

The fixed and permeabilized cells were then blocked using Image IT signal enhancer (as per manufacturers instructions; Invitrogen Corp.) and incubated for 1 hour with a 1:20 dilution of the primary antibody (mouse anti-vimentin or mouse anti-p53; Sigma Aldrich) in PBS with 10% fetal bovine serum. The secondary antibody, goat anti-mouse IgG conjugated to Alexa Fluor 555 was used at a concentration of 20 µg/mL and incubated for 1 hour. The cells were then quickly washed (1 minute) in 1 µg/mL 4',6-diamidino-2-phenylindole (DAPI), and mounted in phosphate buffered glycerol containing 5 mg/mL *n*-propyl gallate as an anti-fade agent.

2.5.2 – Lectin-based Fluorescence Staining

Viable cells settled on glass cover slips were treated to varying degrees of centrifugal force, fixed in 4% paraformaldehyde, and incubated in a solution of 1.0 mg/mL of Alexa Fluor 555 pre-conjugated to wheat germ agglutinin for 10 minutes. The cells were then washed in PBS and mounted in phosphate buffered glycerol (containing *n*-propyl gallate).

2.5.3 – Imaging of Fluorescent Samples

Prepared slides of lectin or antibody stained cells were imaged using a Zeiss AxioImager Z1 upright motorized microscope and a cooled AxioCam MRm camera. Image acquisition was performed using Zeiss AxioVision software. Image processing and manipulation was limited to contrast and brightness manipulation using Photoshop software (Adobe Inc.)

2.5.4 – In Situ Viability Determination

Viability determination was performed within microcarriers using fluorescence microscopy. Cells were removed from actively proliferating cultures, entrapped within microcarriers, and incubated in solutions of fluorescein diacetate (25 mM; Sigma Aldrich) and TO-PRO-3 Iodide (1 μM; Invitrogen Corp.). Viable cells catalyze the non-fluorescent fluorescein diacetate to fluorescein, which was observed through a fluorescence microscope. TO-PRO-3 Iodide stained all cells, living and non-viable, allowing the calculation of the percentage of viable cells within the population.

2.6 – 2D Electrophoresis and Sample Preparation

Two-dimensional electrophoresis was performed using Differential In-Gel Electrophoresis (DIGE) technology according to the manufacturer's instructions (GE Healthcare) in collaboration with Dr. Brendan McConkey at the University of Waterloo.

2.6.1 – Sample Preparation

Cells (approximately $2.5x10^6$) were harvested and washed three times in TRIS-Sucrose buffer (20 mM TRIS, 250 mM sucrose). The cell pellet was resuspended in a reducing lysis buffer (7M urea, 2M thiourea, 1% ASB-14, 5 mM tributyl phosphine, 2.42 mg/mL TRIS base) and incubated for 25 minutes. 4-vinyl pyrimidine was added to a final concentration of 20 mM and incubated for 1 hour to alkylate any disulphide bonds reduced by the tributyl phosphine.

Excess 4-vinyl pyrimidine was quenched with an equimolar (20 mM) solution of dithiotheritol and the samples were centrifuged at 7000xg for 30 – 60 minutes at 4 - 8°C.

2.7 - Apoptosis Assays

Assays to determine apoptotic activity in cell populations were carried out to investigate to specific apoptotic markers within the cell.

2.7.1 – Caspase 3/7 Assay

Caspase activity was assayed within the cell using the Caspase-Glo™ 3/7 assay kit from Promega Corporation. A lumingenic substrate containing the amino acid sequence aspartic acid-glutamine-valine-aspartic acid, is cleaved specifically by caspases 3 and 7, and measured using a Synergy 2 multi-modal plate reader (BioTek Corp.).

2.7.2 – Agarose Electrophoresis based detection of Caspase Activated DNAses

DNA "laddering", a fragmentation pattern characteristic of caspase activating DNAse activity and apoptosis was assayed for using the Apoptotic DNA Ladder Kit from Roche Applied Science. The manufacturer's methods were followed with some modifications. Briefly, genomic DNA was isolated from $2.0x10^6$ cells using glass fiber chromatography, and visualized on an ethidium bromide-free 1% agarose gel with bromophenol blue-free loading buffer run at 75V for 1 hour. The gel was stained in a solution of 0.5 µg/mL ethidium bromide post electrophoresis and imaged on an Alpha Innotech gel documentation system.

2.8 - Statistical Analyses

Statistical significance was determined through the use of unpaired T-tests ($P \leq 0.05$) between equal or approximately equal numbers of data points. Regression lines were calculated using numerous mathematic models (described within each figure). T-tests, standard error calculations and linear regressions were preformed using SigmaPlot 2000 version 6.1 (Systat Software Inc.).

Chapter 3 - Maximizing Recombinant Protein Expression under Hypothermic Conditions through Manipulation of Culture Temperature

Chapter 3.1 – Introduction

The production of therapeutically useful recombinant proteins, also referred to as heterologous proteins or biologics, under mild hypothermic temperatures (30°C to 33°C) is a method of protein production which as been described at length in published literature and has been employed industrially. Lower temperature growth offers a simple and effective strategy to modulate cell growth and increase protein expression, without the need for previously performed additional genetic manipulation or the addition of any exogenous chemical agents.

Chapter 3.2 – Results

Populations of β-interferon-producing Chinese hamster ovary (CHO) cells were cultured at temperatures below their physiological normal in an effort to simultaneously reduce heterologous protein aggregation and increase production yields. However, these elevated protein yields came at the cost of dramatically reduced cell growth; proportional to the magnitude of the temperature decrease. The aim of this thesis is to build from the initial work of Rodriguez et al.(74), further optimizing the hypothermic processes employed in the context of increasing the production of monomeric β-interferon.

3.2.1 – Hypothermic Growth and Optimization of Bi-phasic Bioprocesses through the Induction of Hypothermic Temperature Shifts

In an effort to alleviate the low temperature growth reduction, strategies which divided the cultures into two phases; an initial physiological (37°C) phase followed by a hypothermic (30°C to 33°C) phase were employed. Optimization of these strategies was performed to maximize the protein production and product quality through the modulation of cell growth.

3.2.2 – The Effect of Hypothermic Temperature on Cell Growth and Recombinant Protein Expression

To determine the role of temperature in the production of biologics, cultures were inoculated at $1x10^5$ cells/mL and maintained in small-scale (100 mL) stirred glass vessels over a range of sub-physiological temperatures and maintained for either 8 days (for 37°C cultures) or 12 days (for hypothermic cultures). Temperatures between 31°C and 33°C were selected for a strategy to simultaneously reduce intermolecular aggregation and increase recombinant protein expression. This range was selected by expanding on the 30°C culturing performed by Rodriguez et al.(74), in an effort to increase the hypothermic titres which had been previously achieved.

Growth (enumerated using a hemocytometer) was suppressed in a temperature-dependent manner (Figure 3.1); essentially halted at 31°C ($\mu = 0.0003\ h^{-1}$; doubling-time = 87 days). Increasing the culture temperature to 32°C increased cell proliferation 3-fold ($\mu = 0.001$

h^{-1}; doubling-time = 29 days), while growth at 33°C resulted in nearly a 9-fold increase (μ = 0.0087; doubling-time = 3.3 days); up to 40% of the growth which occurs under physiological conditions (37°C) (μ = 0.0215; doubling-time = 1.3 days).

The growth profiles which resulted from temperature manipulation varied between a typical physiological culture (max. cell yield = $2.2x10^6$ cells/mL at day 6) to an essentially non-proliferative culture (which did not exceed $0.11x10^6$ cells/mL after 12 days). Figure 3.2 illustrates the growth of cultures between 31°C and 37°C. However, in the context of biopharmaceutical production, other factors in addition to growth rate must be considered; including specific recombinant protein expression (Q_P; measured in units/cell per day) and product quality. β-interferon, the glycoprotein product investigated in this work, is a hydrophobic cytokine prone to temperature-dependent in-culture aggregation(116). As only the monomeric form of β-IFN is suitable for therapeutic use, in-culture product aggregation was also considered in determining an optimum culture temperature.

Specific β-IFN production, a key factor in determining product yields exhibited a slight inverse relationship with temperature, however did not vary appreciably between 31°C, 32°C and 33°C degrees (0.956, 0.868, and 1.009 units/cell per day). As a result temperature optimization was based only on the interplay between cellular proliferation (μ) and the rate of product aggregation.

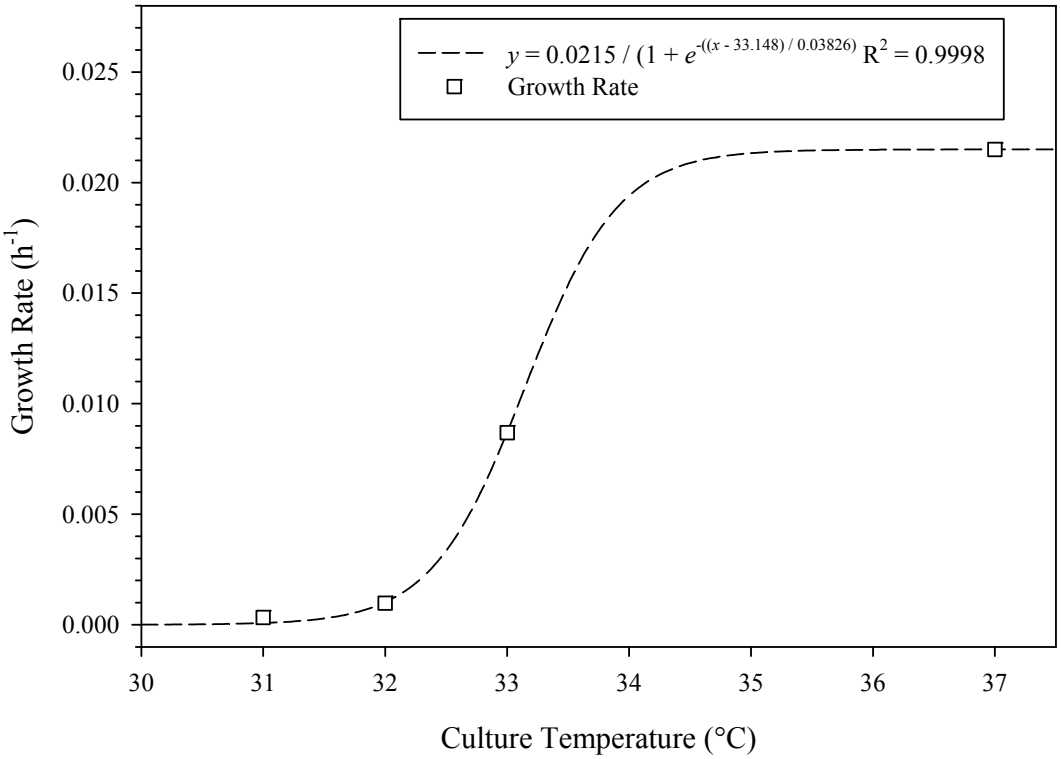

Figure 3.1: The effect of temperature on the growth rate (μ) of β-IFN producing CHO cells. Non-linear (3-parameter sigmoidal) regression illustrates the response over the mild-hypothermic and physiological range.

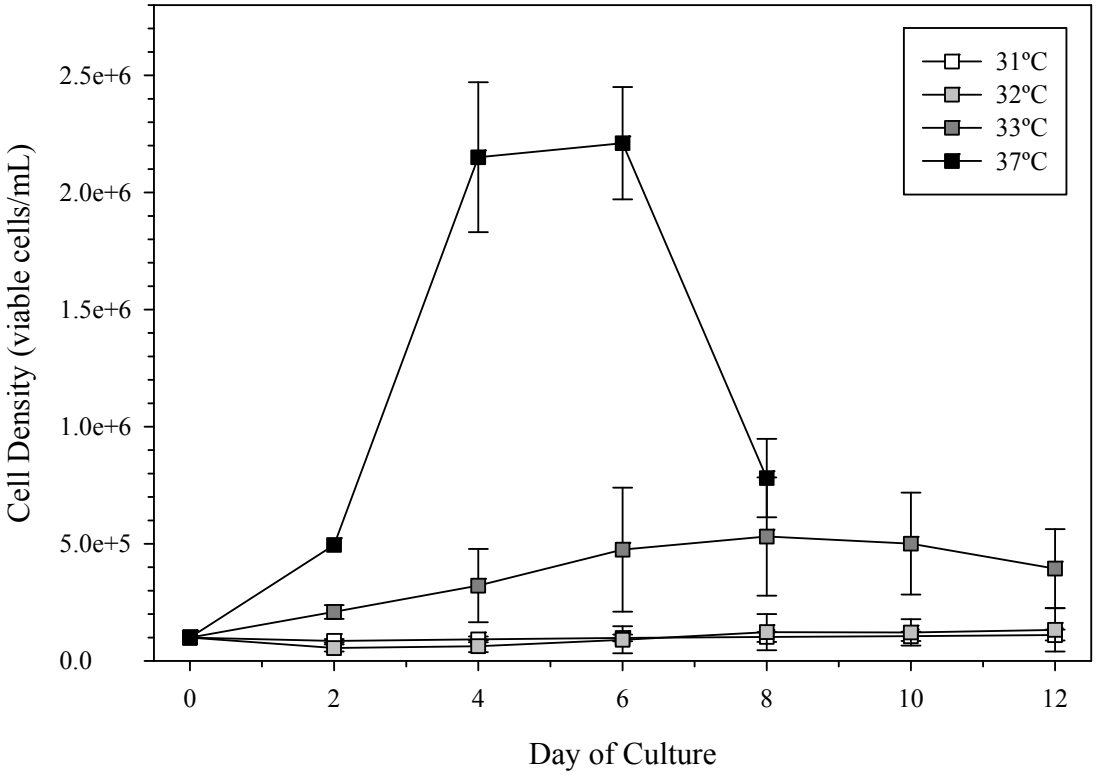

Figure 3.2: The effect of temperature on cell growth profiles of β-IFN producing CHO cells. Cultures were incubated at varying hypothermic temperatures (31-33°C) and 37°C in 100 mL suspension cultures. (n = 2 ± standard error).

Intermolecular aggregation of β-IFN is a function of numerous parameters; one of which is the environmental temperature. Cultures were maintained at varying sub-physiological temperatures (31°C, 32°C, and 33°C); allowing the aggregated proportion of their respective product yields to be compared to that of a physiological culture (37°C). Temperature was found to have a sigmoidal relationship with β-IFN aggregation, with the 31 – 33°C temperature range having a particularly pronounced effect (Figure 3.3). Interferon-beta aggregation was quantified in this work through the ratio of two ELISA responses. The β-IFN titres of untreated and denatured supernatants (supernatants adjusted to 14.2 nM β-ME and 0.001% SDS and heated at 100°C for 5 minutes). The SDS within the denaturing mixture dissociates intermolecular aggregation stabilized through hydrophobic interactions between protein monomers, while the β-ME reduces any covalent bonds which may have formed between sulfide groups on external serine residues. The extent of the process was determined using an ELISA, with the percent of non-aggregated β-IFN calculated as a ratio of the non-denatured ELISA response to the denatured. Intermolecular aggregation would reduce the ELISA response within the sample by blocking access to exterior epitopes on the interferon molecule.

Although product aggregation at 31°C was minimal (approximately 10%), hypothermic growth arrest was so severe (μ = 1.4% of a 37°C culture) at this temperature that there was no significant cell growth throughout a 12 day culture. Determining the optimal temperature between 32°C and 33°C was more complex. Proliferation at 32°C was

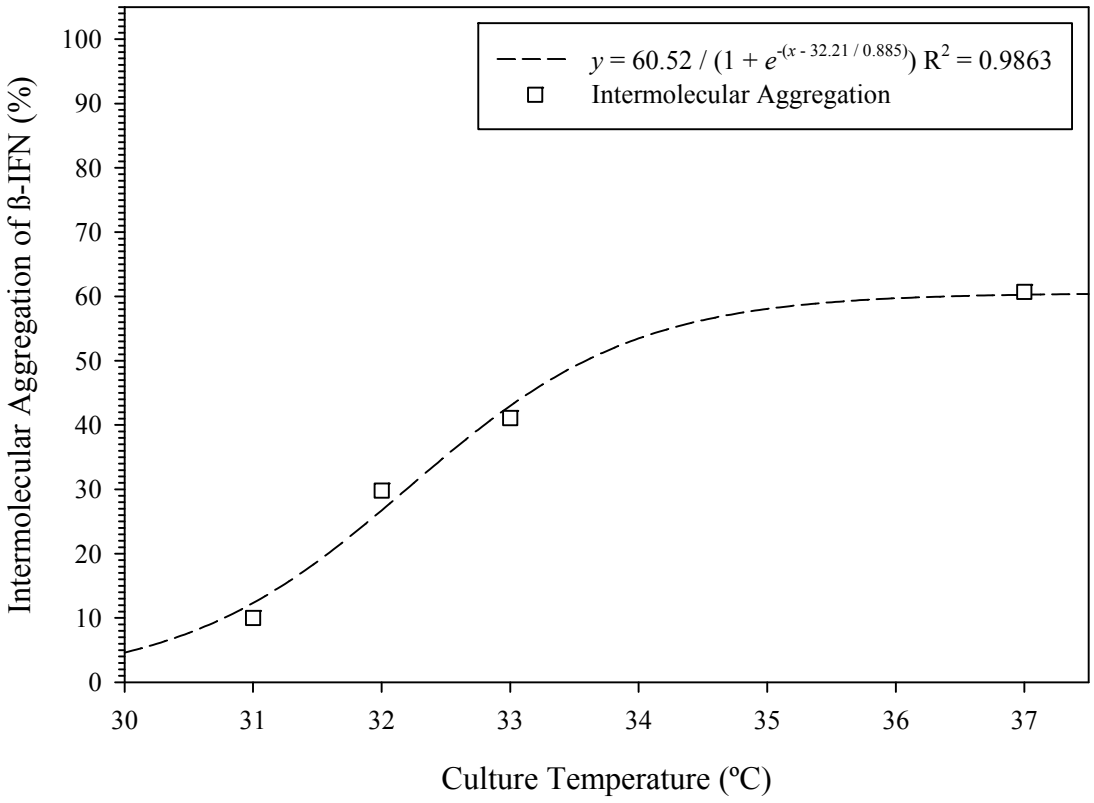

Figure 3.3: The effect of temperature on in-culture intermolecular aggregation of β-IFN produced by CHO cells. Non-linear (3-parameter sigmoidal) regression illustrates the effect over mild-hypothermic and physiological temperatures.

increased 3.5-fold over 31°C (although still only 5% of a 37°C culture); and product aggregation was limited to less than 50% of physiological conditions. Increasing the temperature further to 33°C increased cell growth significantly (40% of a 37°C), but also increased product aggregation to nearly 70% of a physiological culture (resulting in a loss of nearly 50% of the product yield).

3.2.3 – Bi-phasic (Temperature-shift) Cultures to Increase Recombinant Protein Yields

Raising the culture temperature from 32°C to 33°C induced an increase in cellular growth which was significantly greater than that of the increase in product aggregation (8-fold and 1.4-fold respectively). Product yields at 33°C were also 26% greater; indicating that the warmer temperature may increase production more than it aggregates product monomers. However intermolecular aggregation is irreversible and self-perpetuating, therefore production strategies should aim to minimize β-IFN aggregation.

Temperature-shift strategies were therefore employed to increase cellular growth without significantly increasing product loss. By initiating cultures under physiological conditions (37°C) and then lowering their incubation temperature to sub-physiological temperatures, growth under sub-physiological conditions is enhanced. Temperature shifts were performed with the two most promising hypothermic temperatures (32°C and 33°C), as determined in Chapter 3.2.1, in an effort to increase low temperature growth. By preceding sub-physiological growth with a period of 37°C incubation, growth arrest was alleviated in a time-dependent manner. Temperature shifts (to 32°C and 33°C) were initiated after 24, 48 and 72 hours of physiological growth; increasing the maximum cell

yields from less than $0.5x10^6$ to over $2.0x10^6$ cells/mL in a non-linear (sigmoidal) response (Figure 3.4).

3.2.3.1 – Growth and Production Responses to 37°C – 32°C Temperature Shifts

Growth of cells within a 32°C temperature-shifted cultures is illustrated in Figure 3.5. Continuous hypothermic incubation resulted in minimal cell growth, reaching only $0.13x10^6$ cells/mL after 12 days of incubation. The induction of temperature shifts at 24 and 48 hours increased maximums to $0.48x10^6$ and $1.15x10^6$ cells/mL respectively, while a 72-hour shift yielded near physiological growth ($2.2x10^6$ cells/mL). β-IFN expression also increased with an extended 37°C phase. However, unlike cell growth, production under physiological conditions did not outperform cultures which underwent a period of low temperature growth.

The product yields of a 1-day temperature-shift (T_{shift} = 1 day) culture was 1.75-fold greater than 37°C cultures after 8 days of incubation. Increasing T_{shift} to 48 and 72 hours subsequently increased product titres to 3-fold and 3.3-fold respectively; however increased aggregation at T_{shift} = 72 hours reduced monomeric β-IFN titres to less than (95%) a 48-hour temperature shift (Figure 3.6).

3.2.3.2 – Growth and Production Responses to 37°C – 33°C Temperature Shifts

Temperature shifts induced at 33°C demonstrated a similar T_{shift}-dependent proliferation response; however at a reduced rate compared to 32°C cultures (Figure 3.4). Maximum

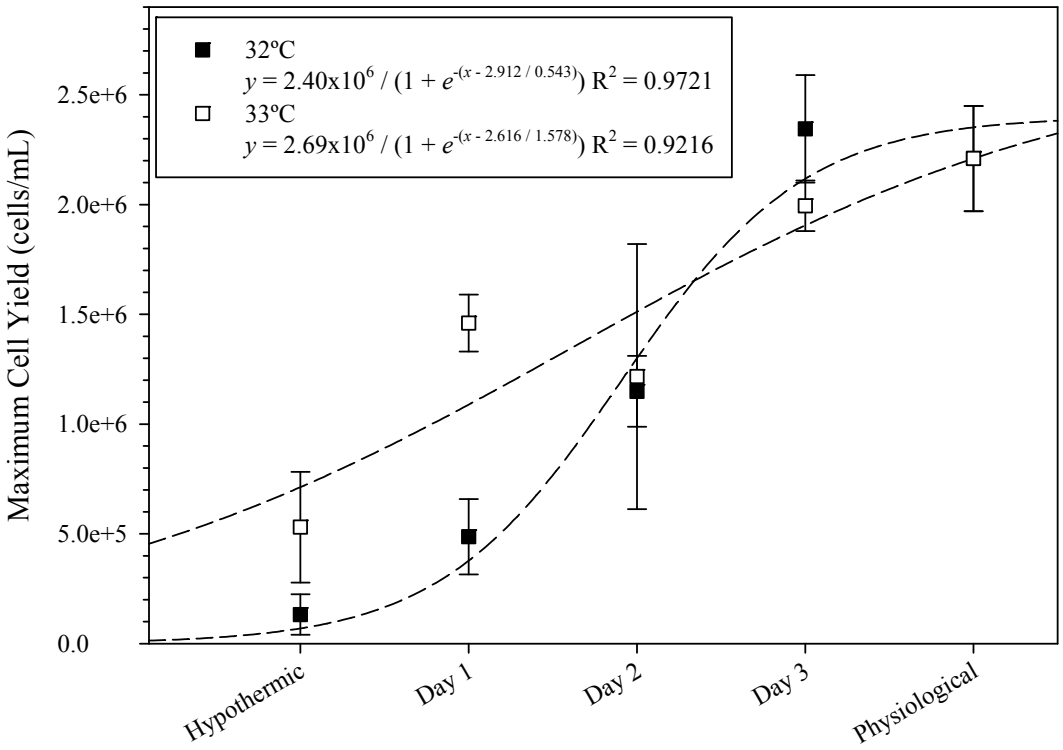

Figure 3.4: The effect of time of temperature shift on maximum cell yields in small-scale agitated (100 mL) cultures of β-IFN-producing CHO cells. Time of induction was varied (at 32°C and 33°C) between 24 and 72 hours, as well as non-shifted (hypothermic) and physiological (37°C) cultures. All titres were measured after 8 days of incubation, with the exception of the physiological culture which was measured after 4 days due to decreased cell viability. Non-linear (3-parameter sigmoidal) regression illustrates the response over the mild-hypothermic, temperature shifted and physiological range. (n = 2 ± standard error).

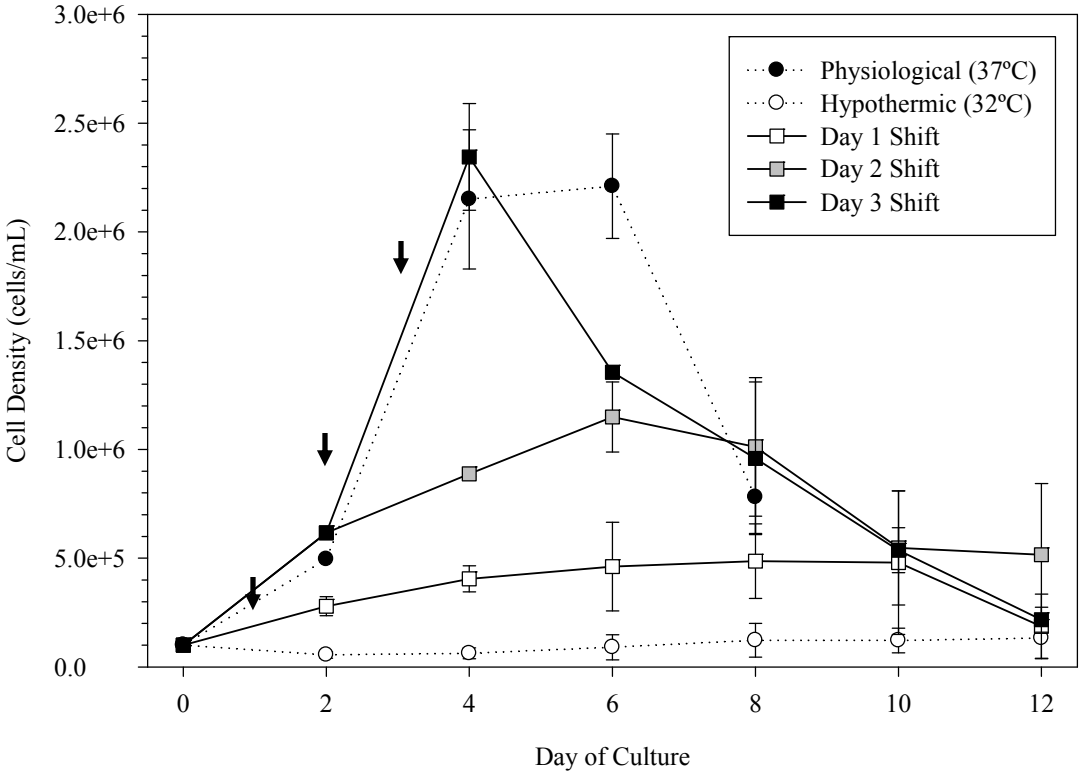

Figure 3.5: Growth response of CHO cells under physiological (37°C), hypothermic (32°C) and temperature-shifted conditions in small-scale (100 mL) agitated cultures. Arrow indicates times of temperature shift. (n = 2 ± standard error).

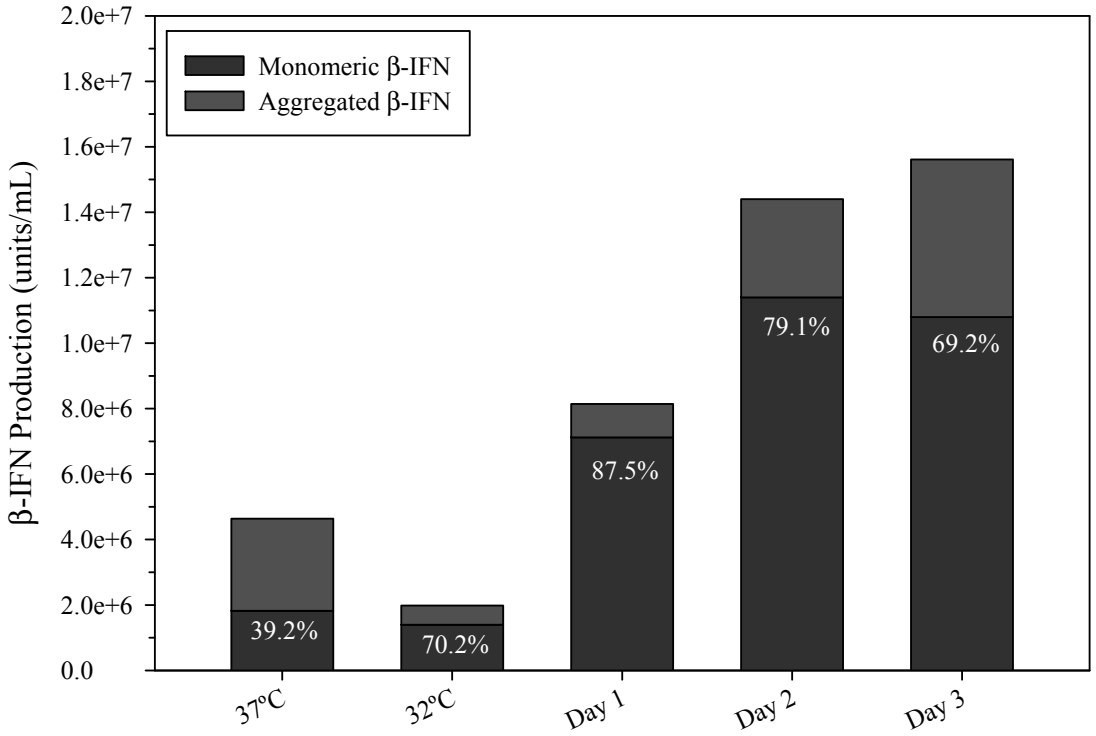

Figure 3.6: β-Interferon titres (day 8) from physiological (37°C), hypothermic (32°C) and temperature-shifted agitated (100 mL) cultures. Monomeric (black) and aggregated (grey) product concentrations as well as the percent of non-aggregated β-IFN are illustrated.

cell yields increased 2.25 to 2.75-fold over a non-shifted culture (at T_{shift} of 48 and 24 hours respectively). Increasing T_{shift} to 72 hours further increased the maximum cell yield to 3.75-fold; 90% of a completely physiological culture (Figure 3.7). At both 32°C and 33°C, extending the 37°C growth phase transformed the culture further towards a physiological growth profile.

The volumetric production response at 33°C was proportional to that of 32°C cultures; with the increased the cell yields at 33°C increasing titres under all conditions (Figure 3.8). Product titres were elevated between 12% to 37%, with maximum production induced by a day 3 temperature shift ($1.8x10^7$ units/mL); 4.3-fold greater than a physiological culture. The magnitude of the production increase over 32°C cultures was inversely proportional to the length of the initial 37°C production phase (inversely T_{shift}-dependent), with diminished increases occurring in cultures with a later T_{shift} (Figure 3.9). As the increased product yields at 33°C (over 32°C) were reduced by bi-phasic culturing (Figure 3.9) and the intermolecular aggregation was also increased (Figure 3.3); T_{shift} = 48 hour 32°C cultures were determined to maximize monomeric β-IFN production. These conditions were utilized for all subsequent temperature-shift cultures.

3.2.4 – Enhanced Proliferation is not a Response to Elevated Cell Density at Time of Shift.

Temperature-shift strategies result in a significant accumulation of cellular biomass prior to the induction of the hypothermic production phase. The population generated during

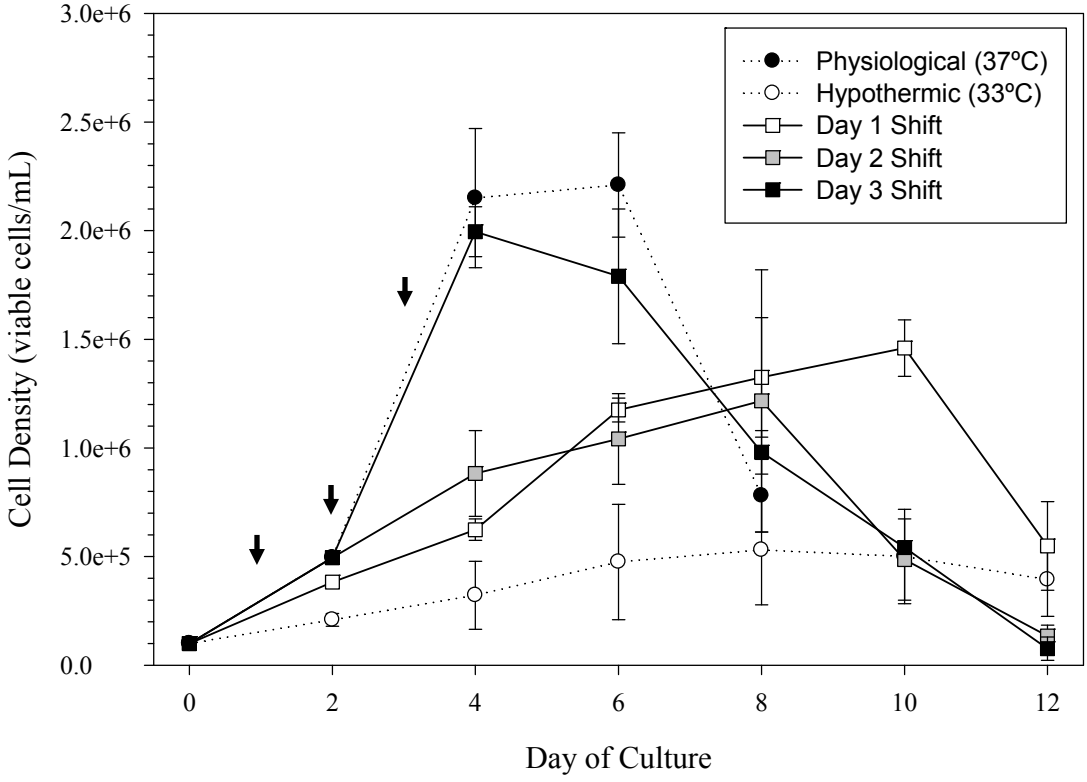

Figure 3.7: Growth response of CHO cells under physiological (37°C), hypothermic (33°C) and temperature-shifted conditions in small-scale (100 mL) agitated cultures. Arrows indicate time of temperature shift. (n = 2 ± standard error).

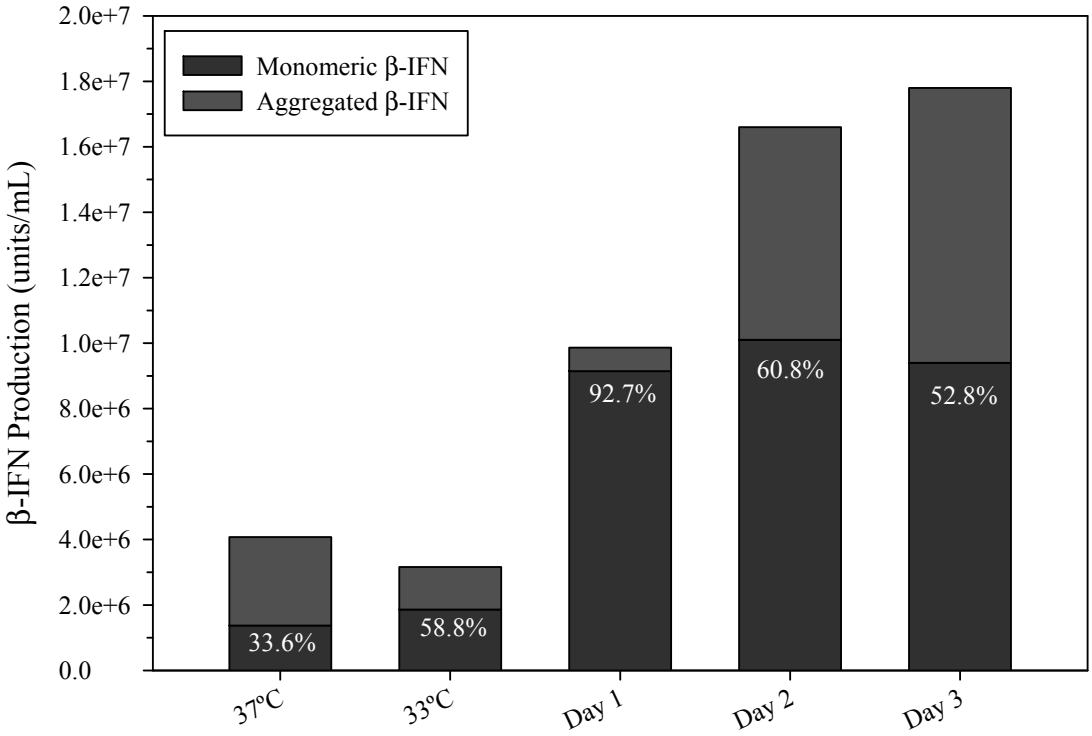

Figure 3.8: Interferon-beta titres (day 8) from physiological (37°C), hypothermic (33°C) and temperature-shifted agitated (100 mL) cultures. Monomeric (black) and aggregated (grey) product concentrations as well as the percent of non-aggregated β-IFN are illustrated.

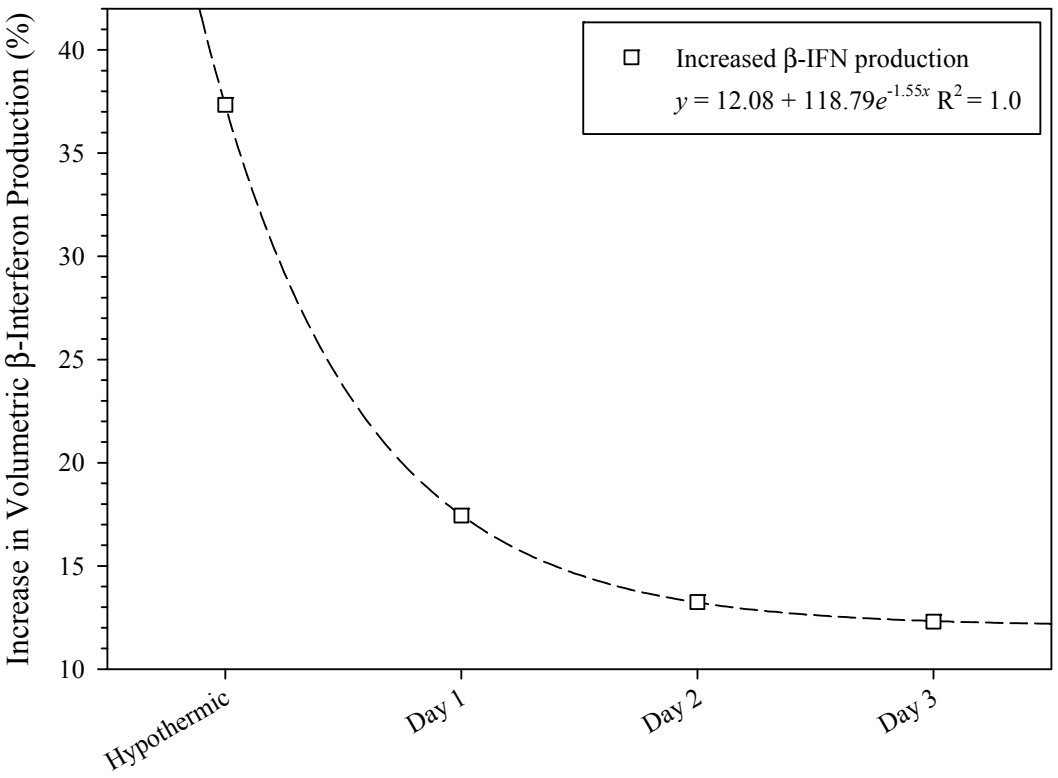

Figure 3.9: The effect of increased T_{shift} on β-IFN production at different culture temperatures (32°C and 33°C). This figure illustrates the increased product titre from culturing the cells at 33°C over 32°C during a series of increasingly delayed temperature shifts. Production enhancement from the increased temperature decreases in response to a delayed T_{shift} when the incubation temperature is raised from 32°C to 33°C; with no significant gain after 48 hours. Product titres were normalized to physiological control cultures. Non-linear (3-parameter exponential decay) regression illustrates the response over increased lengths of the initial culture growth phase (from a non-shifted culture to T_{shift} = 72 hours).

to the induction of the hypothermic production phase. The population generated during the initial physiological growth phase is necessary to maximize the benefit of the enhanced hypothermic Q_P. While the benefits of bi-phasic culturing are multiplied by increased cell titres and an increased rate of hypothermic growth, enhanced growth during a temperature-shifted culture's post-shift hypothermic phase is not due directly to an elevated inoculum upon entering the hypothermic production phase.

To demonstrate this, hypothermic (non-shifted) cultures were inoculated with varying inoculums ($0.1x10^6$ to $1x10^6$ cells/mL) and incubated continuously at 32°C (Figure 3.10A). Regardless of inoculation density, all populations exhibited little or no growth. The populations of inoculated cultures steadily declined at rates between $0.15x10^3$ to $4.91x10^3$ cells/hour; proportional to their initial inoculum. This is in contrast to a temperature-shift (37°C to 32°C; T_{shift} = 48 hours) culture which continued to actively proliferate under hypothermic conditions ($5.62x10^3$ cells/hour) (Figure 3.10B). The significantly different responses of high-inoculum and temperature-shifted cultures demonstrated that the cell density at T_{shift} is not the sole contributing factor to enhanced hypothermic growth within temperature shifts. Inoculating hypothermic cultures at a density equivalent to that of a temperature-shifted population (at time of shift; $0.5x10^6$ cells/mL) did not induce a shift-like growth profile. A moderate hypothermic proliferative response was observed in cultures where the inoculum was not pre-washed in an isotonic phosphate buffered saline solution prior to inoculation (Figure 3.11). After inoculating at $1x10^6$ cells/mL, the unwashed culture increased to $1.7x10^6$ cells/mL

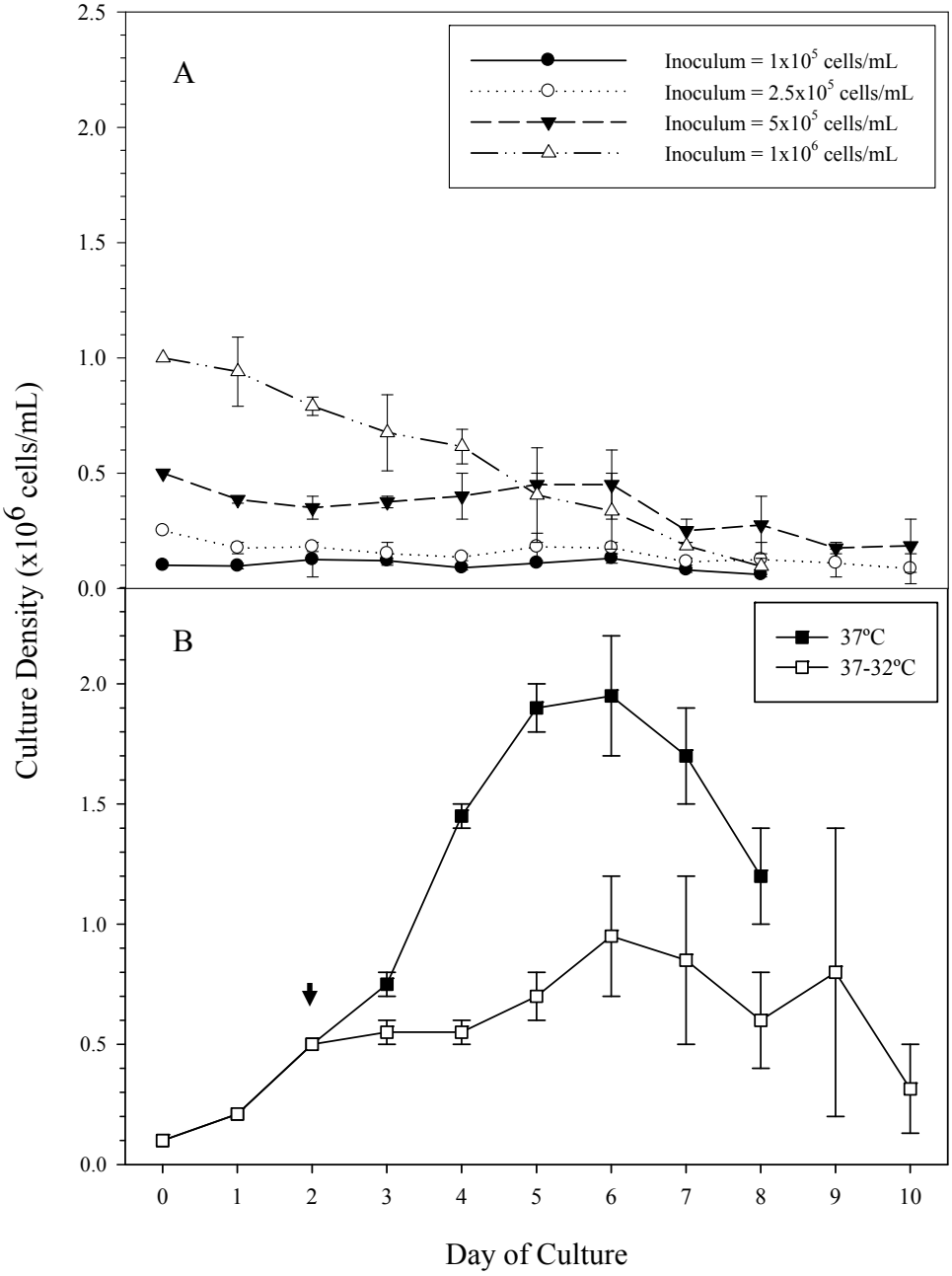

Figure 3.10: The effect of initial inoculum on hypothermic (32°C) culture growth in 100 mL agitated cultures (panel A) compared to physiological (37°C) and temperature-shifted cultures (panel B). Arrow indicates time of temperature shift. (n = 2 ± standard error)

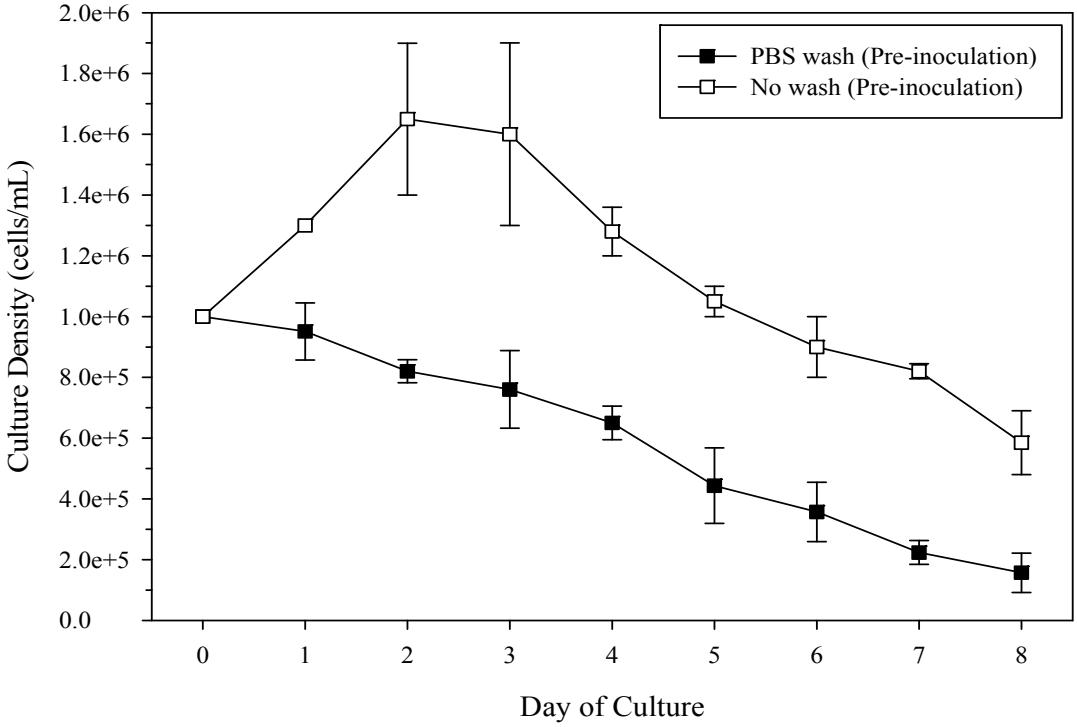

Figure 3.11: Effect of a pre-inoculation wash (isotonic phosphate buffered saline; pH 7.1) on hypothermic (32°C) culture growth. (n = 2 ± standard error).

after 48 hours, before decreasing at a similar rate ($7.3x10^3$ cells/hour) to the PBS-washed culture. This indicates the possibility that in-culture secreted factors, which in this experiment would have been transferred as part of the inoculum, may play a role in active hypothermic proliferation.

Chapter 3.3 – Discussion

3.3.1 – Maximizing Recombinant Protein Expression under Hypothermic Conditions

The development of bioprocesses for the production of β-interferon production was begun as a collaborative research project between our research group at the University of Manitoba (under the supervision of Dr. Michael Butler) and Cangene Corporation. Interferon-beta (Figure 3.12), a class I interferon, is a hydrophobic cytokine involved in the innate anti-viral immune response and used therapeutically in the treatment of multiple sclerosis (by limiting the interaction of activated T-cells with the central nervous system)(117).

3.3.2 – Hypothermic Growth and Optimization of Bi-phasic Bioprocesses through the Induction of Hypothermic Temperature Shifts

High yields of recombinant protein were obtained through a bi-phasic culture strategy involving a temperature shift from a physiological temperature (37ºC) to hypothermic temperatures; increasing cell specific productivity (Q_P) (94). The ability to attain high

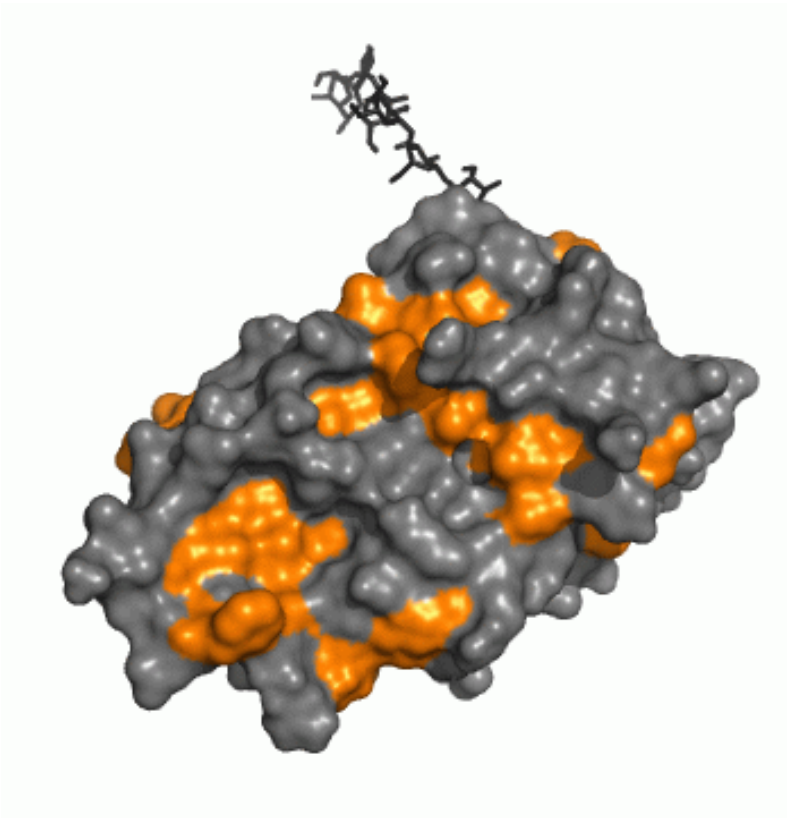

Figure 3.12: Structure (2.2Å resolution) of the Human β-interferon glycoprotein monomer. Hydrophobic residues are indicated in orange. Based on the structure of Karpusas et al. 1997; PBD 1au1 (1) and rendered using PyMOL molecular visualization software.

product titres is dependent upon the balance of the internal state of the cell as well as the timing and magnitude of the temperature change (118).

3.3.2.1 – Improving β-IFN Product Quality through Hypothermic Production Strategies

Immediately upon exposure to near hypothermic temperatures (30°C – 33°C) cell proliferation was dramatically reduced. The reduction in cell growth was proportional to the decrease in culture temperature; following a sigmoidal relationship (Figure 3.1). Incubation between 30°C and 32°C resulted in a nearly complete growth arrest. Between 34°C and 37°C proliferation approached physiological rates, while 33°C represented a mid-point between the two ranges (Figure 3.2). This illustrates how temperature can be used as a parameter to influence cell growth in-culture.

Also induced under hypothermic conditions was a general down-regulation of cap-dependent protein translation; believed to be the initiating response of the low temperature cellular response. β-interferon, typical of heterologous products, was among a population of genes(62) up-regulated in response to mild cold-shock. Internal ribosome entry sites (IRES) are believed to allow these genes to circumvent the cell-wide down-regulation of translation, and have been engineered into recombinant expression vectors for this purpose(119). The exact molecular connections between the detection of decreased environmental temperature, non-specific down-regulated cap-dependent translation, cellular growth arrest and the up-regulation of IRES-specific transcripts is still not understood; however from the perspective of recombinant protein manufacturing these systems can be manipulated to favour increased production.

The effect of the cap-independent increase of β-IFN formation was significant. The cellular rate of β-IFN production (Q_P) increased 2-fold, comparable to productivities of many published hypothermic production strategies (Table 1.2). Product titres increased accordingly to the increased Q_P, however the hypothermic conditions decreased cell proliferation dramatically (approximately 2.5-fold more than production was increased). Although total product yields did not exceed physiological yields at any of the hypothermic temperatures investigated; product quality must be considered when evaluating interferon titres. Aggregated interferon monomers cannot be employed therapeutically; therefore only increases in monomeric (non-aggregated) β-IFN represent biotechnologically relevant improvements.

A further advantage of low temperature cultivation on the production of β-IFN is the reduction of the intermolecular aggregation of the protein product. Aggregation is caused by interactions between the hydrophobic monomers, attempting to sequester their external non-polar residues (represented in orange in Figure 3.11) from their aqueous environment. This results in aggregates which are ineffective as therapeutic agents (116). In our system, aggregation is monitored by a reduction in the ELISA response as the epitopes become unavailable for binding to the detecting antibody, a correlation which has been confirmed through SDS-PAGE and gel permeation chromatography (74). Although the hypothermic conditions cannot prevent aggregation, they can increase the threshold of product concentration or residence time at which molecular aggregation occurs (74). This relationship (Figure 3.3) demonstrates that production under increasingly hypothermic environments results in decreased in-culture aggregation, and is

further illustrated in Figures 3.6 and 3.8 where monomeric β-IFN approximately meets or exceeds physiological production at 32°C or 33°C respectively; despite significantly reduced overall product titres (and concurrent with dramatically reduced cell growth)..

3.3.2.2 – Circumventing Hypothermic Growth Arrest with Bi-phasic Bioprocesses

The combining of physiological and hypothermic phases within a single culture is capable of inducing near physiological growth while maintaining the enhanced productivity of low temperature cultures. Manipulating the balance between these two phases, through adjusting the time of the temperature shift (T_{shift}), provides a culture parameter which allows an essentially seamless transition between hypothermic and physiological proliferation (Figure 3.4). The mechanism through which the physiological growth phase alleviates G1-growth arrest is still not understood. As physiological cultures remain proliferative throughout the length of their culture, a significant portion of their cells have been found to reside in S-phase. However in both temperature-shifted and hypothermic cultures the percentage of S-phase cells was very low (below 5% in bi-phasic cultures and lower within non-shifted). This was proportional to their rate of cell growth, and concurrent with increasing G1-arrested cells (78). It can only be assumed that during the initial physiological period the cells accumulated unidentified factors which allowed for sustained proliferation into the hypothermic phase.

3.3.2.3 – Increased Bi-phasic Growth is not a Factor of Increased Biomass at Time of Shift

As the initial culture inoculations and hypothermic temperature shifts both occur while the cells are undergoing exponential growth; there appears to be few remarkable differences between a (non-shifted) hypothermic culture and a bi-phasic culture except for the cell density at the time of initial hypothermic exposure. Hypothermic cultures within this work (unless otherwise described) were inoculated with a population of cells harvested from a culture maintained at 37°C ($1x10^5$ cells/mL). Bi-phasic cultures were initiated using identical inoculums; however the cells were maintained for an additional 24 to 72 hours at 37°C prior to hypothermic exposure. As the shift occurred during exponential cell growth, from the perspective of cells within the hypothermic phase of a bi-phasic culture, it could appear indistinguishable to a non-shifted 32°C culture inoculated at a higher cell density (typically around $5x10^5$ cells/mL).

To determine whether the enhanced hypothermic growth exhibited during the production phase was attributed to this, hypothermic cultures were inoculated at varying cell densities; from $1x10^5$ to $1x10^6$ cells/mL. Unlike the hypothermic production phase of a temperature-shift culture; all hypothermic cultures, regardless of inoculum exhibited no significant proliferation at sub-physiological temperatures. Therefore it must be concluded that the effectiveness of the bi-phasic culture system is not a result of entering hypothermic state with an increased culture biomass. Other factors which have been hypothesized to aid cell proliferation during sub-physiological temperatures, such as

cellular energy state (adenylate energy charge) were not found to be affected by low temperature exposure(78).

Throughout the cultures described in this thesis, subculturing occurred through the inoculation of new cultures with an inoculum harvested from a viable, exponentially growing population of cells. The cells were then washed in an isotonic solution of phosphate buffered saline, resuspended in fresh media, and diluted to a concentration of $1x10^5$ cells/mL. Inoculums which were not washed; removed from viable cultures and immediately resuspended into new media exhibited a short period of active hypothermic growth (Figure 3.11). It is apparent that inoculum volume (approximately 0.5 to 1 mL), carried over from the preceding culture, contains secreted factors which increased proliferation under hypothermic conditions. Although these factors remain unidentified, their mitogenic effects were completely absent once the inoculum was washed and resuspended in fresh media. Characterization of these factors and their effect on cell proliferation remains an unexplored aspect of hypothermic bioprocesses which could aid in the development of low temperature-specific media formulations, further increasing recombinant protein titres.

Chapter 4 – The Adaptation of Recombinant CHO Cells to Hypothermic Temperatures to Enhance Heterologous Protein Expression

Chapter 4.1 – Introduction

Chinese hamster ovary cells, typical of all cells of mammalian origin, are capable of their maximum cellular growth at physiological (37°C) temperatures. Reducing their environmental temperature proportionally reduces cell growth through the range of mild-hypothermic temperatures (30°C through 35°C). This hypothermic growth arrest is induced through an active mechanism of cell cycle regulation; inducing arrest at the G1/S checkpoint and concurrently increasing heterologous protein expression.

Chapter 4.2 – Results

Despite increased hypothermic proliferation during post-shift production phases (5-fold greater than non-shifted hypothermic cultures), growth was still significantly reduced from physiological conditions (μ = 0.0067 and 0.0307 respectively). The limiting effect of cold-induced growth reduction on recombinant protein expression could be alleviated through the culturing of cells inherently capable of further enhanced hypothermic growth. The isolation of cells which were capable of active hypothermic growth would likely select for cells with comprised cell cycle regulation; allowing for growth at otherwise inhibitory temperatures.

4.2.1 – Growth Properties of Cold-Adapted Cell Lines

Two populations of cold-adapted cells were isolated which exhibited enhanced and sustained growth at hypothermic temperatures (32ºC). To achieve this, parallel subcultures of a β-IFN-producing CHO cell line (maintained at 37°C) were cultured continuously for 400 days (50 eight-day passages) under hypothermic conditions (32°C) in 75 cm^2 (non-agitated) T-flasks. Their response to low temperature selection was characterized in three distinct phases: (I) an initial pre-adaptation phase, (II) an "adapted" phase during which the cells exhibited stable growth (μ) and specific productivity (Q_P), and (III) a final phase during which growth and production rates began to fluctuate dramatically.

Both β-IFN-producing populations exhibited a similar adaptation response. This is in contrast to a population of ATCC purchased tissue plasminogen activator (t-Pa)-producing CHO cells which underwent the same hypothermic selective process yet no successful isolation was achieved.

4.2.1.1 – β-IFN Population "A" Growth and Production Kinetics throughout the Adaptation Process

During the initial pre-adaptation phase (phase I; passages 1 to 12) the first of the two β-IFN adapted populations ("Population A") immediately exhibited a reduced growth rate ($\mu = 0.007\ h^{-1}$) compared to 0.034 h^{-1} at 37ºC, and a 3.3-fold enhanced Q_P over 37ºC (Q_P = 1.383 and 0.419 units/cells per day respectively). This response was typical of recombinant CHO cells lines cultured under mild hypothermic conditions(94). In the

subsequent four passages μ decreased further, correlating with a dramatic rise in Q_P. By the fifth passage μ had decreased nearly 5-fold, while Q_P increased approximately 2-fold (Figure 4.1A and 4.2A). After this initial period (phase I) of low temperature exposure, the cell's rate of growth and recombinant protein expression began to approach levels similar to those during their first hypothermic passage. By passage 12, both μ and Q_P had returned to these initial levels; 0.0125 h^{-1} and 1.031 units/cell per day respectively.

During phase II (passage 12 to 32) the population sustained an enhanced Q_P typical of hypothermic conditions; 1.343 ± 0.390 units/cell per day (Figure 4.2A), while μ gradually increased to a mean value of 0.012 h^{-1}, which was sustained over 20 passages. This period (passages 12 to 32) was designated phase II and chosen to be representative of the cold-adapted cell population "A". The mean growth rate of these cells was almost 2-fold higher than the mean growth rate (0.007 h^{-1}) (Table 4.1) of a comparable set of "non-adapted" cultures growing cells at 32ºC with no previous hypothermic exposure (the inoculum taken directly from a physiological environment). This enhanced growth rate of the cells maintained over phase II was the basis for designating these cells as cold-adapted. The increased growth rate was statistically significant ($P < 0.0001$) and was not associated with a change in specific productivity (Q_P). The effect of cold-adaptation on the growth rate of population "A" is summarized in Table 4.1.

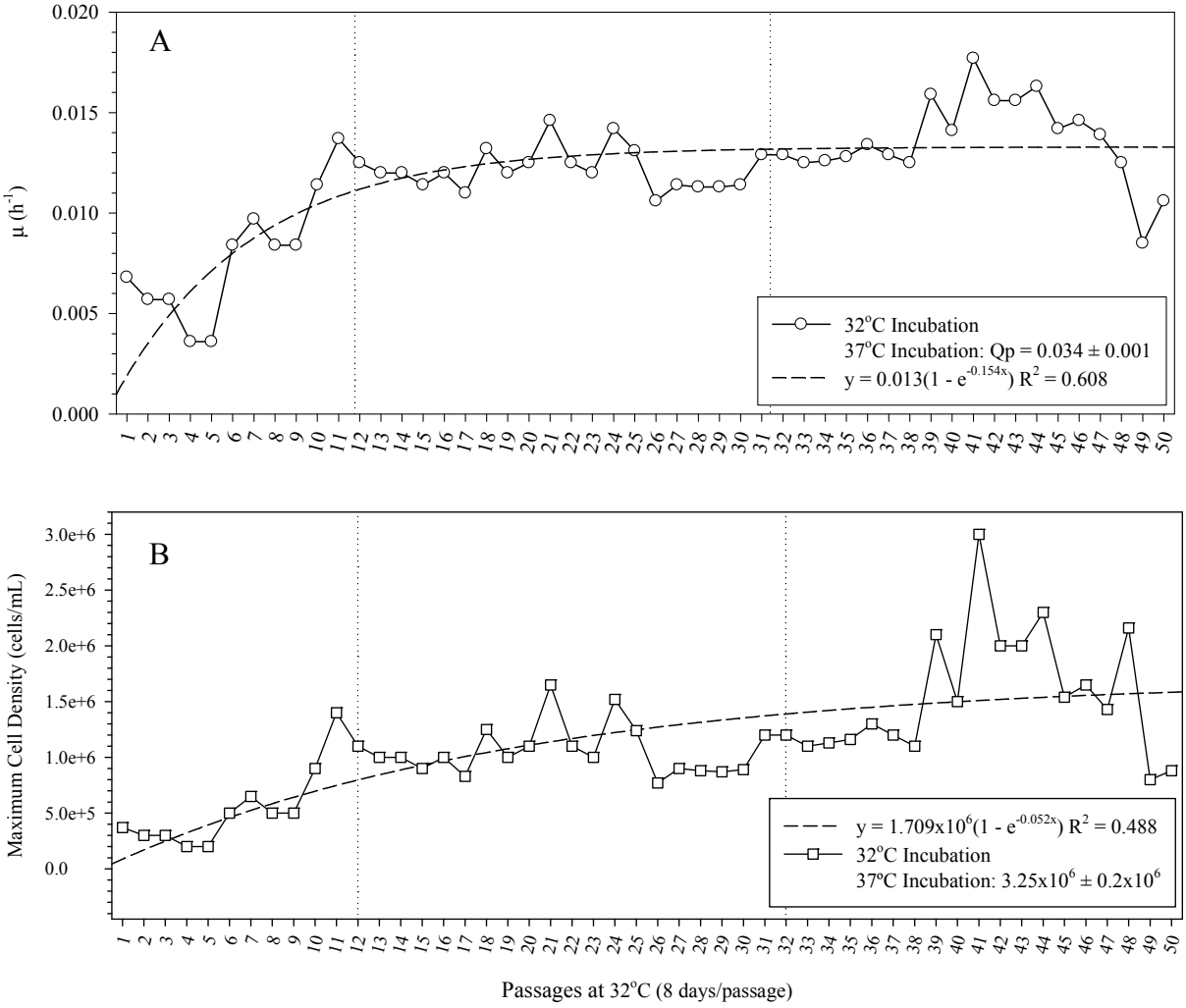

Figure 4.1: Growth rate (panel A) and maximum achieved cell densities (panel B) over the low temperature adaptation process of β-IFN producing adapted population "A". Vertical breaks indicate sub-divisions (phase I, II and III) of the adaptation process.

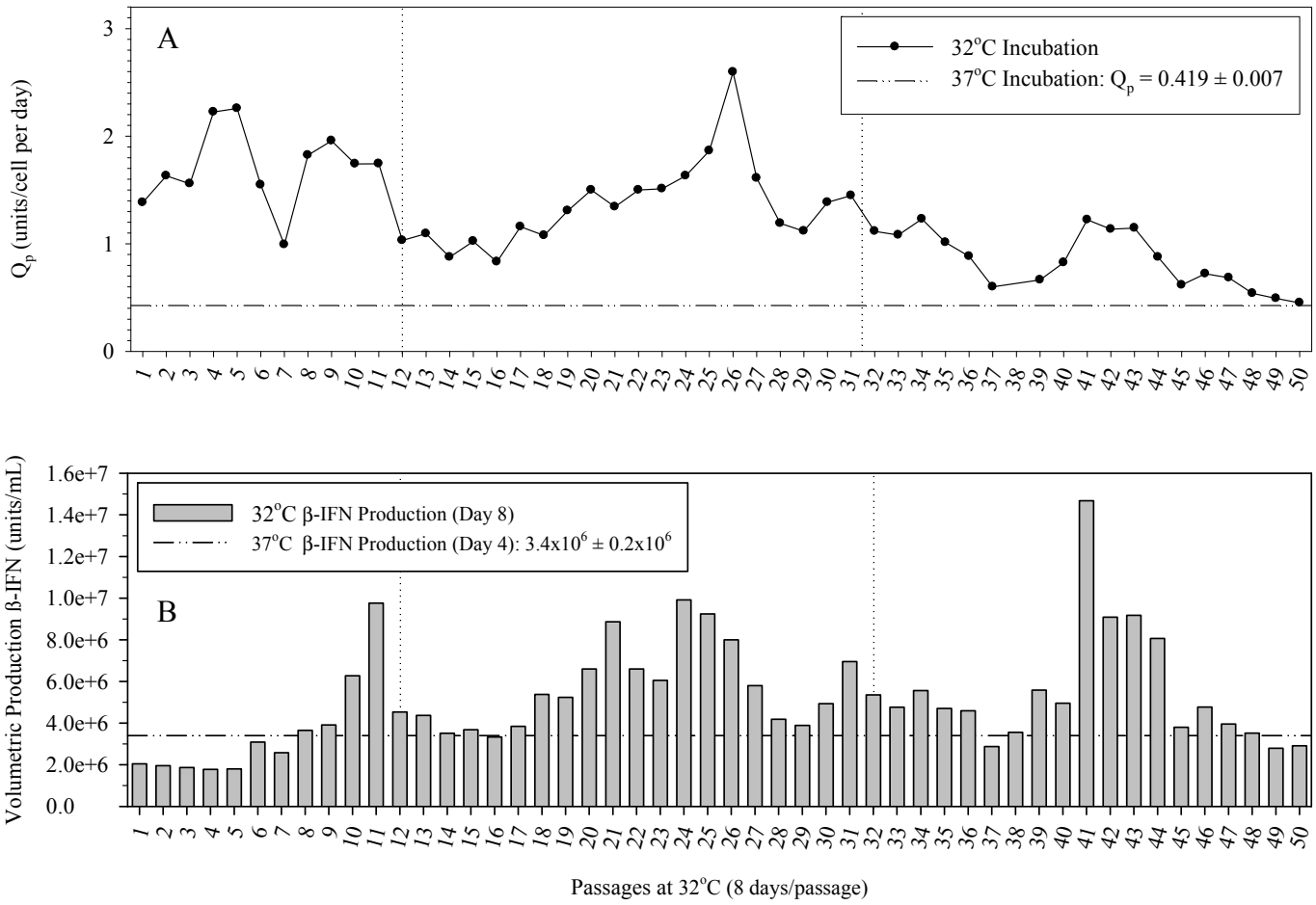

Figure 4.2: Specific (panel A) and volumetric productivities (panel B) achieved throughout the low temperature adaptation process of β-IFN producing population "A". Representative physiological values indicated as dashed line (−···). Vertical breaks indicate sub-divisions (phase I, II and III) of the adaptation process.

Throughout phase III (passages 33 through 50) μ remained elevated (increasing 1.5-fold to a maximum of 0.018 h^{-1} at passage 41), however specific β-IFN production was inconsistent and decreased nearly 70% by end of the adaptation process. This indicated that phase II of the adaptation process; which exhibited stable, predictable and enhanced protein expression, is the preferred window of passages from which further characterization should be performed.

4.2.1.1 – Cell and Recombinant Protein Yields of the β–IFN-Producing Population "A" in Response to Sustained Low Temperature Growth

Under hypothermic conditions both the non-adapted and cold-adapted population "A" maintained a Q_P at least 2-fold greater than that of a non-adapted culture under physiological conditions (Table 4.1). Both populations sustained a Q_P at 32°C of 0.805 ± 0.013 and 1.343 ± 0.390 units/cells per day respectively which was significantly increased from that of a physiological population (0.419 ± 0.007 units/cells per day; $P < 0.0001$).

The volumetric protein yield generally increased with increased hypothermic exposure, reaching a maxima of 1.4×10^7 units/mL at passage 41 (Figure 4.2B). This also corresponded to the highest recorded cell yield (3.0×10^6 cells/mL; Figure 4.1B). These high product titres and cell densities were observed in within phase III, however during this phase yields were not sustained and product expression quickly declined due to decreasing Q_P.

4.2.1.3 – β-IFN Population "B" Growth and Production Kinetics throughout the Adaptation Process

The second population (population "B") of the two β-IFN-producing CHO cells subjected to cold-adaptation exhibited a very similar response to extended low temperature cultivation. The growth response during phase I (passages 1 – 12) mirrored that of population "A"; a 5-fold reduced growth rate compared to physiological cultures (0.007 h^{-1} and 0.034 h^{-1} respectively) and a 2.8-fold increase in the Q_P of β-IFN (1.193 from 0.419 units/cell per day). Cell proliferation continued to decrease, reaching a minimum of 0.002 h^{-1} (passage 3), before increasing and surpassing the initial low temperature response by nearly 2-fold. The adapted population achieved a stable growth rate of 0.012 h^{-1} by passage 12, which was maintained into phase II (Figure 4.3A).

Specific β-IFN production further increased 2.3-fold to 2.795 units/cell per day during the first five low temperature passages (40 days), however returned to its initial levels prior to phase II (Figure 4.4A).

During phase II μ and Q_P remained stable (0.012 ± 0.001 h^{-1} and 0.868 ± 0.035 units/cell per day) (Table 4.1). The growth rates of both population "A" and "B" were identical; although the specific β-IFN of population "B" was 35% lower. Despite a decreased rate of product expression, the productivity of population "B" was more stable; with 10-fold less variability between passages (standard deviations of 0.390 and 0.035 respectively). Due to this stability; with variations of less than 8% (μ) and 4% (Q_P), phase II cells from

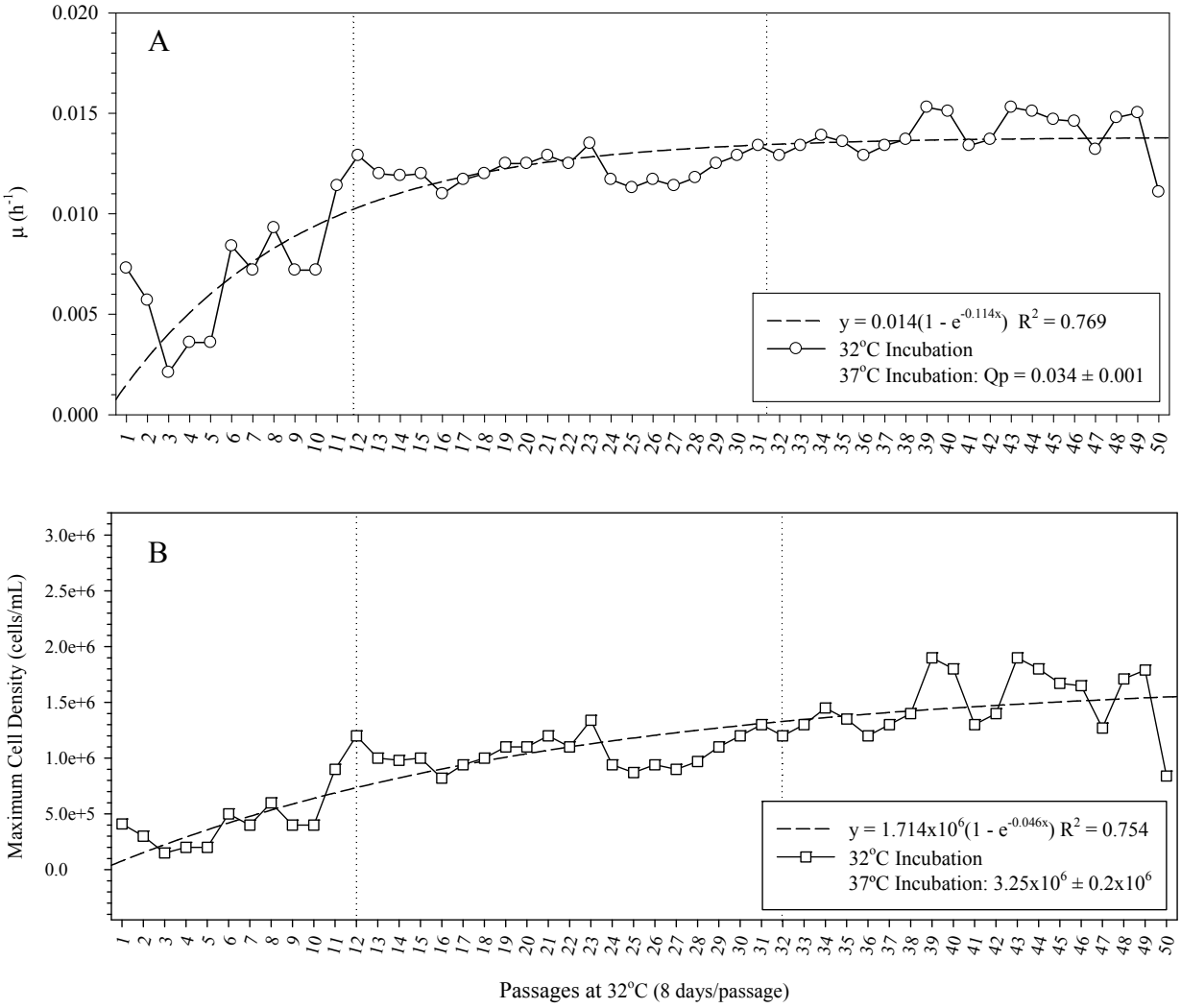

Figure 4.3: Growth rate (panel A) and maximum achieved cell densities (panel B) over the low temperature adaptation process of adapted β-IFN producing population "B". Vertical breaks indicate sub-divisions (phase I, II and III) of the adaptation process.

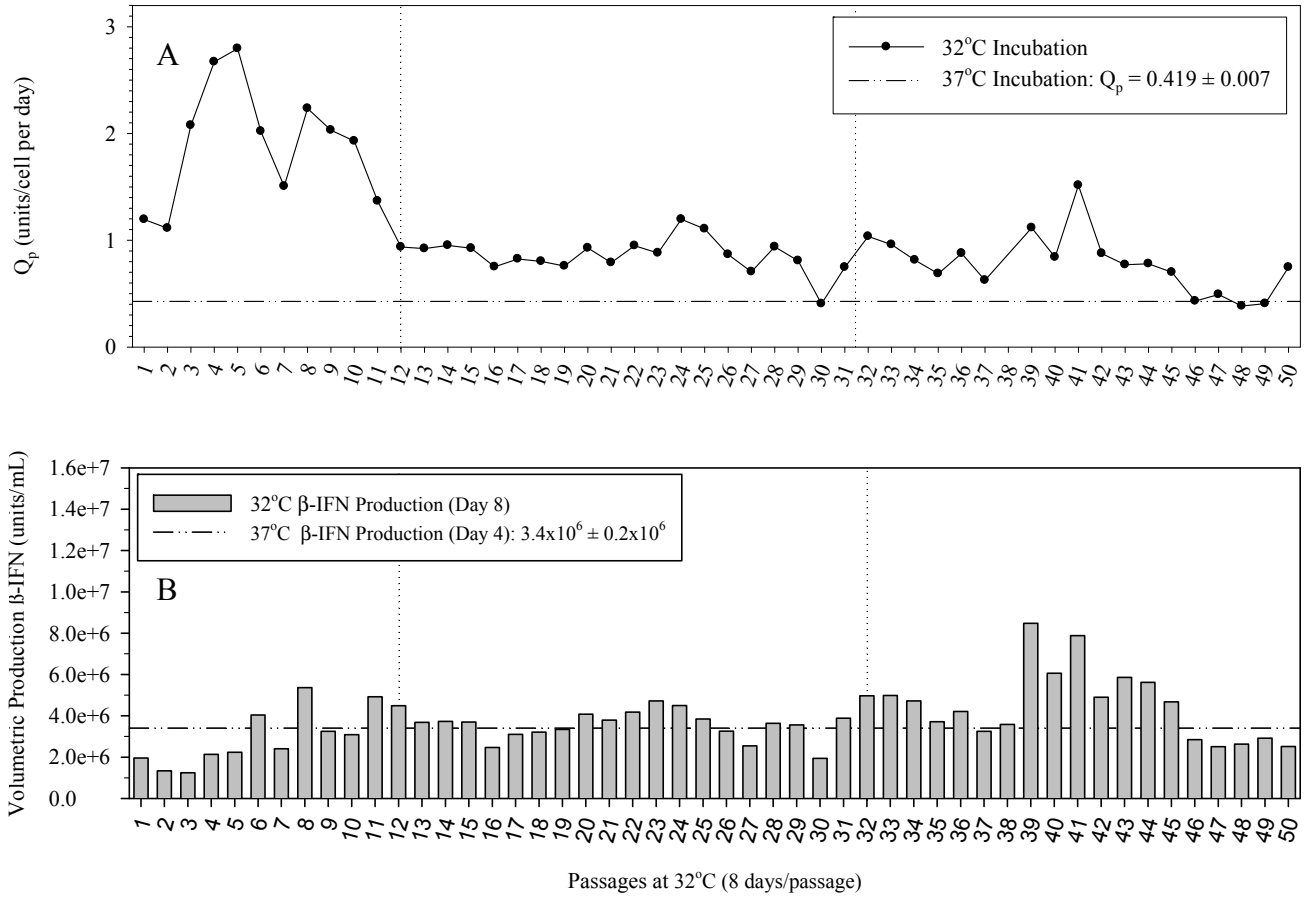

Figure 4.4: Specific (panel A) and volumetric productivities (panel B) achieved throughout the low temperature adaptation process of β–IFN producing population "B". Representative physiological values indicated as dashed line (– · · –). Vertical breaks indicate sub-divisions (phase I, II and III) of the adaptation process.

Table 4.1: Effect of Low Temperature Adaptation on μ, Q_P and maximum volumetric productivity of β-IFN-producing cells in stationary cultures

Culture	**Temperature (ºC)**	**Growth Rate μ (h^{-1})**	**Specific Productivity Q_P (units/cell per day)**	**Total Volumetric Production (units/mL) ‡**
Non-adapted	37ºC	0.034 ± 0.001	0.419 ± 0.007	$3.40x10^6$
	32ºC	0.007 ± 0.002	0.805 ± 0.013	$2.72x10^6$
Adapted †	32ºC *A*	0.012 ± 0.001	1.343 ± 0.390	$5.72x10^6$
	B	0.012 ± 0.001	0.868 ± 0.035	$5.77x10^6$

† Values based on averages of cultures during phase 2 (n = 20)
‡ Based on culture lengths of four and twelve days for 37ºC and 32ºC respectively
A, *B* indicate two individual isolated cold-adapted cell populations

population "B" were selected to be representative of cold-adapted cells for all subsequent characterization and experimentation. Table 4.1 summarizes the growth and production kinetics of this population.

Phase III cultures, similar to their counterparts in population "A", exhibited increased instability in cellular growth (although to a lesser extent than in population "A") (Figures 4.3A and 4.1A). Specific productivity declined throughout phase III, reaching a minimum of 0.384 units/cell per day (passage 48) (Figure 4.4A).

4.2.1.4 – Cell and Recombinant Protein Yields of the β–IFN-Producing Population "B" in Response to Sustained Low Temperature Growth

Maximum cell yields at each passage were consistent throughout phase II ($1.06x10^6 \pm 0.14x10^6$ cells/mL), peaking at $1.34x10^6$ cells/mL (passage 24) (Figure 4.3B). Fluctuations in β-interferon yields were therefore proportional to changes in Q_P, which during phase II and the majority of phase III exceeded the production of a physiological CHO culture (Figure 4.4B). This demonstrates that the loss of specific productivity during late phase III lead to substantially reduced protein titres, emphasizing the importance of stable cellular Q_P and the selection of phase II cells in overall bioprocess design.

4.2.1.5 – Growth and Production Kinetics of t-PA-Producing CHO Cells during Sustained Low Temperature Exposure

Contrary to the adaptation response observed in β-interferon cell lines, prolonged hypothermic culturing of a t-PA-producing CHO cell line failed to select for enhanced low temperature growth.

Immediately following incubation at 32°C the growth rate of the t-PA-producing population was reduced nearly 50% to 0.008 h^{-1} (from 0.017 h^{-1} at 37°C). Over subsequent passages μ was further reduced to below zero levels (at passage 6), where after 8 days there were fewer cells in culture than in the initial inoculum. Following this minimum the growth rate recovered to initial hypothermic levels (increasing to 0.008 h^{-1} by passage 10). Although this response is typical of hypothermic growth and mirrored the responses of both β-interferon lines; unlike the β-IFN populations, μ decreased again to 0.002 h^{-1} and did not recover from this level of near-zero growth (Figure 4.5A)

Specific t-PA production also initially followed a typical hypothermic response. Productivity was increased 4-fold following initial low temperature exposure, and followed μ in an inversely proportional manner (increasing another 430% by passage 4). However following this maximum, Q_P dramatically decreased to near zero levels during the next passage, resulting in essentially no t-PA production. (0.4 units of t-PA/cell·day) (Figure 4.6A)

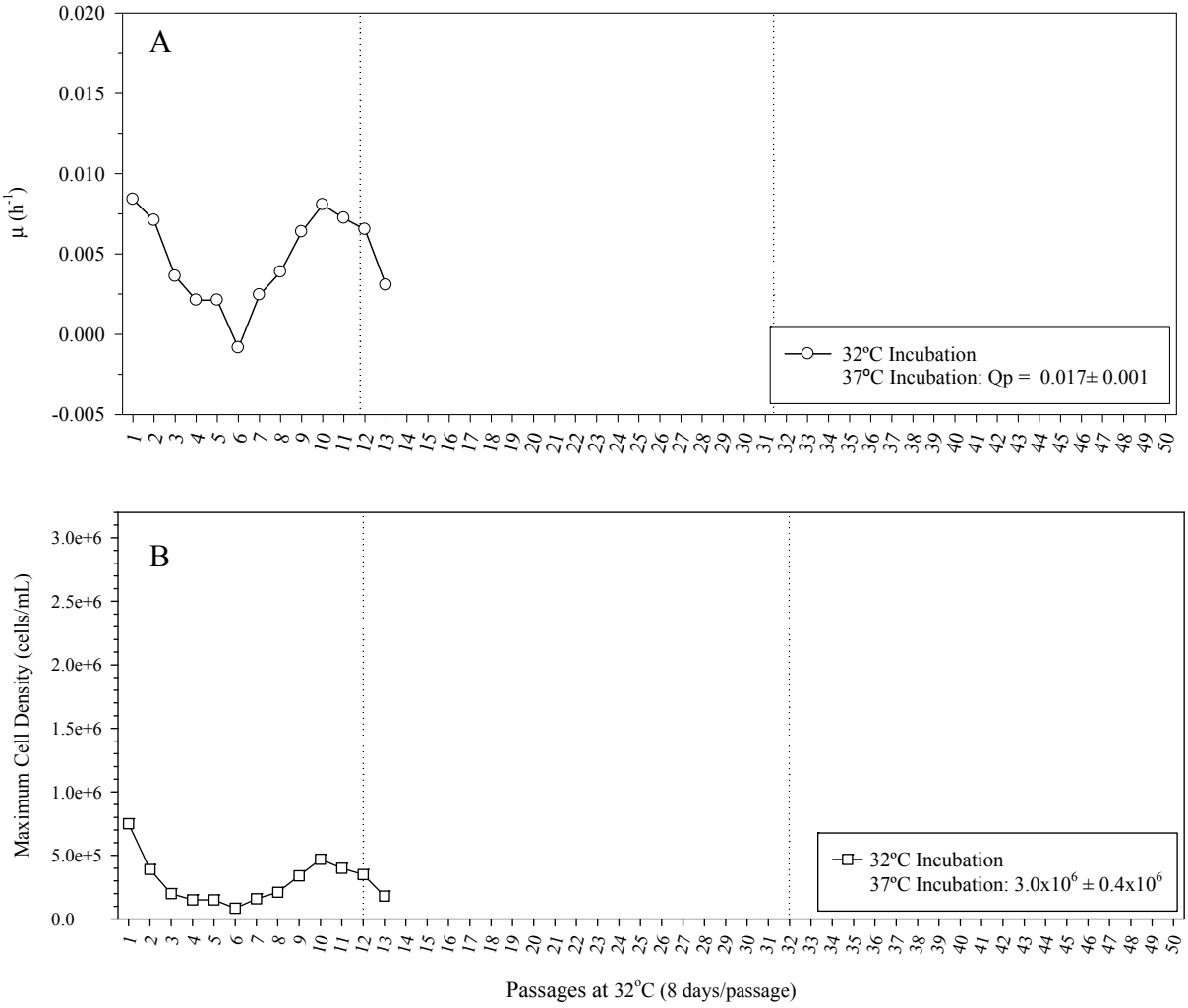

Figure 4.5: Growth rate (panel A) and maximum cell densities (panel B) achieved over the low temperature adaptation process of a t-PA-producing CHO cell population. Vertical breaks indicate sub-divisions (phase I, II and III) of the adaptation process. Culture terminated at passage 13 due to low cell growth and viability.

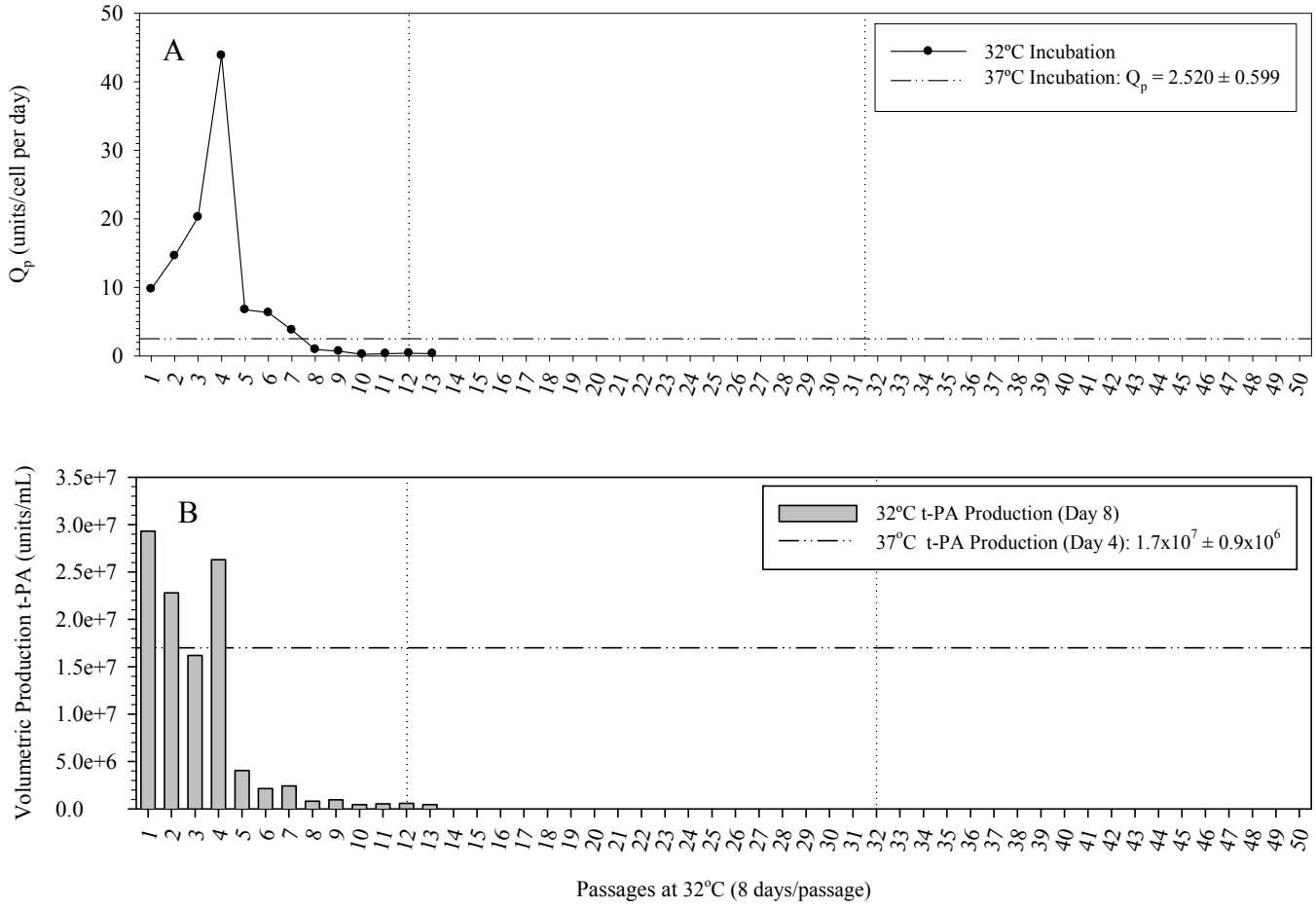

Figure 4.6: Specific (panel A) and volumetric productivities (panel B) achieved throughout the low temperature adaptation process a t-PA-producing population of CHO cells. Representative physiological values indicated as dashed line (– · · -). Vertical breaks indicate sub-divisions (phase I, II and III) of the adaptation process. Culture terminated at passage 13 due to low cell growth and viability.

4.2.1.6 – The Effect of Continuous Low Temperature Growth on Cell and Recombinant Protein Yields of t-PA-Producing CHO Cells

As a result of low temperature growth reduction and the lack of any adaptation response, the t-PA-producing population did not increase in cell yield beyond the initial hypothermic response (reduced 74% from physiological conditions). Cell yields declined 10-fold (from $0.75x10^6$ cells/mL) to a minimum of $0.085x10^6$ cells/mL (at passage 6); the t-PA-producing population then recovered to 60% of its initial hypothermic yield ($0.47x10^6$ cells/mL). However this increase was not sustained; cell yields progressively declined between passage 10 and 14 ($0.18x10^6$ cells/mL) when the adaptation process was discontinued (Figure 4.5B)

Product yields, determined through ELISA assays, were affected two-fold: through the gradual reduction in population densities and the nearly complete loss of specific productivity which occurred at passage 5. Product yields, as a result, immediately dropped to 23% of those of a 37°C culture (which previously had met or exceeded physiological levels). In subsequent passages, titres further decreased to $0.45x10^6$ units/mL (1.5% of initial hypothermic production) (Figure 4.6B). This catastrophic decrease in production resulted in the termination of the adaptation process for this cell population at passage 13.

4.2.2 – Successful Isolation of a Cold-Adapted Population

Based on the growth and production kinetics of the two β-interferon- and the t-PA-producing CHO cells lines, the β-IFN population "B" was selected as a model for further

characterization and bioprocess development. The t-PA-producing cell line was excluded as it did not demonstrate any adaptive properties. Both β-IFN-producing populations exhibited enhanced low temperature growth (increased 1.7-fold over a non-adapted population); however there was significant passage-to-passage variation in the specific productivity of population "A" (± 30%). The β-IFN population "B" was more consistent, 7.5-fold less variable than population "A" (± 4%).

To minimize variations between cultures, the window of passages already described as phase II was defined. This period, mid-way through the adaptation process, demonstrated the most consistent growth and production properties between consecutive passages in both adapted β-IFN cell lines; with population "B" the most consistent of the two. As a result all ensuing experimentation was performed using inoculums harvested from phase II, population "B" cultures. All further references to cold or low-temperature adapted cells will be referring to cells derived this sub-set of the low temperature adaptation process, unless otherwise stated.

4.2.3 – Morphological Changes in Cold-adapted Populations

In addition to affecting cell growth and recombinant protein production kinetics, the low temperature-adaptation process induced changes in other aspects of the population's physiology; including physical alterations to cellular structure.

4.2.3.1 – Cold-adapted Population Significantly Enlarged through Adaptation Process

While monitoring the low temperature-adapted cells in T-flask cultures, it was observed that the cells from the adapted populations appeared enlarged; including a small percentage of cells which were up to 10-fold larger than an average 37ºC cell. The areas of cells from adapted and non-adapted populations grown in stationary cultures were determined microscopically using a differential interference contrast (DIC) equipped Zeiss AxioImager Z1 with a Plan-Apochromat 20x/0.8 objective and AxioVision software (Figure 4.7A). Representative images of the two populations are presented in Figures 4.7B and C.

The size of the cold-adapted cells increased significantly, on average 52% larger and more varied in size than those from the non-adapted population; with an average size of 237.5 ± 139.4 μm^2 compared to 156.2 ± 48.7 μm^2 in the non-adapted population ($P < 0.0001$). Cells as large as 2205 μm^2 in area were observed within the adapted population, although this extraordinarily large phenotype was not representative of the majority of cold-adapted cells. The proportion of cells larger than 1000 μm^2 in area was less than 0.5% of the total adapted population; cells of this size are indicated by arrows in Figure 4.7. There were no cells larger than 500 μm^2 in area observed in any of the non-adapted cultures, while 3.8% of the adapted cells were larger than the largest non-adapted cell.

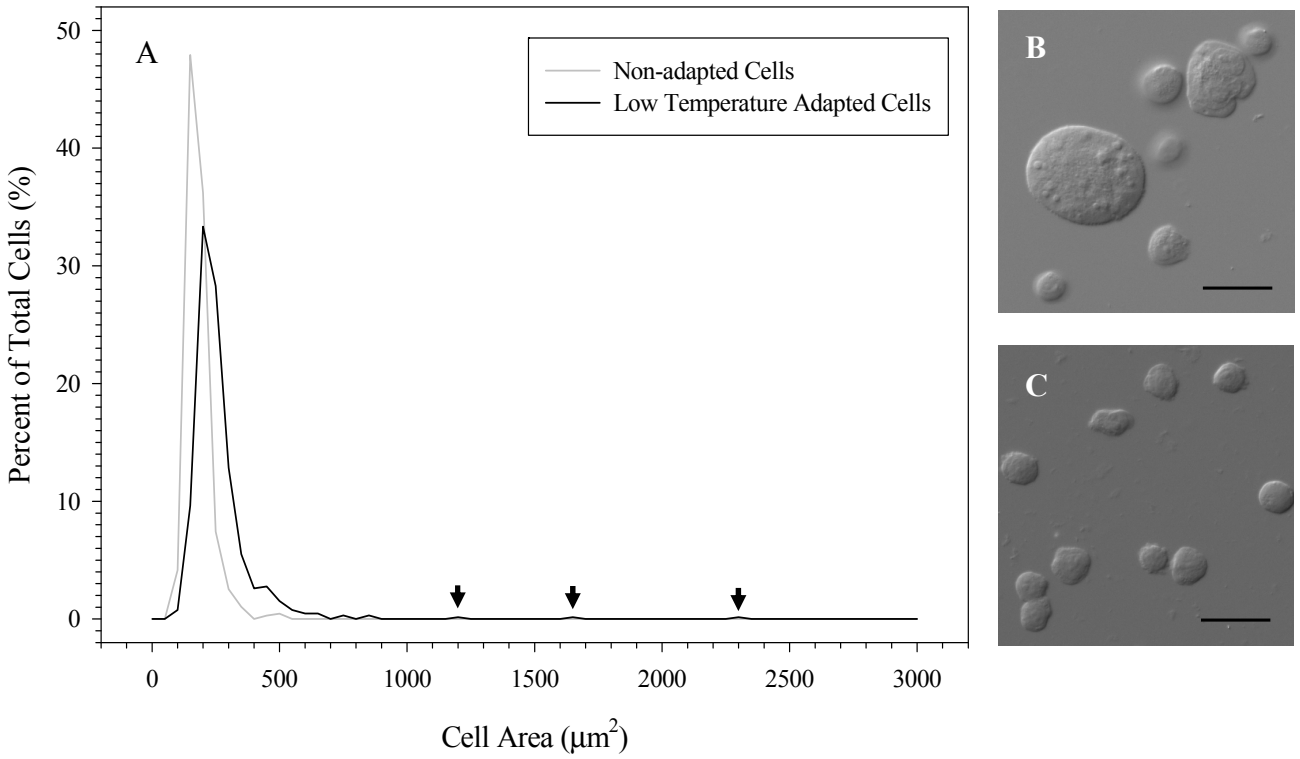

Figure 4.7: Distribution of cell sizes of low temperature-adapted and non-adapted CHO cells (panel A; *n* = approx. 650 cells per group). Arrows indicate presence of atypically enlarged (5-10 fold) cold-adapted cells. Images of low temperature-adapted cells (panel B) and non-adapted cells (panel C) to illustrate the increased variability of the adapted population (Bar = 25 μm).

4.2.3.2 – Enhanced Multi-nucleation/Nuclear Fragmentation within the Population of Low Temperature-Adapted Cells

Within the population of adapted CHO cells it was noticed that in addition to an overall larger cell size, the cells appeared to have either become significantly more multi-nucleated or to have undergone an extensive amount of nuclear fragmentation. The number of nuclei per cell in populations of low temperature-adapted and non-adapted interphase cells is presented in Figure 4.8A.

The adapted population contained significantly more nuclei and/or nuclear fragments per cell ($P < 0.0001$). The non-adapted CHO cell population was predominantly mononucleate, with 87% of the population having only one nucleus. The remainder of the population was binucleate, with less than 2% of the population containing 3 or 4 nuclei or nuclear fragments. No cells in the non-adapted culture were found to contain more than 4 nuclear bodies.

Cells which had been adapted to low temperature growth had a significantly different nucleation profile. While the majority of the cells were still mononucleate, only 64% of the cells had only one nucleus. Approximately 15% of the remaining cells were binucleate, with an additional 10% containing 3 or 4 nuclear bodies. In contrast to the non-adapted population, nearly 10% of the low temperature-adapted cells contained

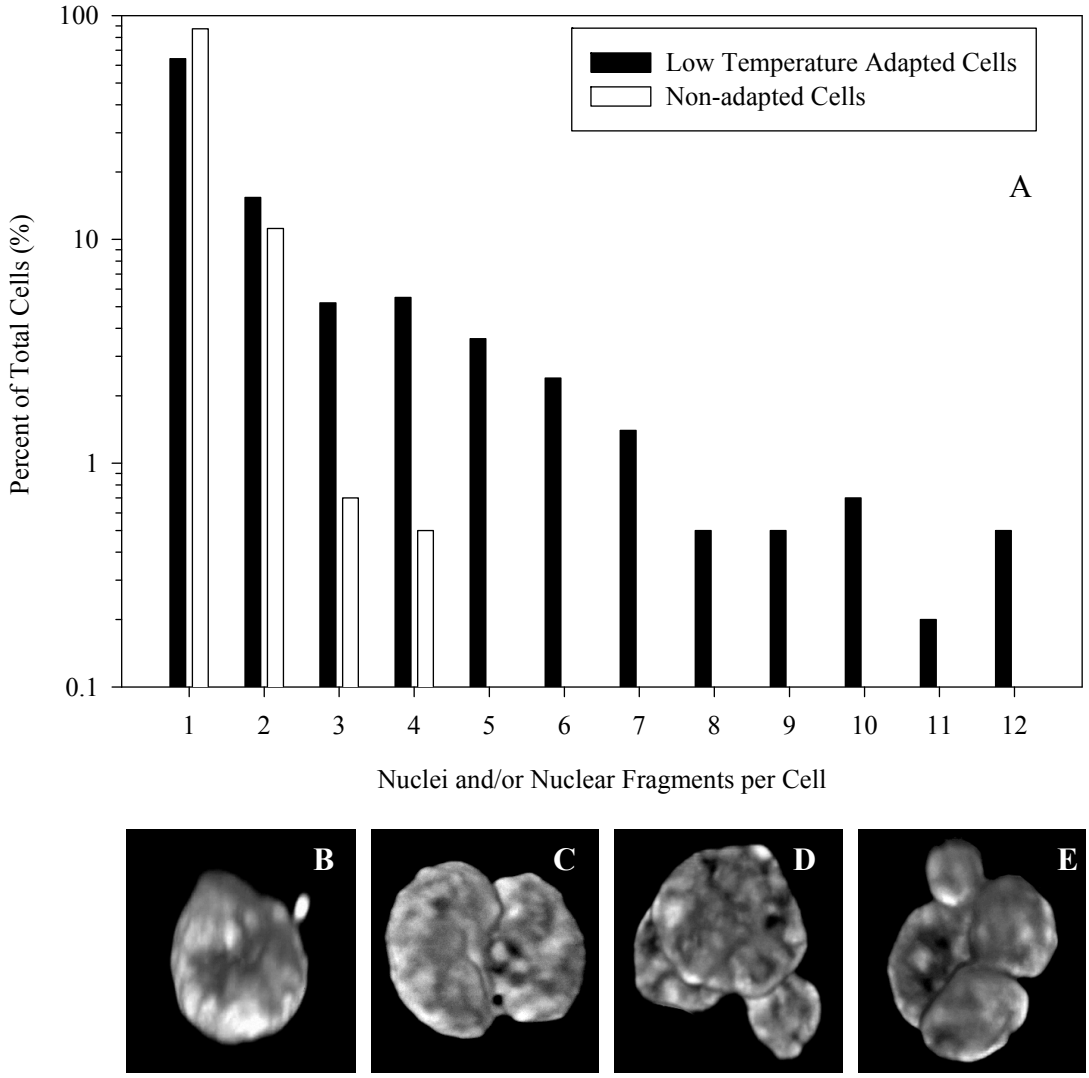

Figure 4.8: Multi-nucleation and/or nuclear fragmentation (panel A) in response to the low temperature adaptation of CHO cells (n = 400 cells per group). 3D reconstructions typical of mononucleate to tetranucleate nuclear complexes are illustrated (panels B through E).

more than 4 nuclei or nuclear fragments. A small proportion of the cell population (<1%) was observed to contain up to 12 nuclei and/or nuclear fragments.

The non-adapted population had on average 1.15 nuclei and/or nuclear fragments per cell, while cells in the adapted cultures contained 1.97, an increase of approximately 70%. 3D reconstructions of DAPI-stained nuclear complexes containing various numbers of nuclear fragments are illustrated in Figure 4.8B through E and again in Figure 4.9 in context with their cellular morphology. These are representative of the populations described within Figure 4.7A, and illustrate both symmetric and asymmetric nuclear fragmentation. The increase in fragmentation may be indicative of elevated rates of genetic instability, improper chromosome segregation, disrupted cytokinesis or overall mitotic failure within a subset of the adapted population (120).

No distinction was made between cells which were fully bi-nucleate, containing a complete additional set of genetic material (a result of completed mitosis and failed cytokinesis) and cells in which their nuclei had fragmented during mitosis into distinct, incomplete nuclear bodies. The terms nuclei, nuclear fragments and nuclear bodies are used interchangeably throughout this section due to this lack of intra-nuclear analysis.

4.2.4 – Proteome Level Analysis of Low Temperature-adaptation Induce Changes

A proteomic-level analysis of adaptation-induced changes was performed, quantifying differential protein expression levels between the two adapted populations and a non-adapted β-interferon-producing CHO population.

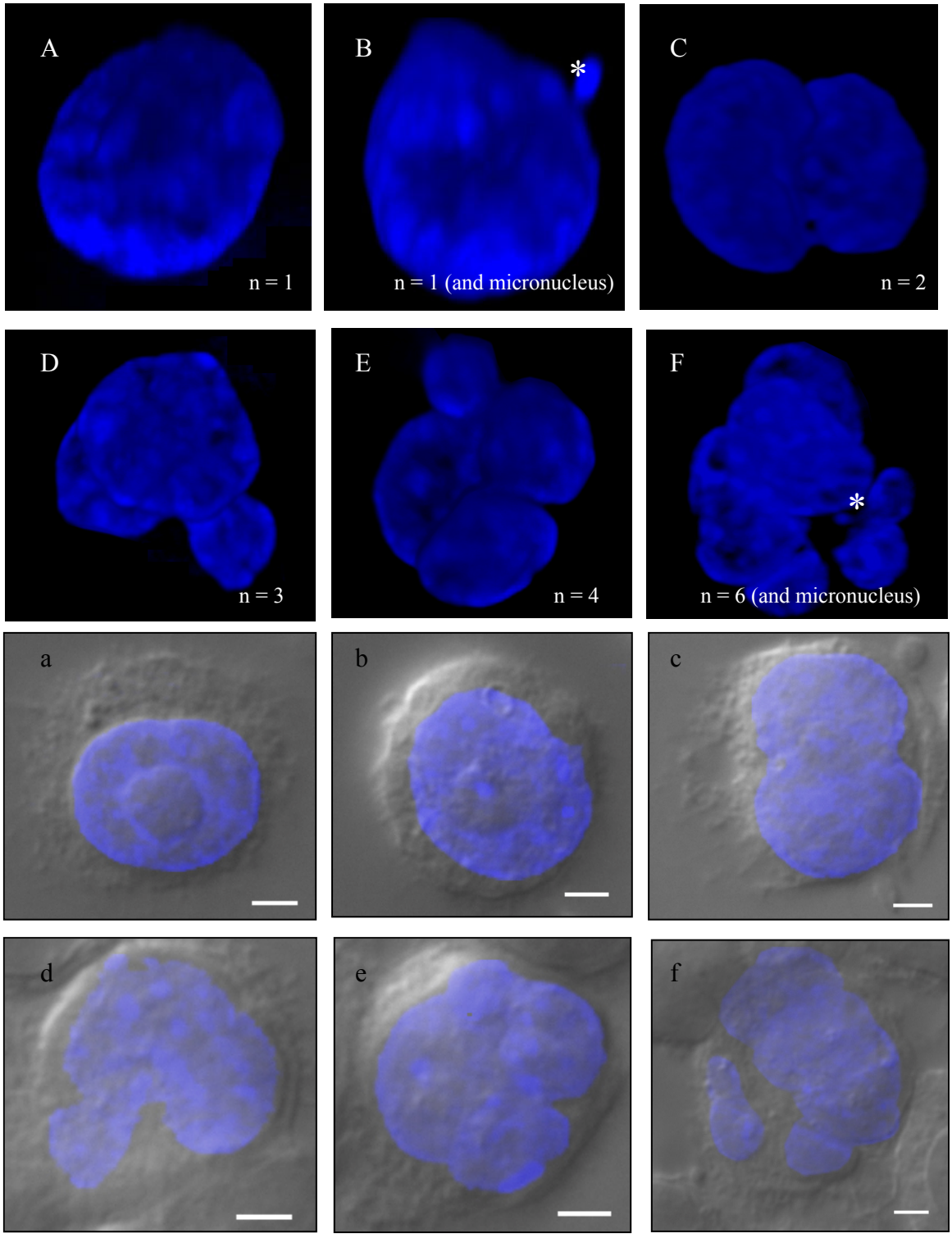

Figure 4.9: 3D representations and 2D micrographs of single and multi-nucleated/fragmented complexes. Panels A through F represent 3D reconstructions of mono- and multinuclear complexes. Asterisks identify presence of micronuclei. Number of distinct nuclear fragments indicated in each frame. 2D micrographs from the represented cells (panels a through f) illustrate relationship between nuclear material (blue) and cell morphology. (Bar = 2 μm)

Two-dimensional fluorescence differential in-gel electrophoresis (DIGE) was employed, allowing a broad-based investigation of expression changes between the populations. Proteins were isolated through two-dimensional electrophoresis; separating based on their apparent molecular weight and isoelectric point (pI) (Figure 4.10) Identities of the proteins which exhibited statistically altered expression levels (T-test calculated p-values < 0.1) were predicted based on the electrophoretic response of a set of internal molecular weight and pI standards.

Electrophoretically isolated proteins which demonstrated similarly altered expression in both adapted populations are described in Table 4.2. Nine statistically significant proteins were detected; identifications of four of these were possible using a 2D electrophoresis map of the Chinese hamster proteome(121). An unidentified heat-shock protein was found to be up-regulated 1.7 and 2.3-fold in both populations of the adapted cells. A second isolate, determined to be either lactate dehydrogenase A (LDH-A) or phosphoribosylpyrophosphate synthetase I was up-regulated 1.3-fold in both populations. The remaining proteins were down-regulated varying degrees (between 1.21 and 1.74-fold); two of these were identified as cytoplasmic dynein intermediate chain 2 homologue and UV excision repair protein.

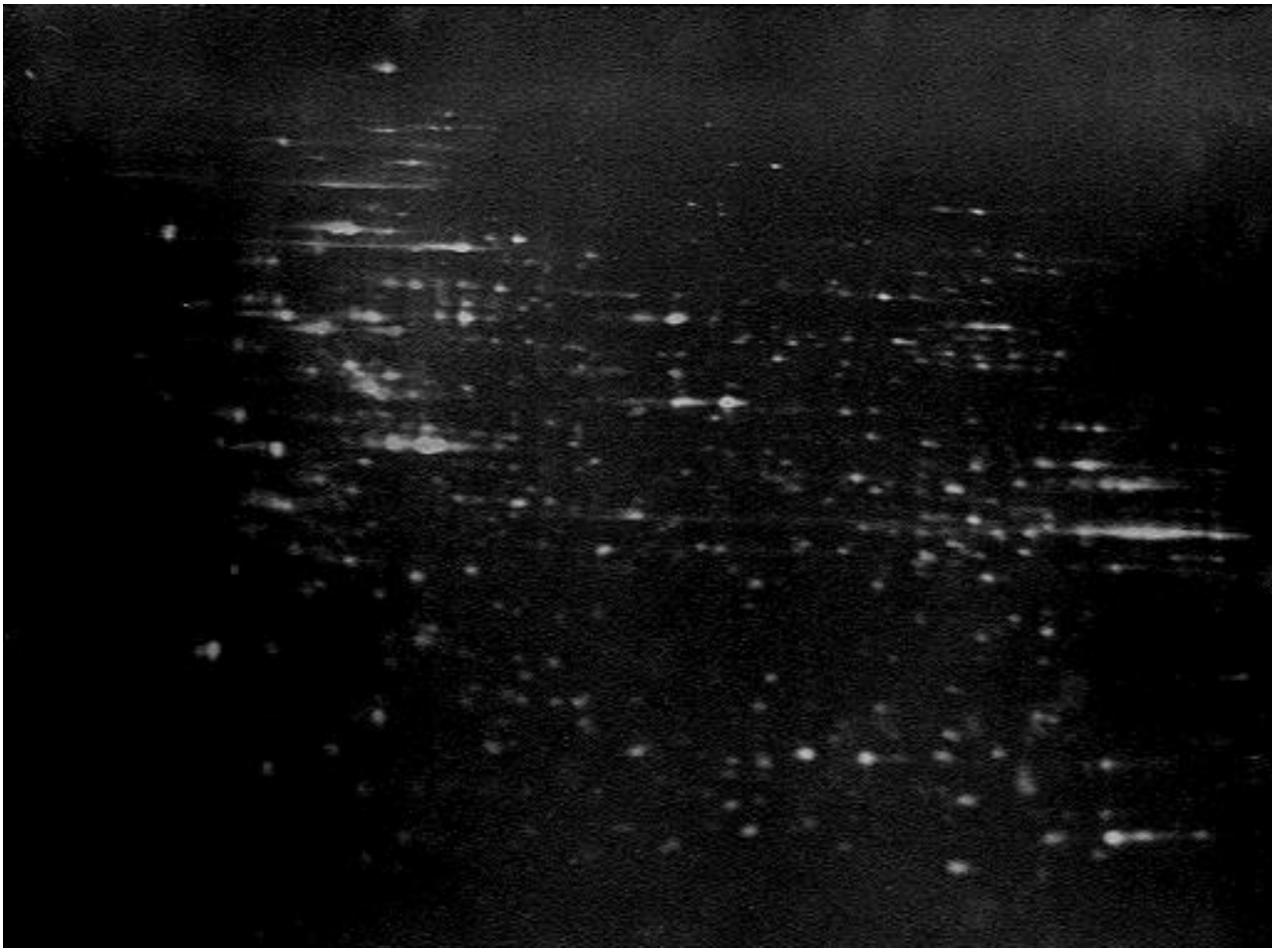

Figure 4.10: Representative 2D-SDS polyacrylamide gel image used for DIGE proteome analysis of adaptation-induced cellular changes. Proteins were separated based on their isoelectric point (X-axis) and molecular weight (Y-axis). Individually resolved spots were detected; their relative abundance quantified and compared to a non-adapted population using DeCyder™ Differential Analysis Software (GE Healthcare). Statistically significant alterations in expression levels are described in Table 4.2.

Table 4.2: Changes in levels of protein expression within the two low temperature-adapted cell populations versus their parental (non-adapted) cell line

Protein ID #	pI / Molecular Weight	Change in Expression (fold) Population A	Population B	Identification
269	5.16/100.0 kDa	1.67	2.28	Unknown heat shock protein
764	5.76/69.7 kDa	-1.45	-1.36	
765	5.65/69.7 kDa	-1.74	-1.52	
803	6.02/48.7 kDa	-1.45	-1.63	
841	5.08/47.8 kDa	-1.74	-1.62	Cytoplasmic Dynein Intermediate Chain 2 Homologue
1093	6.38/53.1 kDa	-1.59	-1.27	
1163	4.78/44.1 kDa	-1.35	-1.21	UV Excision Repair Protein
1909	6.84/20.3 kDa	1.3	1.31	LDH-A or Phosphoribosylpyrophosphate Synthetase I
183	5.90/19.5 kDa	1.93	1.61	

4.2.5 – Adaptation Response is Retained After Re-introduction to Physiological Growth

Successfully adapted cells were re-introduced to physiological temperatures (37°C) to determine whether the adaptation response would be retained in the absence of selective pressure. A population of low temperature-adapted cells was transferred to 37°C after subculturing and maintained at physiological temperatures for three 4-day passages. After each passage the population was divided; maintaining one subculture at 37°C and the second under hypothermic conditions. The cultures were maintained at physiological temperatures for an additional two 8-day passages (Figure 4.11).

After subsequent 37°C passages the maximum physiological cell yields of each adapted culture increased; reaching that of a typical non-adapted culture ($3.6x10^6$ and $3.25x10^6$ cells/mL respectively). The low temperature-adapted response was maintained in all populations after re-introduction to 32°C, regardless of the duration of physiological exposure (4 to 12 days). Cells continued to reach maximum cell yields 5-fold greater than a typical non-adapted hypothermic culture ($1.53x10^6$ and $0.33x10^6$ cells/mL respectively) for two 8-day passages after re-introduction.

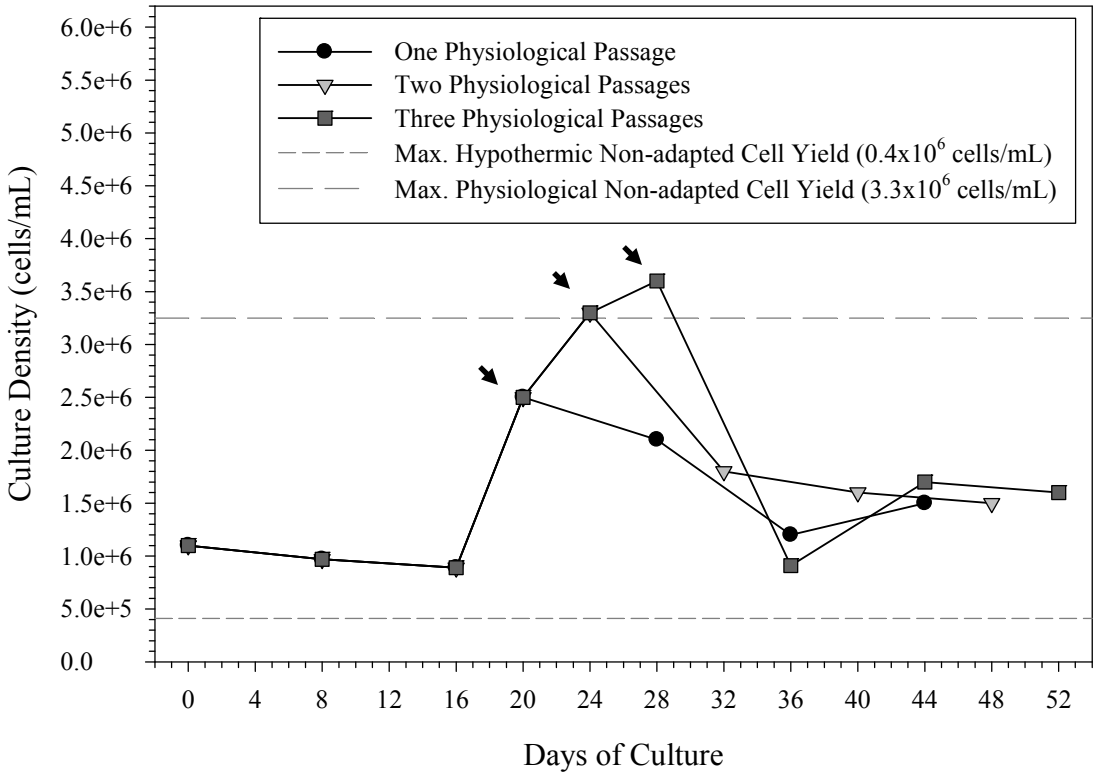

Figure 4.11: Hypothermic maximum cell yields of low temperature-adapted cells after re-introduction to physiological (37°C) temperatures. Cells were returned to hypothermic conditions after a period (4-12 days) of physiological growth. Points of re-introduction indicated by arrows. All populations retained enhanced hypothermic growth upon re-introduction.

Chapter 4.3 – Discussion

4.3.1 – The Adaptation of Recombinant CHO Cells to Hypothermic Temperatures to Enhance Heterologous Protein Expression

The work presented in this chapter describes the isolation a cell population which has been adapted to sub-physiological conditions through continuous culturing at 32ºC. These cells exhibit an enhanced performance under hypothermic (32°C) conditions, allowing further improvement to the process described by Rodriguez *et al*.(74); which previously reported the hypothermic culturing of this β-interferon producing cell line.

The adaptation process produced a population of cells capable of enhanced hypothermic growth which did not compromise the elevated hypothermic Q_P characteristic of many recombinant cell lines. The ability of Chinese hamster cells to adapt themselves to non-physiological temperatures (32°C through to 41°C) was first described by Li and Hahn in 1980(112); seven years prior to CHO cells being utilized in recombinant production(4). Despite hypothermic production strategies first being reported over 15 years ago, it was only in the last three years that adaptation had been attempted to further increase protein yields. Yoon et al. (111) described the successful isolation of two low temperature-adapted recombinant CHO cell populations. However they reported that in both cases the increase in μ occurred concurrently with a proportional decrease in Q_P. As a result, there was no net increase in protein production in either cell line. Unlike the cultures utilized in this thesis, both populations described by Yoon et al.(111) were isolated in successive agitated spinner cultures. The β-IFN-producing CHO cell lines in this work were adapted to hypothermic temperatures through a series of stationary T-flask cultures. This

resulted in an adaptation which, in addition to increased μ, sustained a hypothermically-elevated Q_P.

4.3.2 – Morphological changes in cold-adapted populations

A particularly notable characteristic which resulted from the adaptation process was a significant increase in the average cell size, the variability of cell sizes, and an increased rate of multi-nucleation and/or nuclear fragmentation within the adapted population. Whether there is a direct correlation between increased nucleation and/or cell size and cold-adaptation is unknown, however the prevalence of these traits within the population makes it difficult to overlook their potential role in the low temperature-adaptation response.

For adaptation-induced active hypothermic growth to occur, regulatory systems within the cycle cell checkpoints must be circumvented to avoid G1-phase cell cycle arrest. This has been achieved previously by Fox et al.(84) through the supplementation of hypothermic cultures with high concentrations of mitogens(84). Increased cell size and aberrant cellular nucleation could be a result of same cell cycle dysregulation, resulting in the interruption of M-phase processes, including mitosis and cytokinesis(120).

4.3.3 – Low Temperature-Adaptation is a Sustained Response Affecting Numerous Cellular Processes

Proteomic analysis of adaptation-induced changes did not produce a clear mechanism for low temperature-adaptation. The proteins identified to have modulated expression

belonged to three general categories: dynein motor protein subunits, metabolic enzymes, and stress response proteins.

4.3.3.1 – Identification of Proteomic Analysis Isolates

Cytoplasmic dynein intermediate chain (CD-IC) 2 homologue (down-regulated approximately 1.6-fold) is a subunit of the cytoplasmic dynein motor protein, involved the attachment of cargo organelles to the protein motor complex(122). CD-IC has been reported to undergo caspase-mediated cleavage during apoptosis(123), resulting in an apparent decrease in CD-IC expression; however no additional evidence to support apoptotic activity was observed. This is further discussed in Chapter 6.

UV excision repair protein (down-regulated 1.3-fold), is a stress response protein involved in nucleotide excision and DNA repair, which is also is involved in degradation of misfolded glycoprotein aggregates(124). Another stress response protein, an uncategorized heat shock protein was found to be up-regulated approximately 2-fold. These proteins are typically induced under thermal stress (hyperthermia) and function as protein chaperones. Significant overlap has been found between the hypo- and hyperthermic stress response(62).

The specific identity of the final protein isolate could not be determined, however two candidates were proposed; both involved in cellular metabolism Phosphoribosyl-pyrophosphate synthetase I, the first of the two possibilities, is a metabolic enzyme involved in the *de novo* and salvage synthesis pathways of guanosine-5'-

triphosphate(125). The second possibility, lactate dehydrogenase A, another metabolic enzyme, is involved in the conversion of lactate to pyruvate under low O_2 conditions(126).

4.3.3.2 – Re-introduction of Low Temperature-adapted Cells to Physiological Conditions

Although the adaptive mechanism was not explained through proteomic analysis, re-introducing the cells to physiological temperatures demonstrated that the adaptation, induced through selective pressure, did not require the maintenance of this pressure to sustain it.

This is an important observation as it confirms that the adaptive response is integral to the cell's regulatory machinery, and can be maintained dormant at typically growth permissive temperatures (37°C) and reactivated upon subsequent exposure to hypothermic conditions.

4.3.4 – Decoupling of the μ and Q_P Relationship

The most significant trait to arise from the adaptation process was the ability to decouple the relationship between μ and Q_P. This allowed increased hypothermic growth without reducing cell specific protein expression. As already described, the link between μ and Q_P has been previously decoupled through the supplementation of hypothermic cultures with high concentrations of mammalian growth factors (84). Genetic alteration, specifically the down-regulation of cold-inducible RNA-binding protein (CIRP), a gene

product believed to be responsible for growth arrest under mild hypothermic conditions, alleviated the growth arrest of mouse fibroblasts at 32ºC (69). However it was subsequently reported that the inhibition of the CIRP protein alone is not sufficient to induce active hypothermic growth in CHO cells under the same conditions(104). The process of low temperature-adaptation presented is this chapter allowed the isolation of the first CHO cell line capable of enhanced hypothermic growth and production without the introduction of exogenous growth factors or additional genetic manipulation to be described in literature.

Aspects of this chapter have been published in the AIChE journal Biotechnology Progress (127):

Sunley, K., Tharmalingam, T. and M. Butler. *CHO Cells Adapted to Hypothermic Growth Produce High Yields of Recombinant beta-Interferon*. Biotechnol. Prog. 2008; 24:898-906.

Chapter 5 - Growth and Recombinant Protein Expression in Low Temperature and Temperature-shifted Stationary Culture of Cold-adapted Cells

Chapter 5.1 – Introduction

Low temperature-adaptation and bi-phasic culture strategies are two distinct methods to achieve the same goal: increase cell proliferation under hypothermic conditions. In an effort to further optimize hypothermic production; cold-adapted cells were cultured within temperature-shifted processes, increasing heterologous protein expression in a combinatorial manner.

Chapter 5.2 – Results

β-IFN production was further increased through the culturing of low temperature-adapted cells in bi-phasic (32°C temperature-shifted) cultures in 75 cm^2 (non-agitated) T-flasks. This process involved a 48 hour growth phase at 37ºC to induce an enhanced μ, then a period under hypothermic conditions to enhance protein expression.

5.2.1 – Bi-phasic Culturing Increase the Cell Yields of Low Temperature-Adapted Bioprocesses in Stationary Cultures

As described in Chapter 3, cells with no prior hypothermic exposure (non-adapted) exhibit very little growth under low temperature conditions (increasing to $1.6x10^5$ cells/mL after 10 days). The same population of cells under temperature-shift conditions increased almost 7-fold, to $6.9x10^5$ cells/mL, from an initial $1.0x10^5$ cells/mL inoculation (Figure 5.1A).

The adapted cells presented in Chapter 4 demonstrated a significantly enhanced μ under low temperature conditions, increasing over 10-fold and resulting in yields of $1.1x10^6$ cells/mL over the 10 day culture. This represents more than a 6-fold increase over non-adapted cell titres under the same conditions. Growth under temperature-shifted conditions increased the cell yields of the adapted population an additional 2.3-fold (to $2.5x10^6$ cells/mL); a 4-fold increase over a non-adapted temperature shift culture (Figure. 5.1B)

Total recombinant protein expression in these cultures was related to the differences in cell growth (Table 5.1). The non-adapted cultures, under both 32ºC and temperature-shifted conditions, produced similar amounts of β-IFN ($2.2x10^6$ and $2.4x10^6$ units/mL respectively). This is explained by the fact that although the Q_P was enhanced significantly at the lower temperature, the decreased growth rate and subsequent cell yields of the non-adapted cells off-set any advantage in terms of total protein production. Alternatively, the adapted cells demonstrated the dual advantage of high Q_P and an enhanced growth rate at the lower temperature. This translated into significantly higher yields of the recombinant protein. At 32ºC, the cultures of adapted cells produced $5.7x10^6$ units/mL of β-IFN, an increase of 2.6-fold over the non-adapted cells; while temperature-shifted cultures increased nearly 3-fold ($7.1x10^6$ units/mL) over an equivalent non-adapted culture.

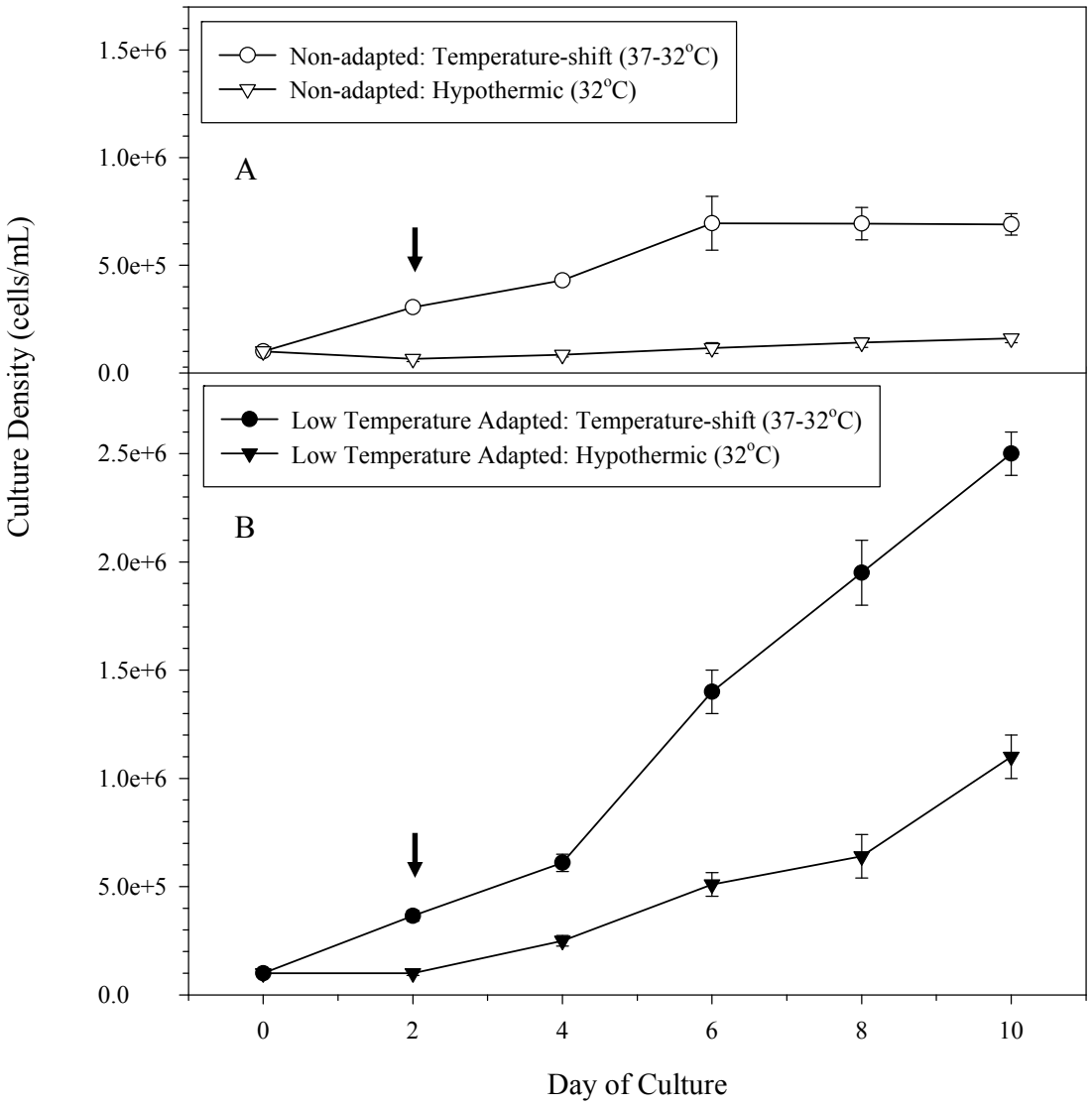

Figure 5.1: Cold and non-adapted stationary (T-flask) cell cultures under hypothermic (32°C) and temperature-shifted (37°C to 32°C) conditions. (n = 2 ± standard error)

Table 5.1: Growth and β-IFN Production of Non-adapted and Low Temperature-adapted Cells in Low Temperature and Temperature-Shifted Stationary Cultures

Culture	Temperature (ºC)	Max. Cell Density (cells/mL)	Total Volumetric Production (units/mL)	End Culture Viability (%)
Non-adapted	32ºC	$1.6x10^5$	$2.2x10^6$	93%
	37→32ºC	$6.9x10^5$	$2.4x10^6$	98%
Adapted †	32ºC	$1.1x10^6$	$5.7x10^6$	93%
	37→32ºC	$2.5x10^6$	$7.1x10^6$	88%

† Low temperature-adapted cells were from within phase II of the adaptation process

5.2.2 – Development of Low Temperature-adapted Scalable Stirred-tank Bioprocesses

The potential for scale-up of adapted cell cultures is dependent on the ability to transfer bioprocesses into stirred-tank (agitated) vessels; such as smaller scale spinner-flasks or bioreactors. The scalability of the cold-adapted cell processes was assessed in a series of 100 mL agitated spinner flasks.

5.2.2.1 – Growth of Low Temperature-adapted Cells in Stirred-tank Suspension Cultures

The growth profile of the non-adapted cultures matched those exhibited in stationary T-flask cultures at 32ºC (Figure 5.2A and Figure 5.1A respectively). During the 18 day culture, cells in suspension only reached a density of $0.17x10^6$ nuclei/mL (Figure 5.2A). However, unlike the proliferative cell growth within the adapted stationary cultures, the growth of the cold-adapted cells was minimal in agitated suspension cultures and did not exceed a density of $0.25x10^6$ nuclei/mL; 10-fold lower than the maximum cell yield attained in an equivalent stationary culture (Figure 5.1B and Figure 5.2B respectively).

5.2.2.2 – Growth of Low Temperature-adapted Cells in Stirred-tank Microcarrier Cultures

These low cell yields were concurrent with dramatically decreased cell viability; only 40% of the cells remained viable to the end of the culture (2-fold less than in stationary

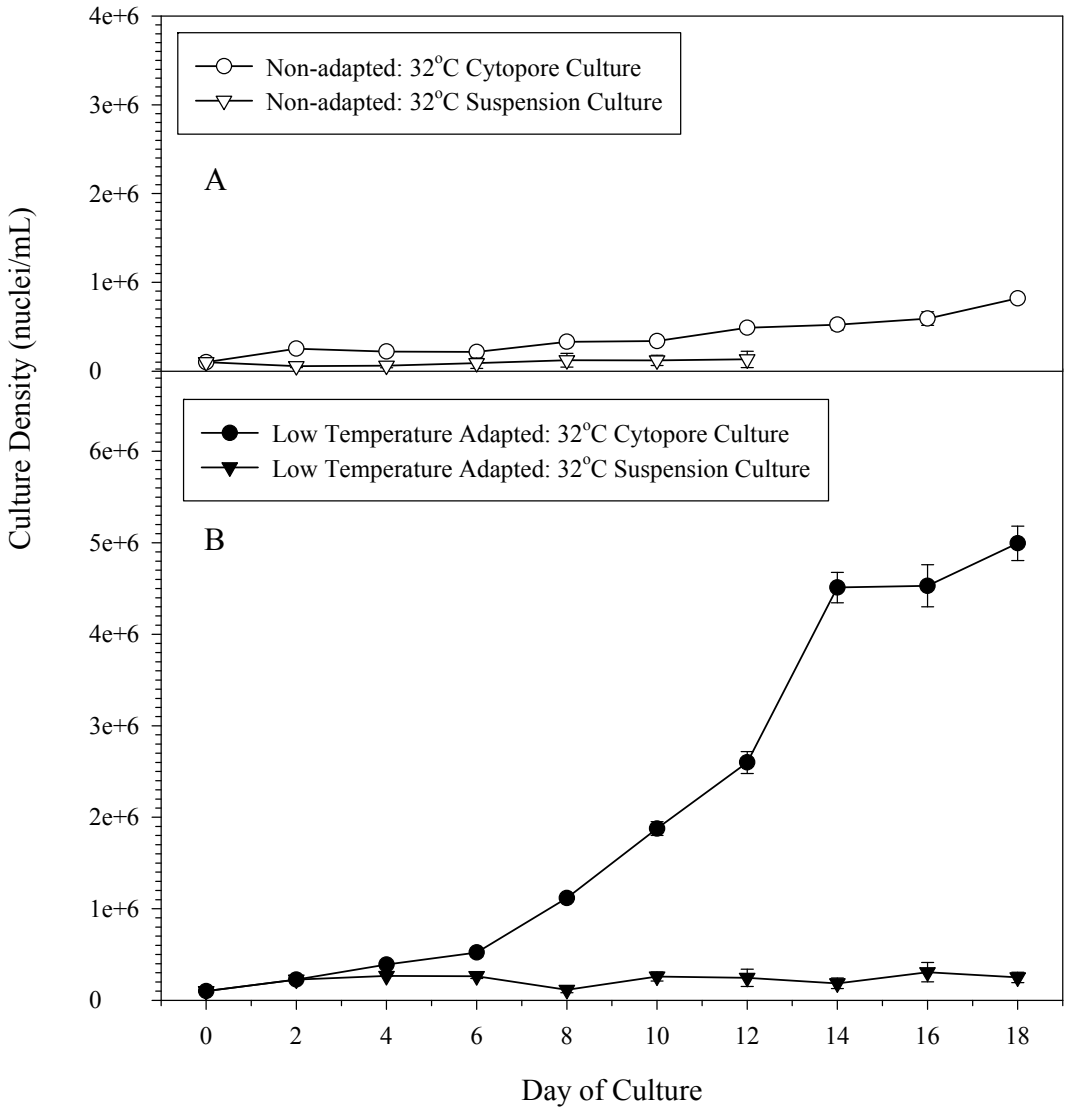

Figure 5.2: Cell growth of non-adapted (panel A) and low temperature-adapted (panel B) CHO cells at 32ºC grown in suspension or entrapped within macroporous microcarriers in 100 mL magnetically-stirred cultures. (n = 2 ± standard error per condition)

cultures). As a result of the apparent fragility of the adapted cells under agitation, the potential of microcarriers to protect the cells and support growth was assessed. Cytopore 2 are macroporous microcarriers that have been shown to support the growth of CHO cells in previous studies in our laboratory (114). The cells become embedded within the pores of the microcarrier; a matrix of cross-linked dextran polymers and are protected from the hydrodynamic shear forces generated through agitation.

The growth profiles of the microcarrier cultures are illustrated in Figure 5.2. The low temperature-adapted cells reached a density 20-fold higher than in microcarrier-free cultures (reaching $5x10^6$ nuclei/mL) under the same culture conditions (Figure 5.2B). However, the increased growth within the non-adapted population from the addition of microcarriers was negligible (reaching only $0.8x10^6$ nuclei/mL) (Figure 5.2A). The specific rates of β-IFN production within the Cytopore cultures of adapted cells (Table 5.2) were not significantly different from those in the stationary T-flask cultures at 32ºC; 0.920 units/cells per day and 0.868 units/cells per day respectively. This indicates that a transition to an agitated culture system utilizing Cytopore microcarriers did not alter cell specific protein production (Q_P).

The total volumetric β-IFN production was enhanced significantly in the low temperature-adapted microcarrier cultures as a result of the enhanced Q_P and μ at 32°C (Table 5.2). The product titre ($1.0x10^7$ units/mL at day 12) was 3-fold higher than the equivalent in non-adapted cell cultures at 32°C, even though Q_P was only increased by

Table 5.2: Growth and β-IFN Production of Non-adapted and Low Temperature-adapted Cells in Cytopore 2 (1 mg/mL) and Microcarrier-free Agitated Cultures at 32ºC

Culture	Temperature (ºC)	Microcarrier Concentration (mg/mL)	Max. Cell Density (nuclei/mL)	Specific Productivity Q_P (units/nuclei per day)	Total Volumetric Production (units/mL) ‡
Non-adapted	37ºC	0	4.14x106	0.341	$4.24x10^6$
	37ºC	1.0	2.53x106	0.954	$5.19x10^6$
	32ºC	0	$0.17x10^6$	0.784	$1.32x10^6$
	32ºC	1.0	$0.82x10^6$	0.847	$3.27x10^6$
Adapted †	32ºC	0	$0.25x10^6$	0.233	$0.73x10^6$
	32ºC	1.0	$5.01x10^6$	0.920	$10.1x10^6$

† Low temperature-adapted cells were from within phase 2 of the adaptation process

‡ Total protein production as of culture day 6 or day 12 (37ºC and 32ºC respectively)

10%. Although β-IFN production from the non-adapted physiological cultures was also increased by the addition of the microcarriers; their product yields were only 50% of those obtained from cold-adapted hypothermic microcarrier cultures.

Significantly higher quantities of β-IFN could be obtained through the maintenance of the microcarrier cultures beyond day 12; however product analysis demonstrated that culturing beyond this gradually reduced titres of monomeric β-IFN through increased product aggregation. This phenomenon of in-culture intermolecular β-IFN aggregation has been studied previously in our laboratory and has been found to occur at high product titres (typically above $1.0x10^7$ units/mL) (74).

It should be noted that the cell yields described in this section were assayed by nuclei enumeration (visualized by crystal violet nuclei staining) rather than the trypan blue dye-exclusion method used throughout the remainder of this thesis. This was essential for microcarrier cultures because of the inability of extracting intact cells from the microcarrier core. The same method was applied to the equivalent suspension cultures to enable valid comparisons. Due to the multi-nucleation states of the different cell populations, direct comparison between cell counts and nuclei counts would not have been valid, although the inaccuracies would likely not have exceed ± 1.7-fold (based on the nucleation states described in Chapter 3.3.1)

Chapter 5.3 – Discussion

5.3.1 – Combinatorial Effect of Bi-phasic Low Temperature-adapted Cultures

Low temperature adaptation increases hypothermic proliferation through a still uncharacterized mechanism which circumvents G1 cell cycle arrest, typically induced through cyclin-dependent kinase inhibitor activation. Bi-phasic culturing is a second mechanism for achieving increased hypothermic proliferation, also through a mechanism which is poorly understood. The combination of these two processes results in a synergistic effect which further increases hypothermic growth without compromising elevated recombinant protein expression, resulting in significantly increased β-IFN titres.

5.3.2 - Development of Low Temperature-adapted Scalable Stirred-tank Bioprocesses

For developed recombinant production processes to be biotechnologically relevant they must be able to be scalable to industrial volumes. Non-agitated (T-flask) cultures, used routinely in cell culture laboratories (Figure 5.3A) rely on vessels of low volumes and high surface areas, which can not be easily scaled to multiple litre vessels. High volume, low surface area vessels can be constructed up to volumes of 20,000 litres, yet require significant agitation and sparging to ensure sufficient oxygenation and pH control. To scale-up towards these large scale vessels, smaller intermediate stirred vessels (100 – 1000 mL) (Figure 5.3B) and bench-scale bioreactors are used simulate these conditions.

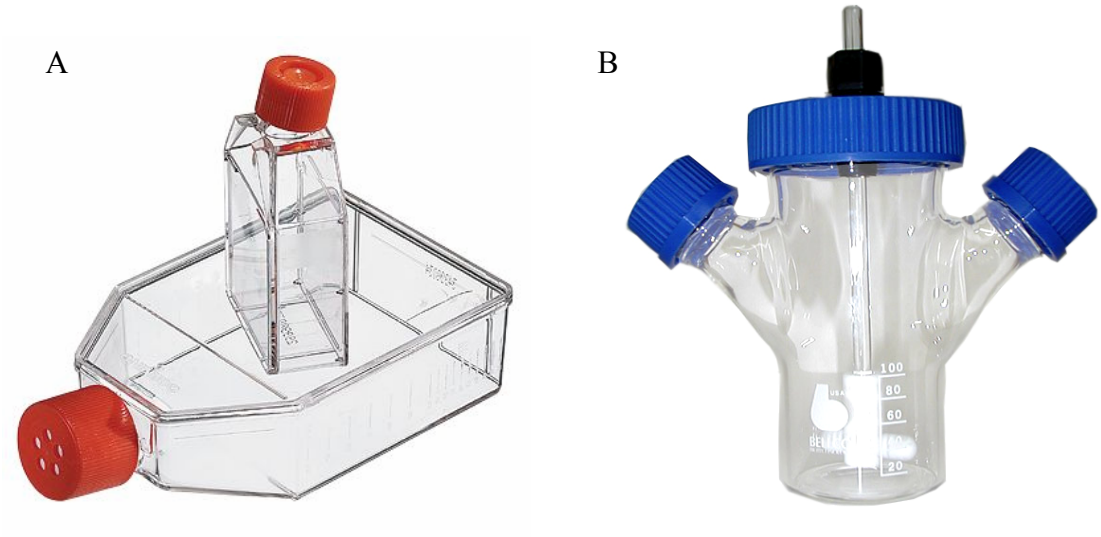

Figure 5.3: Vessels used routinely in cell culture research. Non-agitation (stationary) T-flasks (panel A) are low volume (10-20 mL), high surface area vessels which rely on passive gas diffusion for oxygenation and pH control. Spinner flasks (panel B) are agitated larger volume (100mL), low surface area vessels which are magnetically stirred allow for homogenous gas and pH control. Images courtesy of Corning Life Sciences and Bellco Glass respectively.

5.3.2.1 – Growth of Low Temperature-adapted Cells in Stirred-tank Suspension Cultures

The scale-up of the stationary T-flask adapted cultures to agitated stirred-tank vessels resulted in minimal cell growth with poor viability; presumably due to a sensitivity to mechanical agitation. This sensitivity was observed only in the low temperature-adapted populations, and therefore seems to have been unintentionally selected for through the adaptation process.

5.3.2.2 – Growth of Low Temperature-adapted Cells in Stirred-tank Microcarrier Cultures

In an effort to provide an environment that would reduce in-culture mechanical stress, the cells were inoculated into stirred cultures containing macroporous microcarriers. The Cytopore carriers are cross-linked cellulose beads charged with active DEAE groups, which are capable of entrapping CHO cells (Figure 5.4) within their mesh-like structure (128).

The microcarrier-entrapped adapted cells, when maintained in magnetically stirred cultures at low temperature, were capable of growth profiles very similar to those achieved in stationary T-flasks. The stirred microcarrier cultures also maintained the high rate of recombinant protein production observed in stationary flasks. These cultures were able to reach high cell densities while maintaining an elevated Q_P, which resulted in

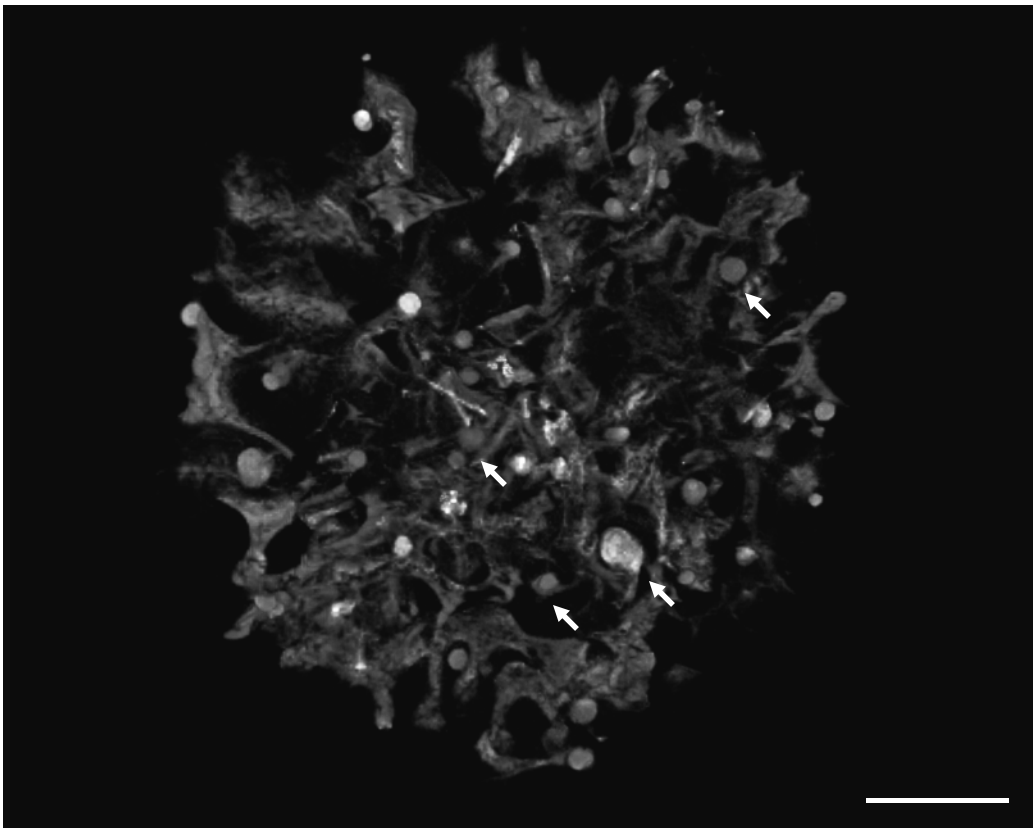

Figure 5.4: Optical fluorescence cross-section of a Cytopore 2 macroporous microcarrier populated with recombinant CHO cells. Carrier imaged through intrinsic auto-fluorescence of the dextran material while cells were visualized by acridine orange staining. Image demonstrates the capacity of the carrier to internalize cell populations (see arrows). Bar = 50 μm.

high product titres; 10-fold higher than non-adapted cells in equivalent suspension cultures and 3-fold higher than equivalent non-adapted microcarrier cultures.

This demonstrates that a strategy which employs a hypothermic temperature-shift on a scalable population of cold-adapted CHO cells is capable of increasing product titres substantially over either of the methods individually.

Chapter 6 - Loss of Cellular Integrity through Enhanced Sensitivity to In-culture Hydrodynamic Stress within Cold-adapted Cells

Chapter 6.1 – Introduction

Cellular robustness is maintained through a strong cytoskeletal structure and an intact cellular membrane(129). As the inability of the cold-adapted cells to proliferate within agitated cultures was determined to be due to a perceived sensitivity to in-culture hydrodynamic stress due to increased cellular fragility (as discussed in Chapter 5), the mechanism of this fragility was investigated.

Chapter 6.2 – Results

The ability of macroporous microcarriers to facilitate growth within stirred cultures suggests that the carriers offer a protective environment for the adapted cell population. The role of in-culture hydrodynamic stresses (induced through culture agitation) and the protective nature of the Cytopore microcarriers was quantified in the context of cell viability. Furthermore, adaptation-induced structural changes were correlated to increased cellular fragility

6.2.1 – Increased Cellular Fragility within Populations of β-IFN-Producing Cold-Adapted CHO Cells and the Protective Mechanism of Macroporous Microcarriers

Cell fragility was investigated through the examination of whole cell populations and at the resolution of the individual cell. This approach allowed for the comparison between different heterogeneous populations of recombinant CHO cells and ability to determine

how the variability within a single population (in terms of cell size and intra-microcarrier localization) affected cellular robustness.

6.2.1.1 – Endogenous Lactate Dehydrogenase as a Marker for Compromised Membrane Integrity in Populations of Low Temperature-adapted Cells

The overall extent of cellular fragility was quantified by subjecting a population of cells ($1x10^6$ cells/mL in a working volume of 5 mL) to increasing rates of mechanical agitation (Figure 6.1). These were performed in triplicate in small-scale (10 mL) magnetically-stirred glass culture vessels using a 10 mm diameter cross-shaped polytetrafluoroethylene (PTFE) coated stir bar (schematically illustrated in Figure 6.1E) in a 37°C, 10% CO_2, humidified environment.

By maximizing the size of the stir bar relative to the size of the culture vessel, the amount of mechanical stress transferred on to the cells was increased, generating an enhanced stress response. The cells were also exposed to rates of agitation over 10-fold higher than in traditional spinner flask culturing (500 RPM and 45 RPM respectively) to further exaggerate the response over the short period of time of this assay (2 hours). This experimental setup was designed as a proof of principle to simulate in-culture hydrodynamic stresses, however able to generate stress levels significant enough to be

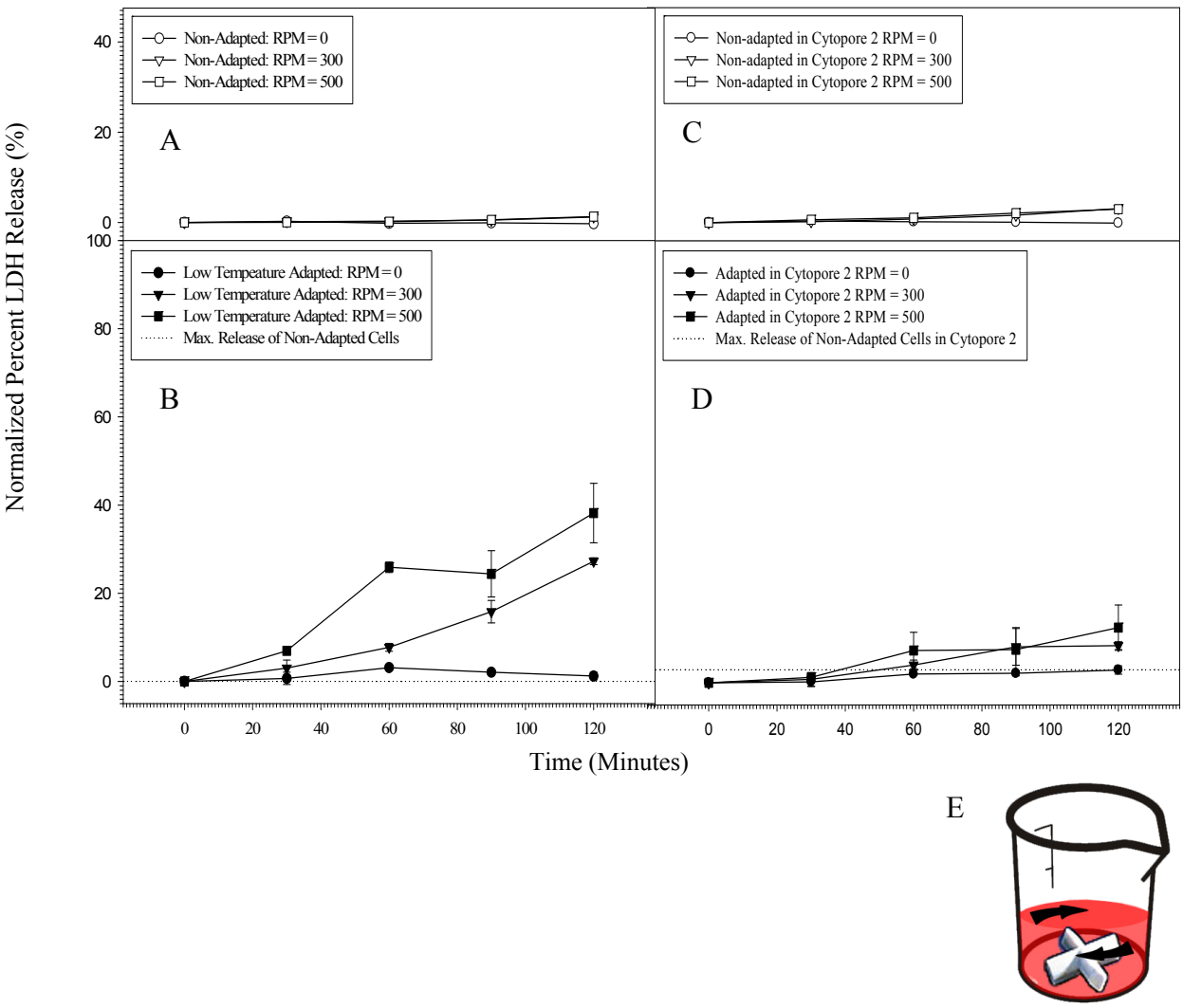

Figure 6.1: Cytosolic lactate dehydrogenase release in response to mechanical agitation of non-adapted (panel A) and low temperature-adapted cell (panel B) populations of CHO cells (n = 3 ± standard error). The release of LDH from non-adapted and adapted populations entrapped within Cytopore 2 microcarriers (Panels C and D) is also represented (n = 3 ± standard error). Lactate dehydrogenase release was used as an indicator of cell damage in response to mechanical stress. A schematic representation of the experimental set-up is illustrated in panel E.

detected during a short-term experiment, rather than the 10 to 12 days typical of hypothermic cultures.

The presence of lactate dehydrogenase (LDH); a non-secreted, cytosolic enzyme in the culture media was assayed over time as an indicator of cell damage; as LDH activity within culture supernatant would be proportional to compromised membrane integrity. This is due to the fact that the only source of LDH within the culture media would be from cell lysis and the rupturing of cell membranes; which over the 2 hours of the experiment can be presumed to be caused by the significantly increased rates of mechanical agitation. The short duration of the experiment, and subsequent elevated rates of mechanical agitation were also necessary to minimize the spontaneous loss of LDH activity, which has a measured half-life of 2 to 2.5 hours(130). LDH was also chosen as a marker due to relatively simple and sensitive methods available for its detection, including the colorimetric assay used in this work(131); where LDH catalyzes the first reaction, and a second enzyme (diaphorase), catalyzes the colourless tetrazolium salt 2-p-(iodophenyl)-3-(p-nitrophenyl)-5-phenyltetrazolium chloride (INT) into a formazan product (detectable by optical absorbance at 492nm) at a rate limited by the first reaction:

$$Lactate + NAD(+) \rightarrow Pyruvate + NADH; \qquad NADH + INT \rightarrow NAD(+) + Formazan$$

The levels of released cytosolic LDH were then normalized as a percentage of the total cellular LDH within the population of cells. This was performed through determining the ratio of the released LDH activity (for a treated population of $1x10^6$ cells) to the activity

total potential LDH activity of a similar population of cells completely lysed through a series of freeze/thaw cycles (at -80°C) and expressing this as a percentage. This allows for the valid comparison between different populations of the same and between different cell lines; acknowledging the significant heterogeneity which exists even between technical replicates of the same cell population using a method which is well established(132) and compatible with cells entrapped in extra-cellular structures, unlike traditional optical methods such as the trypan blue dye exclusion assay(133).

The effect of RPM on the release of LDH was measured over a series of time points (30 minute intervals) between 0 and 2 hours, at varying rates of agitation (stationary, 300 and 500 RPM). This assay system was then applied to both the low-temperature and non-adapted CHO populations, in the presence and absence of macroporous microcarriers to determine the relationship which exists between agitation-induced mechanical stress, the protective nature of the microcarriers and robustness of the different cell populations.

The release of LDH from non-adapted cells in suspension cultures was minimal, with no significant extra-cellular activity (1% of total cellular LDH) after 120 minutes at 500 RPM (Figure 6.1A). However, the low temperature-adapted cells exhibited significant release, with maximum LDH activities of 1%, 27% and 38% after exposure to 0, 300 and 500 RPM respectively (Figure 6.1B).

The protective effect of the Cytopore 2 microcarriers was demonstrated through the LDH release from microcarrier-entrapped cells exposed to equivalent agitation rates (Figures

6.1C and 6.1D). Cells were inoculated into cultures containing 1.0 mg/mL Cytopore 2 microcarriers at a density of $1x10^5$ cells/mL and incubated at 37°C to a density of $1x10^6$ cells/mL (determined by nuclei enumeration). During this incubation, cells migrated into the interior of the microcarrier structure (with less than 1% remaining in suspension). From this culture approximately $1x10^6$ cells were transferred into the assay vessel to determine agitation-induced LDH release.

The LDH release from the entrapped non-adapted cells was again minimal, at approximately 3% of total cellular LDH after exposure to 500 RPM. The release from low temperature-adapted cells with the carriers increased 4-fold, however still at a rate 3-fold lower than the adapted cells in suspension. The maximum LDH release from Cytopore 2 cultures was 3%, 8% and 12% from their respective 0, 300 and 500 RPM trials after 120 minutes. This demonstrated that in-culture LDH release from CHO cells increased in an RPM-dependent manner (Figure 6.2) and that the microcarriers were able to protect the fragile cells under conditions of elevated hydrodynamic stress.

6.2.1.2 – Intra-Microcarrier Localization Determines the Protective Effect of Cytopore Cultures

To further characterize the protective role of macroporous microcarriers against in-culture hydrodynamic forces, cellular viability was quantified as a function of intra-

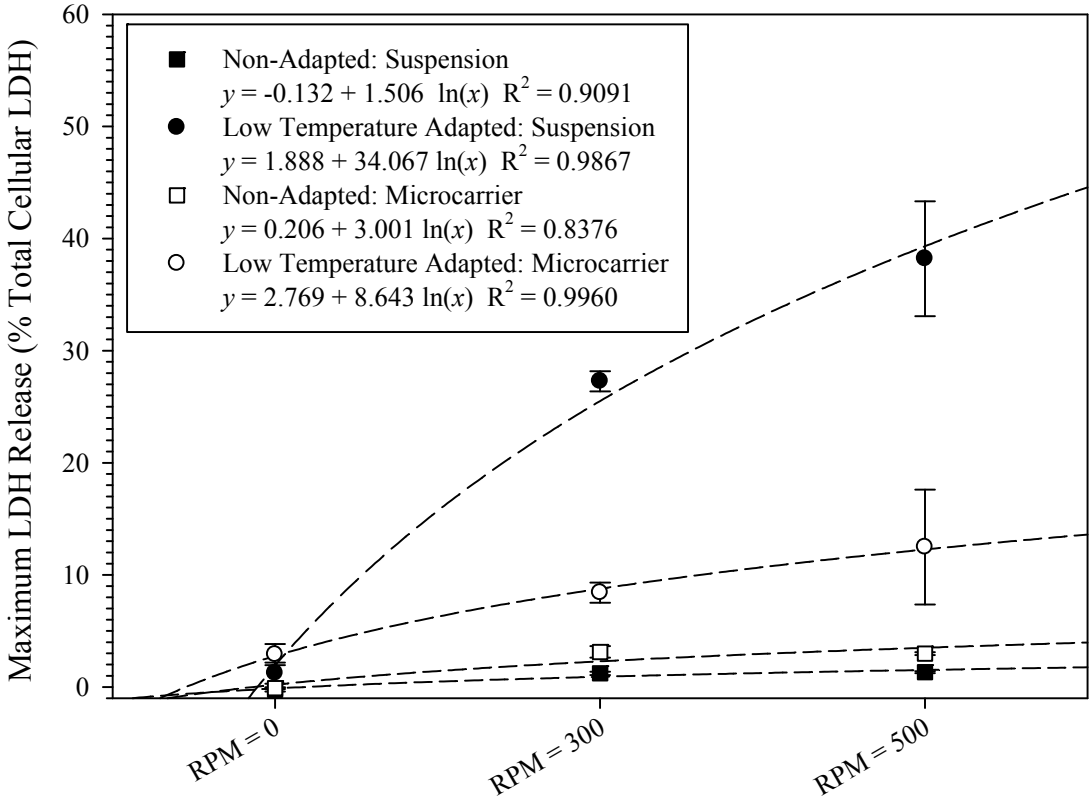

Figure 6.2: The RPM-dependent release of endogenous cellular LDH in response to increased mechanical agitation. Non-linear (2-parameter logarithmic) regression illustrates the response over the increased rates of mechanical agitation (0 – 500 RPM) (n = 3 ± standard error)

microcarrier location. Viability was determined in situ through fluorescence microscopy, adapting the method of Jones and Senft(134), utilizing a combination of fluorescein diacetate (FDA; 25 mM) and TO-PRO-3 iodide (1 μM). FDA; a non-polar, membrane permeable, non-fluorescent ester enters the cytosol passively and is hydrolyzed by intracellular esterases in living cells, cleaving the two acetate groups. Fluorescein, the polar product of esterase hydrolysis then accumulates within the cells to due to its poor membrane permeability, and functions as an inferred marker for viability, reporting the integrity of the cell membrane and intracellular esterase activity through a strong fluorescence signal. TO-PRO-3 iodide was used as a non-selective fluorescent counter-stain and is results in the staining of all cells, viable and non-viable, a property which is necessary to identify the location and quantity of the cells within the carrier. FDA and TO-PRO-3 were detected through green (λ_{EX} = 490 nm, λ_{EM} = 513 nm) and red (λ_{EM} = 642 nm, λ_{EX} = 661 nm) fluorescence respectively. Cells were determined to be viable if they exhibited green and red fluorescence simultaneously and non-viable if only red fluorescence was observed.

Throughout an optical cross-section of the microcarrier (Figure 6.3) cell viability was visually determined, and correlated to regions within the carrier. To facilitate quantification, the carrier was divided up into sequential ring-shaped zones, 25 μm in width, and the cell viability within each region was determined. Structured fluorescence illumination, achieved through the use of a Zeiss Apotome module(135), allowed the exclusion of out-of-focus light, creating an optical section through the middle of the approximately 300 μm bead. Mechanical agitation (2 hours at 300 RPM) compromised

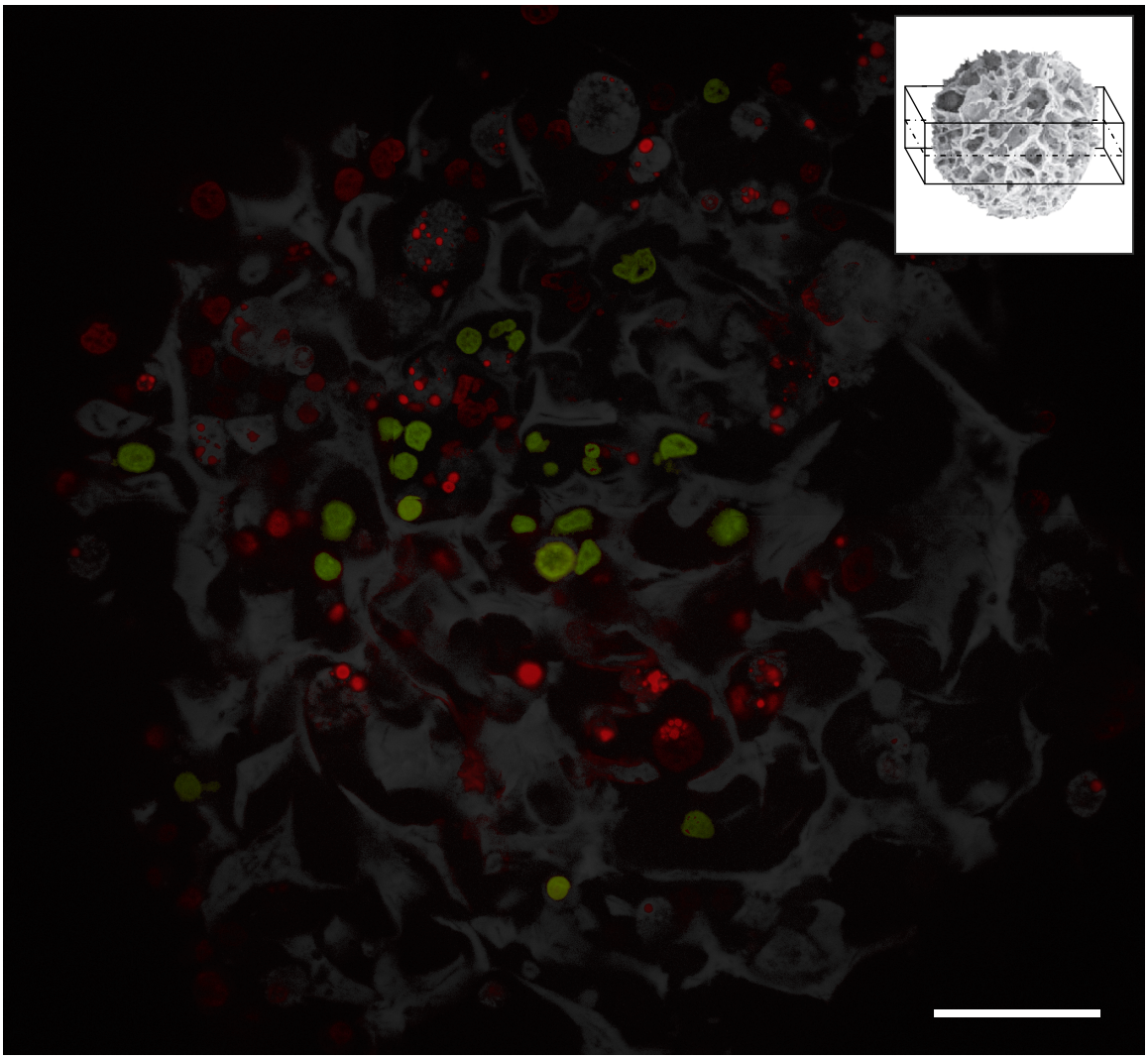

Figure 6.3: A representative composite image used to examine the effect of intra-microcarrier localization on cell viability in response to mechanical agitation (300 RPM; 120 minutes). In situ viability (fluorescein diacetate/TO-PRO-3 Iodide fluorescence) allowed determination of viable (green) and membrane compromised (red) cells within a microscopically observable 3D region of the microcarrier structure (illustrated as horizontal plane through inset image). (Bar = 50 μm)

the membrane integrity of entrapped cells in a relationship inversely to their proximity to the exterior of the microcarrier structure (Figure 6.4), reducing viability to below 10% at the periphery of the carrier. Microscopy analysis was immediately performed after agitation and staining to not compromise the health of the remaining viable cells. All manipulations were performed within sterile phosphate-buffered saline. This experiment confirms that the microcarrier internal structure itself is providing a sheltered environment from in-culture hydrodynamic forces, facilitating the growth of the fragile cold-adapted cells in stirred-tank cultures.

6.2.2.3 – Increased Mechanical Deformability of Low Temperature-adapted Cells

To determine the mechanism which resulted in the increased fragility of cold-adapted cells, the susceptibility of individual cells within the adapted population to mechanical deformation was investigated.

The mechanical strength of the low temperature-adapted cells was compared to non-adapted cells cultured at physiological conditions by measuring their resistance to structural deformation after centrifugation, following the method of Brown et al. (136). Briefly, 100 μL of live cells from mid-exponential viable cultures (>90% at approximately $5x10^5$ cells/mL) were suspended in phosphate buffered saline and dispensed onto poly-L-lysine coated glass coverslips. These were subjected to significant centrifugal force through centrifugation for 10 minutes at 1700g, a force which was found to produce a wide range of deformation responses, and allowed for an overall precise

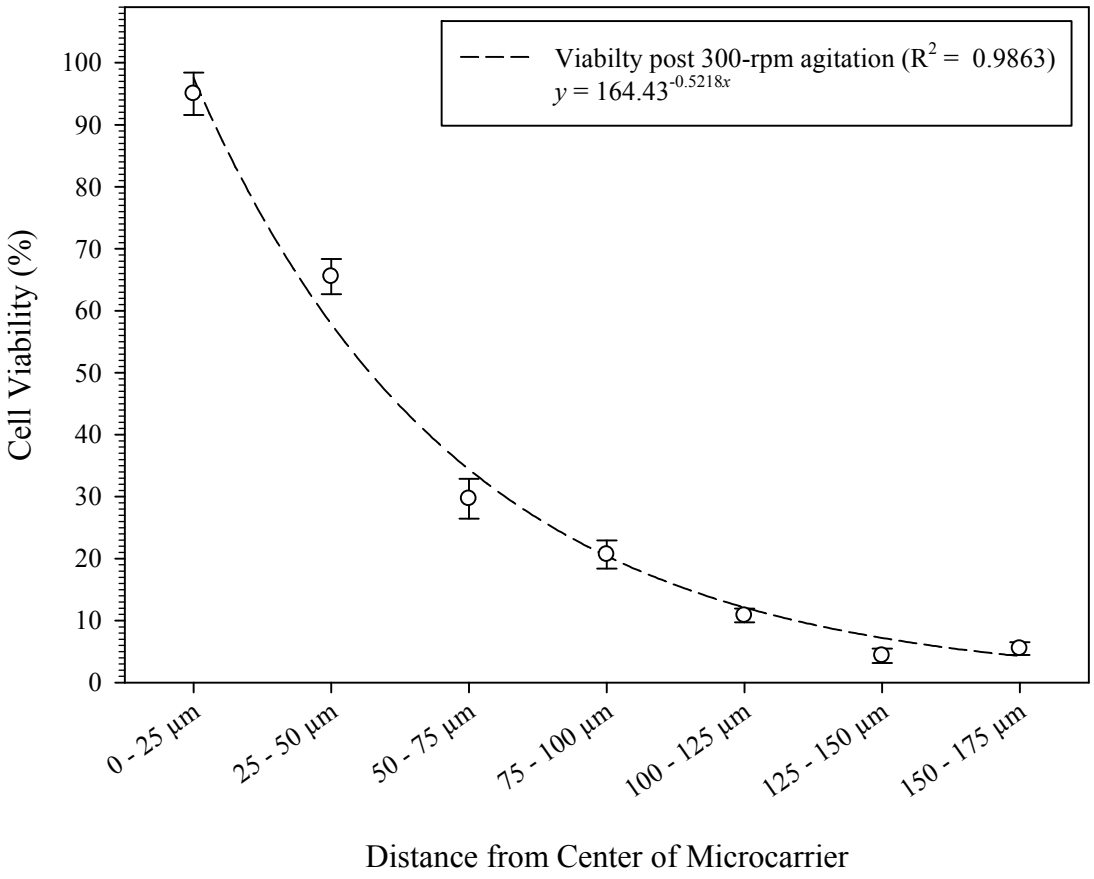

Figure 6.4: Effect of cellular localization within macroporous microcarriers on viability. Protective nature of microcarrier illustrated as the proportion of viable cells decreases (2-parameter exponential decay) as distance from center of matrix increases. (n = 5 ± standard error)

measurement of deformation. Cellular structure was determined microscopically by pre-staining the plasma membrane of the live cells with fluorescently-labeled wheat germ agglutinin (10 μg/mL in PBS), a glycan-binding lectin (specific for N-acetylglucosamine and N-acetylneuraminic sialic acid residues) conjugated to a Alexa Fluor 594 (Invitrogen Corp.). The cells were fixed in 4% paraformaldehyde post-centrifugation to preserve their structure for observation. The relatively high abundance of membrane glycoproteins on mammalian cells results in the seemingly non-selectively staining the exterior cellular structure.

High resolution three-dimensional microscopy (Apotome-equipped Zeiss AxioImager Z1 with a Plan-Apochromat 100x/1.4 objective) was used for the capture of a series of optically-sectioned images at 0.27 μm intervals along the Z-axis of individual cells. This collection of images allowed for accurate three-dimensional reconstruction of the cell's morphology and subsequent measurement of the cell height and diameter. The degree of cell Z-axis compression was quantified by calculating a relative deformation index (DI):

Deformability Index = X or Y-axis Cell Diameter (μm) / Z-Axis Cell Height (μm)

These values were used to categorize the adapted and non-adapted populations in terms of their ability to resist structural change, a property likely correlated with their overall robustness and tolerance for in-culture hydrodynamic stress.

Two distinct sub-populations were observed within the population of non-adapted cells; cells which generally resisted deformation (Low DI or DI < 2) and cells which

compressed to less than half their initial height (High DI or DI > 2). The adaptation process, in addition to selecting for enhanced hypothermic growth, also seemed to select against cells which were able to resist mechanical deformation; as only the latter sub-group (Low DI) was observed within the adapted population.

The inherent variation within the two cell populations is illustrated in Figure 6.5. Post-centrifugation (1700g for 10 minutes), cells within the non-adapted population ranged from 100% of their initial height (DI = 1.0) to only 12% (DI = 8.5). This is in contrast to the low temperature-adapted population, in which all observed cells were compressed to a minimum of 40% of their initial height and over half were reduced to less than 25%. Average deformability indexes, sub-categorized by their resistance (DI < 2) or susceptibility (DI > 2) to deformation are illustrated in Figure 6.6. In the non-adapted population both resistant and susceptible cells were observed (average DI = 5.57 ± 1.98 and 1.48 ± 0.46 respectively), indicating that CHO populations are naturally heterogeneous in terms of their cellular robustness. However in the adapted populations no cells were observed which were able to resist deformation (average DI = 6.17 ± 2.21).

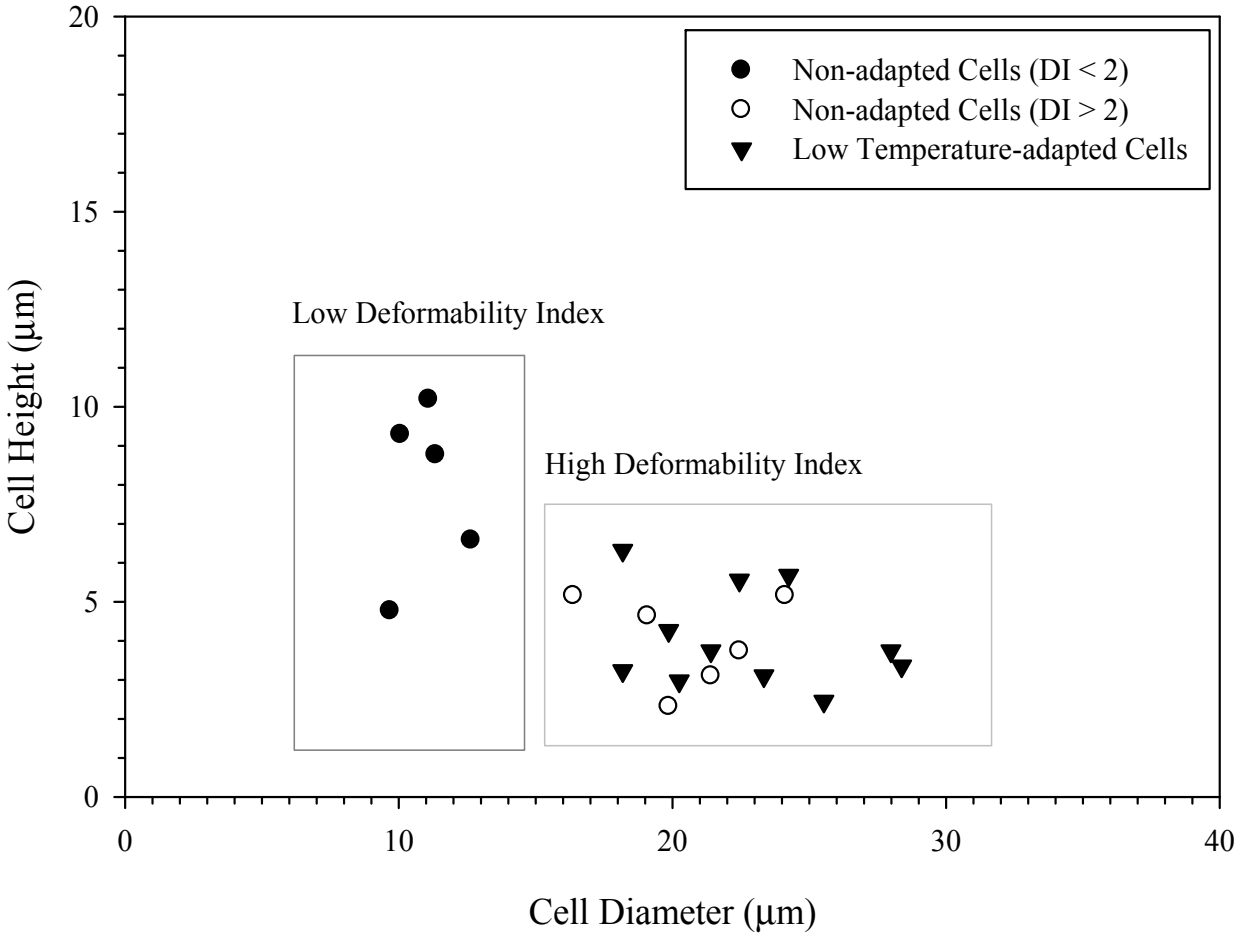

Figure 6.5: Measured cell deformation in response to centrifugal (1700g) force of low temperature and non-adapted CHO cells. Populations are grouped in terms of being generally resistant (low DI) or susceptible (high DI) to mechanical deformation.

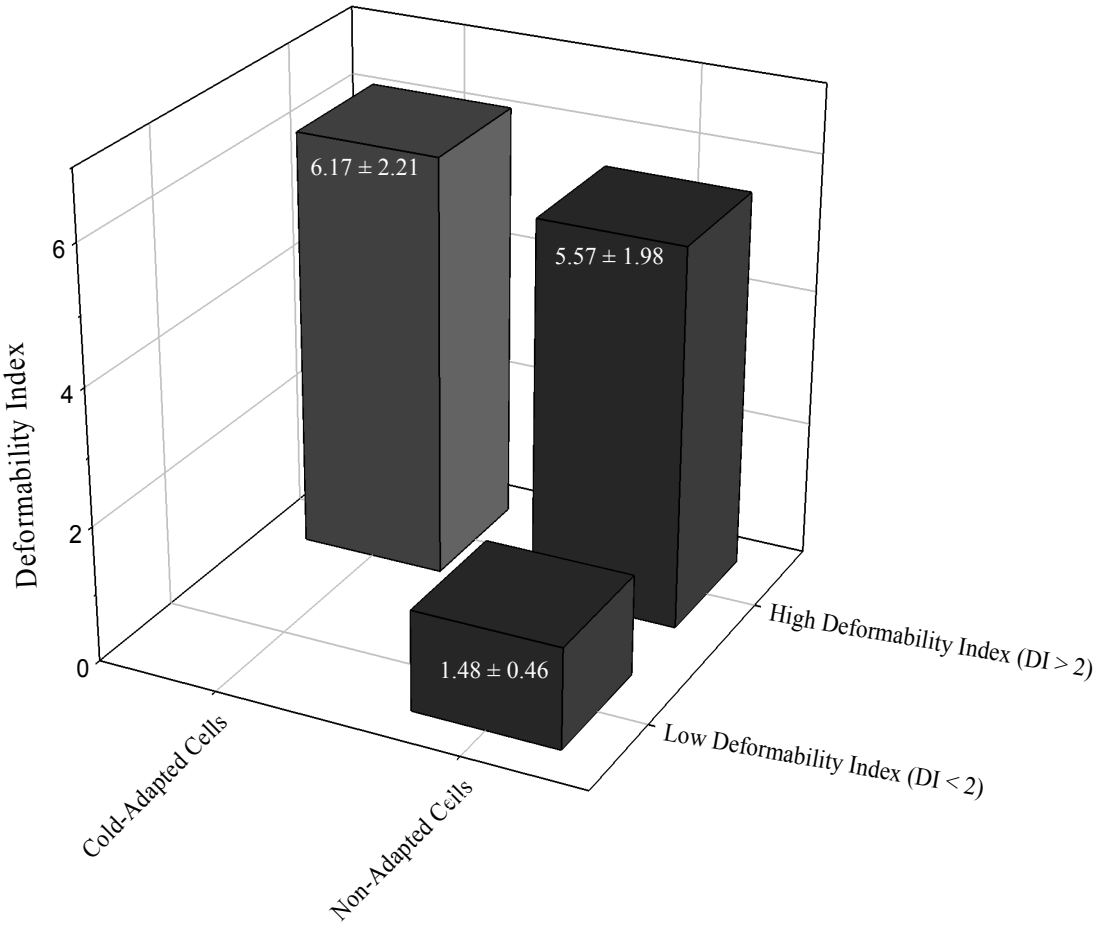

Figure 6.6: Average deformability indices (DI) of low temperature and non-adapted CHO cells, sub-categorized by high and low index values. Low DI cells were absent from the cold-adapted population. (n = 10 per population)

Cells selected through the adaptation process were also on average 70% larger, a trait which likely contributes to their increased cellular fragility. Yet the overall increase in cell size is not the cause of their weakened cell structure, as in the non-adapted populations smaller cells of equal size were be found both resistant or susceptible to structural deformation. X/Y-axis and X/Z-axis projections of resistant and susceptible cells are represented in Figures 6.7A and B, and 6.7C and D respectively.

6.2.2 – The Vimentin Intermediate Filament Network and its Role in Increased Cellular Fragility

Physiological causes for the increased fragility of the adapted cells would likely be based in one of two areas: a weakened cellular membrane or a compromised cytoskeletal structure. Two broad approaches were attempted to quickly screen whether the cell membrane was responsible for the increased cell fragility (Table 6.1): determining whether there was limited availability of a component of the membrane structure within the media formulation, or whether the membrane (through any number of possible reasons) was weaken to where it could simply not withstand the in-culture hydrodynamic shear forces across its hydrophobic surface.

To ensure that no essential membrane components were limited, Ex-cyte™ (Millipore Inc.), a concentrated complex mixture of lipoproteins, cholesterol and fatty acids which

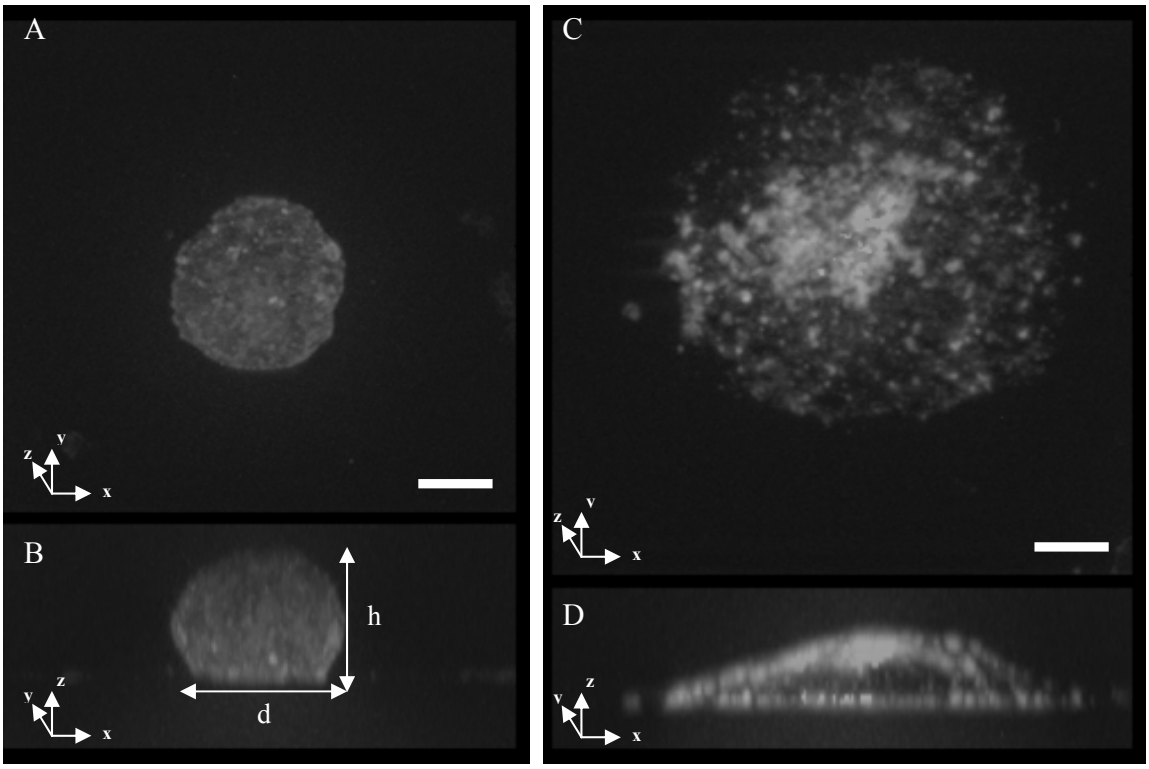

Figure 6.7: Representative X/Y-axis (panels A and C) and X/Z-axis (panels B and D) fluorescence projections of high (left) and low (right) deformability index CHO cells post-1700g centrifugation. (Bar = 5 μm)

has been demonstrated to increase membrane fluidity(137) was supplemented to the CHO-SFM media in concentrations between 0.5 and 5%. This range was selected to cover and exceed the manufacturer's recommended concentration for CHO cells by 5-fold (1% and 5% respectively). However none of the concentrations demonstrated any significantly observable effect on either the cell growth or culture viability, indicating that the fragility is not due to the insufficient availability of common membrane precursors.

Another approach attempted was to reduce the in-culture hydrodynamic shear stress which affects the hydrophobic membrane of the cells in suspension. Pluronic™ F-68 (BASF Corp.) is an FDA-approved, non-ionic surfactant which has been demonstrated to reduce hydrodynamic shear forces on the cell membrane(138) through coating or internalization of the product into the membrane. Pluronic™ F-68 is added routinely as a protective agent to cell culture media, including CHO-SFM at a concentration of 0.1% (previously optimized for the parental CHO population by Tharmalingam et al.(139)). To determine whether increasing the available concentration would have an additive protective effect, the low temperature-adapted cells were cultured in 100 mL agitated spinner flasks in the presence of 0.2% Pluronic™ F-68. At this increased concentration cell growth and viability decreased to below those at 0.1% (Figure 6.8), demonstrating not only the lack of an additional protective role but a possible cytotoxic effect.

These two assays screened the two most likely roles the membrane could play in terms of affecting cellular integrity. By removing the possibility of a limited membrane

Table 6.1: Strategies to determine the cause of increased fragility in low temperature-adapted CHO cells

Investigative Strategy	Cellular Target	Effect of Cell Fragility	Details of Strategy
Increased Pluronic F-68 Concentrations†	Cell Membrane	No	Cultures were supplemented between 0.1 and 0.5%
Addition of cholesterol, lipoprotein and fatty acid concentrate‡	Cell Membrane	No	Cultures were supplemented between 0.5 and 5%

† Pluronic F68 (Sigma Aldrich) is a non-ionic surfactant with well characterized cell strengthening properties

‡ Ex-cyte (Millipore) is a cell culture supplement which increases plasma membrane fluidity

component and observing no beneficial effect of increased Pluronic™ F-68 concentrations, all initial leads to a role for the membrane in the increased cell fragility were eliminated, leaving the alterations to cytoskeleton as the most likely cause.

6.2.2.1 – In situ Examination of the Vimentin Intermediate Filament Network

The cytoskeleton is a dynamic, interactive network of different protein classes which regulate, structure, and coordinate many diverse processes throughout the cell. Composed of distinct sub-networks; actin microfilaments, intermediate filaments and microtubules, each of these sub-groups contain numerous unique protein classes with specialized roles within the cell's physiology. A review of the current literature prior to investigating the potential role of the cytoskeleton in cell fragility found two notable observations; that although microfilaments and microtubules have important and well characterized roles in conferring mechanical strength to a cell, previous proteomic investigations have not observed significant changes to the expression of these proteins at hypothermic temperatures. However, intermediate filaments (IF), and particularly the vimentin IF network has been observed play a significant role in the mechanical stability of mammalian cells (136, 140), with an expression level which has been found to be modulated at sub-physiological temperatures(141). These two occurrences resulted in vimentin being the primary target of an investigation into adaptation-induced cytoskeletal changes.

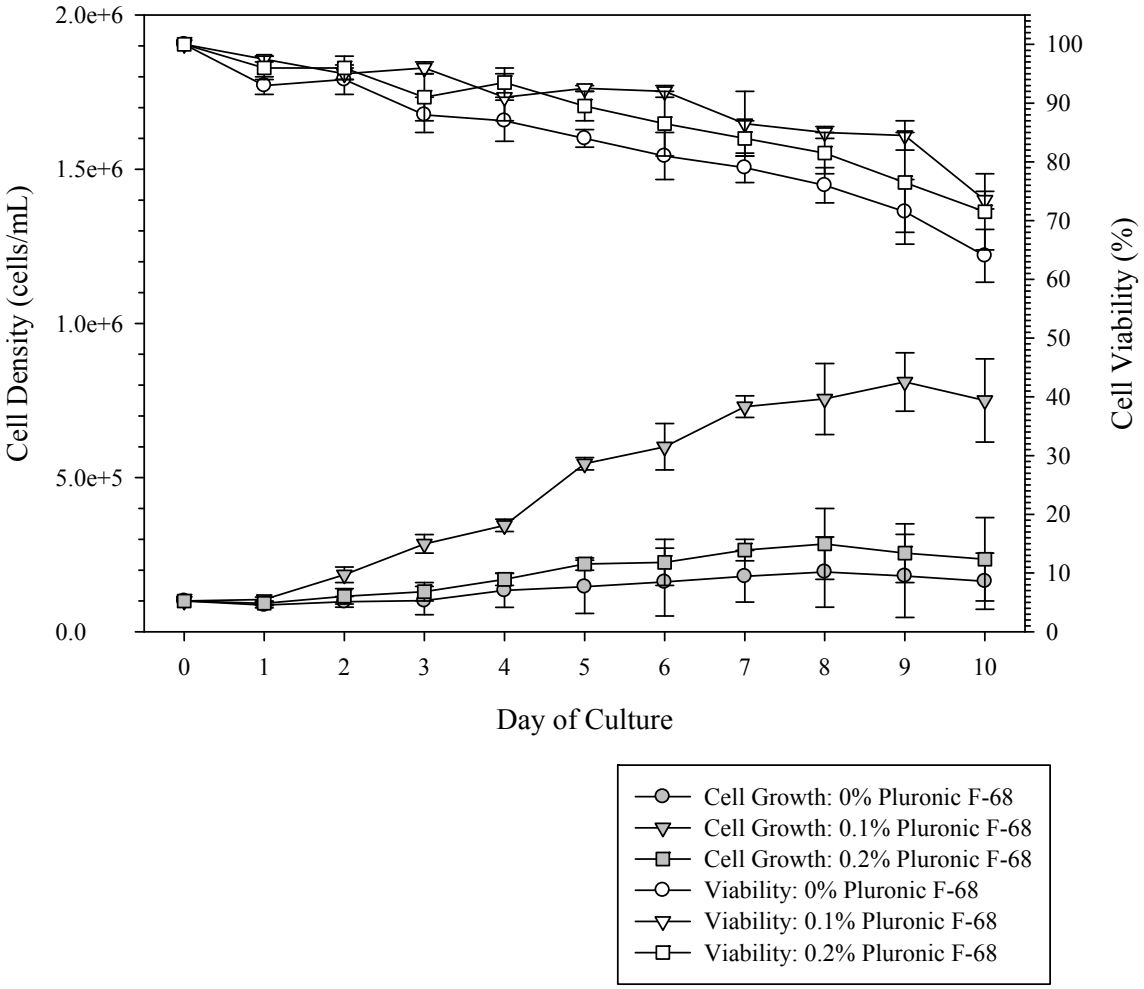

Figure 6.8: The effect of varying concentrations of Pluronic F-68 supplemented to CHO-optimized serum-free media on low temperature-adapted CHO cells in 100 mL spinner flask cultures. (n = 2 ± standard error)

The role the cytoskeleton in cellular fragility was initially investigated by examining the vimentin intermediate filament network through immunofluorescence microscopy. Populations of cells ($1x10^5$ cells per population) were allowed to settle on poly-L-lysine coated glass coverslips. These cells were then fixed in a 4% solution of phosphate-buffered paraformaldehyde, then permeabilized with 0.1% Triton x-100. The vimentin intermediate filament network was detected through a mouse-produced anti-vimentin monoclonal antibody (clone V9 from Sigma Aldrich), which was subsequently detected using an anti-mouse IgG molecule conjugated to the fluorescent dye Alexa Fluor 568 (Invitrogen Corp.). The cells were then briefly incubated (1 – 5 minutes) in 300 nM 4',6-diamidino-2-phenylindole (DAPI) and visualized with a Zeiss AxioImager Z1 using a 100x/1.4 Plan-Apochromat objective. In the non-adapted cells (under physiological or hypothermic conditions) the vimentin network formed a continuous sub-membrane shell around the perimeter of cell (Figure 6.9A). However, within low temperature-adapted cells the vimentin shell appeared irregular and discontinuous, with a significant portion of the network internalized to the perinuclear region of the cell relative to the DAPI-stained nuclei (Figure 6.9B).

6.2.2.2 – Analysis of the Vimentin Protein Monomer

Further characterization of the cellular vimentin network was performed on the molecular level to explore a potential mechanism responsible for the irregular and apparently weakened network structure. It was determined by Western-blot analysis that within the

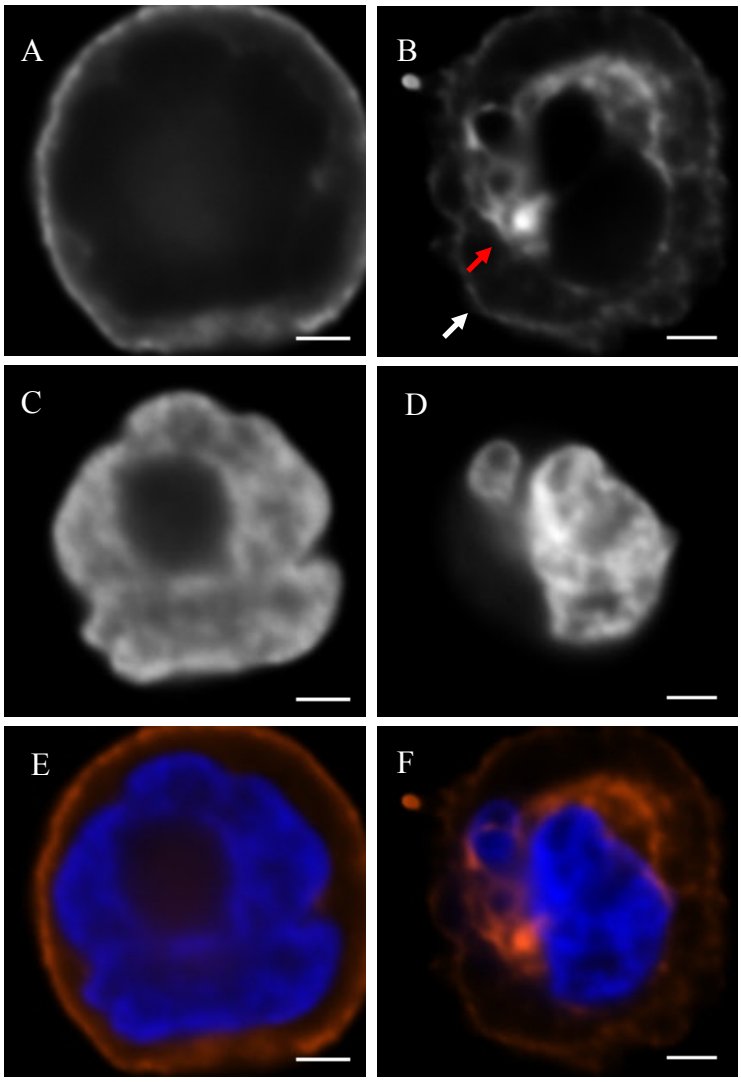

Figure 6.9: The structure of the vimentin intermediate filament network within non-adapted (panel A) and low temperature-adapted (panel B). Arrows indicate weakened external structure (white) and enhanced perinuclear localization (red). To provide reference for the perinuclear region, DAPI-stained nuclear structures are included as panels C and D, as are false-colour superimpositions of the two micrographs (panels E and F). (Bar = 2 μm)

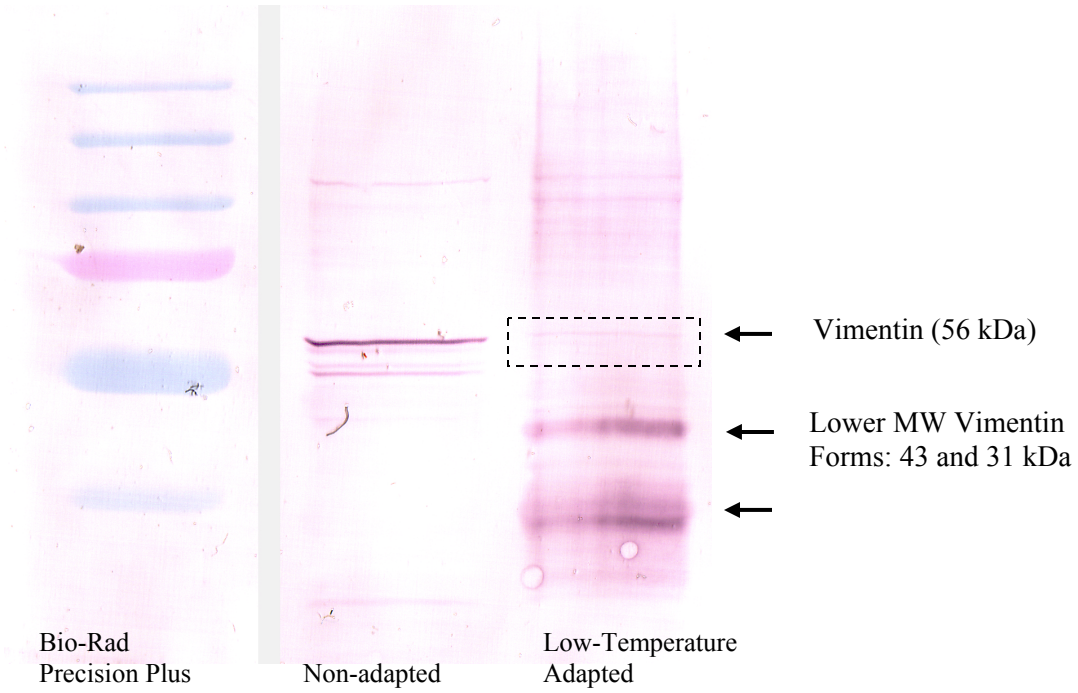

Figure 6.10: Western blot of cellular vimentin intermediate filament protein (56 kDa) from non- and cold-adapted CHO cells. 56 kDa vimentin band was absent in cold-adapted cells, concurrent with an appearance of lower molecular weight (43 and 31 kDa) vimentin fragments.

low-temperature adapted population the vimentin peptide (typically 56-57 kDa) had been truncated or degraded into two smaller molecular weight forms (43 and 31 kDa; Figure 6.10); with no significant quantity of the 57 kDa vimentin form detected by Western blot in the adapted sample (outlined in Figure 6.10). This analysis was performed using a 12% acrylamide SDS-PAGE one-dimensional gel for protein separation of cell lysates (approximately $1x10^7$ cells per sample), with the molecular weight determination calculated from a set of known molecular weight standards (Bio-Rad Precision Plus pre-stained protein standard) (Figure 6.11). Protein detection was carried out using a mouse anti-vimentin monoclonal antibody (clone V9 from Sigma Aldrich) and an anti-mouse alkaline phosphatase conjugated IgG antibody on a nitrocellulose membrane.

6.2.3 – Vimentin Monomers are Degraded through an Apoptosis-Independent Mechanism

The detection of two clear lower molecular forms of vimentin suggests that the modification of the 57 kDa form is likely a specific, targeted degradation; rather than random proteolysis or truncation of the reading frame of the vimentin gene.

Had numerous, randomly distributed lower MW products been detected, this would have implied a non-site specific degradation of the monomer, however it is clear from the Western blot that there are two primary degradative forms (43 and 31 kDa). For this to be a result of gene loss, two independent copies of the vimentin gene would have had to have been randomly truncated at different sites. While this is not impossible,

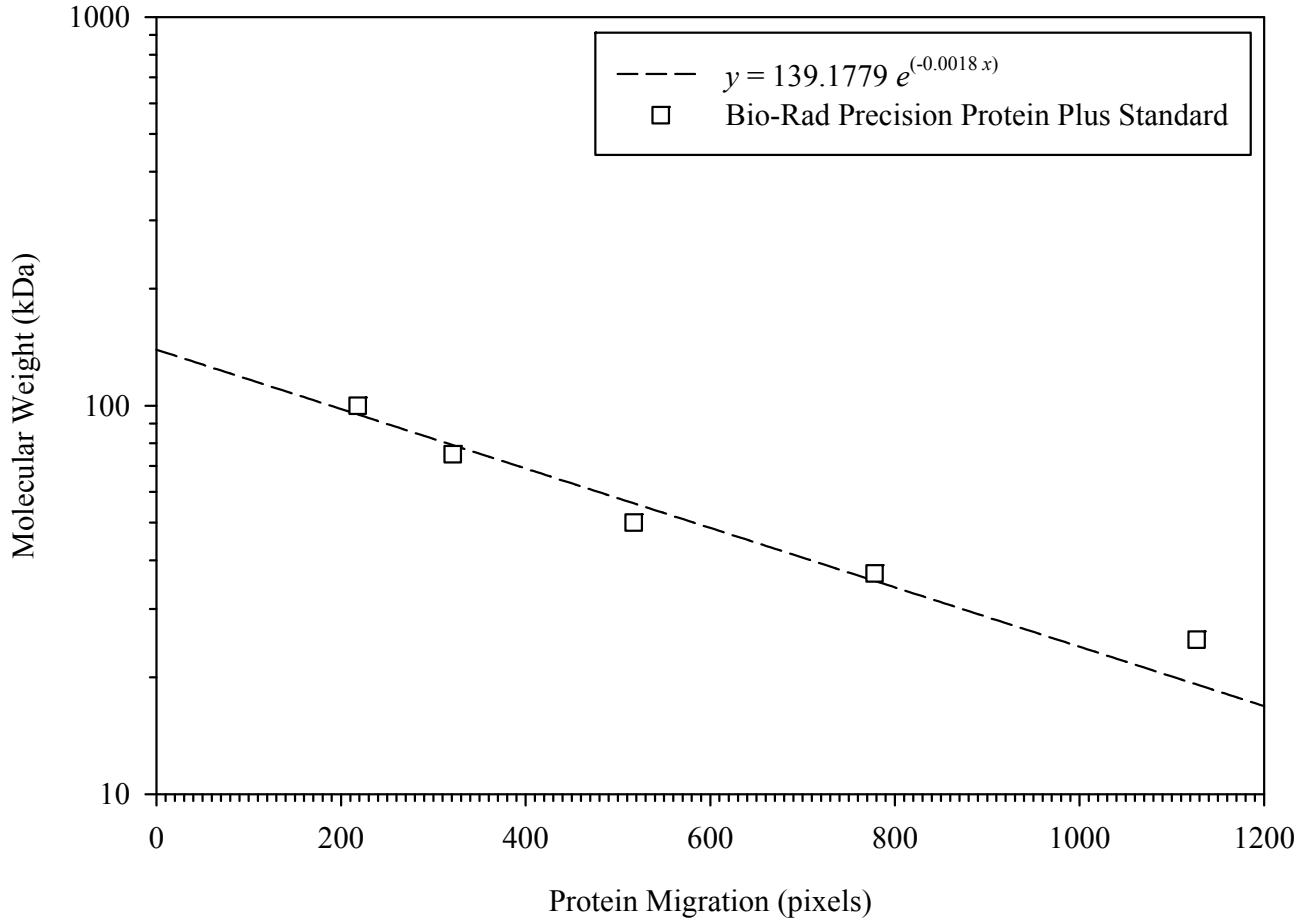

Figure 6.11: Determination of unknown molecular weights isolated by SDS-PAGE. Non-linear (2-parameter exponential decay) illustrates the apparent molecular weight as a function of distance traveled across the gel.

Table 6.2: Common apoptosis biomarkers and their presence/absence in non-adapted and cold-adapted recombinant CHO cells

Apoptotic Biomarker	Non-Adapted Population	Cold-Adapted Population	Method of Determination
Nuclear Fragmentation	-	+	Fluorescence Microscopy
Nuclear p53 Localization	-	-	Immunofluorescence Microscopy
Low-MW Vimentin Protein Forms	-	+	Western Blot
Caspase 3 and/or 7 Activity	-	-	Luminescence Assay
Apoptotic DNA fragmentation	-	-	Agarose Gel Electrophoresis
Apoptotic Bodies/Membrane Blebbing	-	I	Microscopy

I = Inconclusive; blebbing was observed sporadically throughout adapted population, minimally in some cultures. and significantly in others. Blebbing was never a dominant phenotype of any of the examined cultures

it is very improbable. Additionally, there have been no reported observations of lower molecular weight vimentin isoforms resulting from alternative splicing in Chinese hamster ovary cells. Indicating that there is no compelling evidence of vimentin monomer variations regulated at the transcriptional level. Therefore it has become more likely that the vimentin degradation, and subsequently increased fragility is result of vimentin-specific protein degradation. As a result, a review of published mechanisms which targeted vimentin for proteolytic degradation was performed; with the vast majority of research focusing on the interaction between apoptosis-mediation caspase enzymes and the vimentin monomer.

Vimentin, a known substrate for several of caspase proteins(142), is cleaved during early apoptosis. Caspases are a family of cysteine-specific proteases which are instrumental in inducing, regulating and executing apoptosis, otherwise known as programmed cell death. This, when considered with the increased frequency of nuclear fragmentation (Chapter 4.2.3.2) and the obvious dysregulation of the cell cycle (resulting in enhanced hypothermic growth), may suggest that apoptotic pathways are involved in, or triggered by the low temperature-adaptation process. However the absence of significant membrane blebbing and apoptotic bodies (condensed granules of sequestered cellular components); both of which are characteristic microscopically visible phenotypes of apoptosis, and assays for numerous apoptotic biomarkers indicated that there was no detectable apoptotic activity in either the non-adapted or adapted populations (Table 6.2).

6.2.3.1 – Absence of Caspase 3 and/or 7 Activity in Cold-adapted Cells

One of these assays was for intracellular activity of two of the most prominent executioner caspases; caspases 3 and 7. The caspases, called executioner caspases because of their active role in apoptosis, induced through members of the class of "initiator" caspases, begin a cascade of regulated proteolysis which coordinates the organized deconstruction and compartmentalization of the apoptotic cell. Apoptosis cannot proceed in the absence of caspase 3 and 7 activity, as they are key members of the apoptotic pathway.

No significant differences in caspase-3 or 7 activity was detected between the non-adapted and low temperature-adapted cells (Figure 6.12). This was determined through a luminescence-based assay (Caspase-Glo™ 3/7 from Promega Corp.), in which a proluminescent substrate; aminoluciferin covalently bound to the caspase 3/7-specific tetrapeptide aspartic acid-glutamic acid-valine-aspartic acid (DEVD-aminoluciferin) is cleaved by endogenous caspase activity into the aminoluciferin, a substrate for the luminescent reported enzyme luciferase. This assay was performed in a 96-well plate (approximately $1x10^4$ cells/well) and measured on a Synergy 2 multi-modal plate reader (BioTek Instruments Inc.). The absence of endogenous caspase activity indicates that the adaptation-induced truncated vimentin forms and nuclear fragmentation, despite their association with apoptotic processes are not caspase-induced and must be caused by some other, yet to be determined, cellular event.

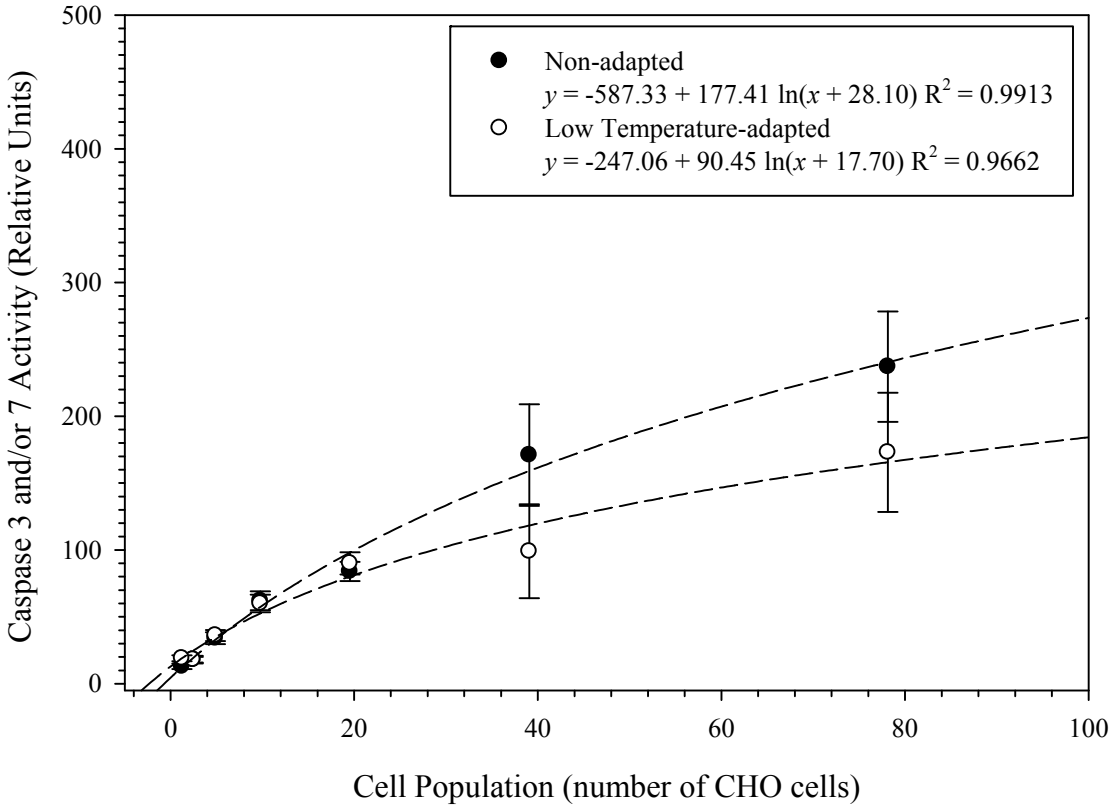

Figure 6.12: Caspase 3 and/or 7 activity in non-adapted and low temperature-adapted CHO cell samples. Non-linear (3-parameter logarithmic) regression illustrates activity over a range of cell populations. (n = 3 ± standard error)

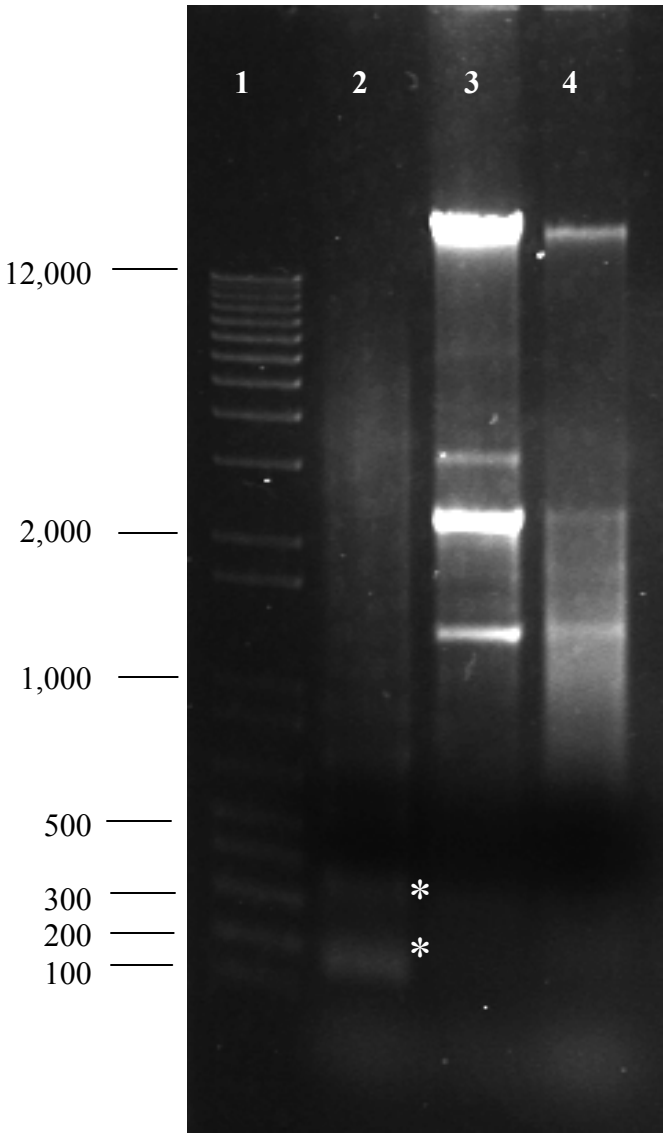

Figure 6.13: Detection of apoptosis-induced nuclease activity in cold-adapted (32°C) and non-adapted (37°C) CHO cells. Asterisks indicate apoptotic internucleosomal fragments. Note the absence of fragments in hypothermic and non-adapted samples.

Lane 1: DNA ladder (1 Kb Plus) ladder
Lane 2: Apoptotic U937 Cells (Positive Control)
Lane 3: Non-adapted CHO cells
Lane 4: Low-temperature adapted CHO cells

6.2.3.2 – Lack of Apoptosis-induced DNAse Activity in Low Temperature-adapted Cells

Confirming the lack of apoptotic activity, DNA was isolated from adapted and non-adapted populations was assayed for apoptotic nucleosomal fragments; 200 base pair (bp) DNA fragments produced by caspase-activated DNAses (CADs). This was performed through the use of an Apoptotic DNA Ladder Kit (Roche Diagnostics), and involves the lysis and DNA extraction from populations ($2x10^6$ cells/mL) of adapted and non-adapted cells on a DNA-binding glass fiber mesh. Cytosolic components were removed through centrifugation (approximately 700xg), and the remaining nuclear material was eluted from the glass mesh and separated electrophoretically on a 1% agarose gel (75V for 1.5 hours at room temperature) using ethidium bromide-free and bromophenol blue-free loading buffer. The DNA bands were visualized by staining the gel post-separation in a solution of ethidium bromide (0.5 μg/mL) and imaged in an Alpha Innotech Gel Documentation station. No DNA fragments of appropriate size (200 or 400 bp) were detectable in either of the populations (Figure 6.13), despite their appearance in a control population of apoptotic U937 human leukemic monocyte lymphoma cells. Short DNA fragments (in intervals of 200 bp) visualized through agarose gel electrophoresis would be indicative of CAD activity and late-apoptotic processes.

6.2.3.3 – No Nuclear p53 Accumulation was Observed in Low Temperature-adapted Cells

In p53-mediated growth arrest and apoptosis, the tumor suppressing protein p53 is translocated to the nucleus; a mechanism necessary for the protein to affect gene expression. p53 localization was determined by immunofluorescence to be sequestered

within the cytoplasm in both non-adapted and low temperature-adapted cells (Figure 6.14) under hypothermic conditions. Cells were harvested from viable (>90%) exponentially growing cultures, fixed and permeabilized using standard immunofluorescence techniques (15 minute incubations in 4% paraformaldehyde and 0.1% Triton X-100 respectively). p53 was targeted through the use of a mouse anti-human p53 monoclonal antibody (clone DO-7 from Sigma Aldrich), briefly incubated for 1 – 5 minutes in a 300 nM solution of 4',6-diamidino-2-phenylindole (DAPI) and then visualized through a goat produced anti-mouse IgG molecule conjugated to the fluorescent dye Alexa Fluor 568 (Invitrogen Corp.) with a Zeiss Plan-Apochromat 100x/1.4 objective on an AxioImager Z1 fluorescence microscope. p53 localization was categorized as either nuclear or cytosolic relative to the location of the DAPI-stained nucleus.

This assay confirmed that the apoptotic-like symptoms within the low temperature-adapted cells (multi-nuclear/nuclear fragmentation and lower MW vimentin forms) occurred in the absence of conclusive apoptotic biomarkers.

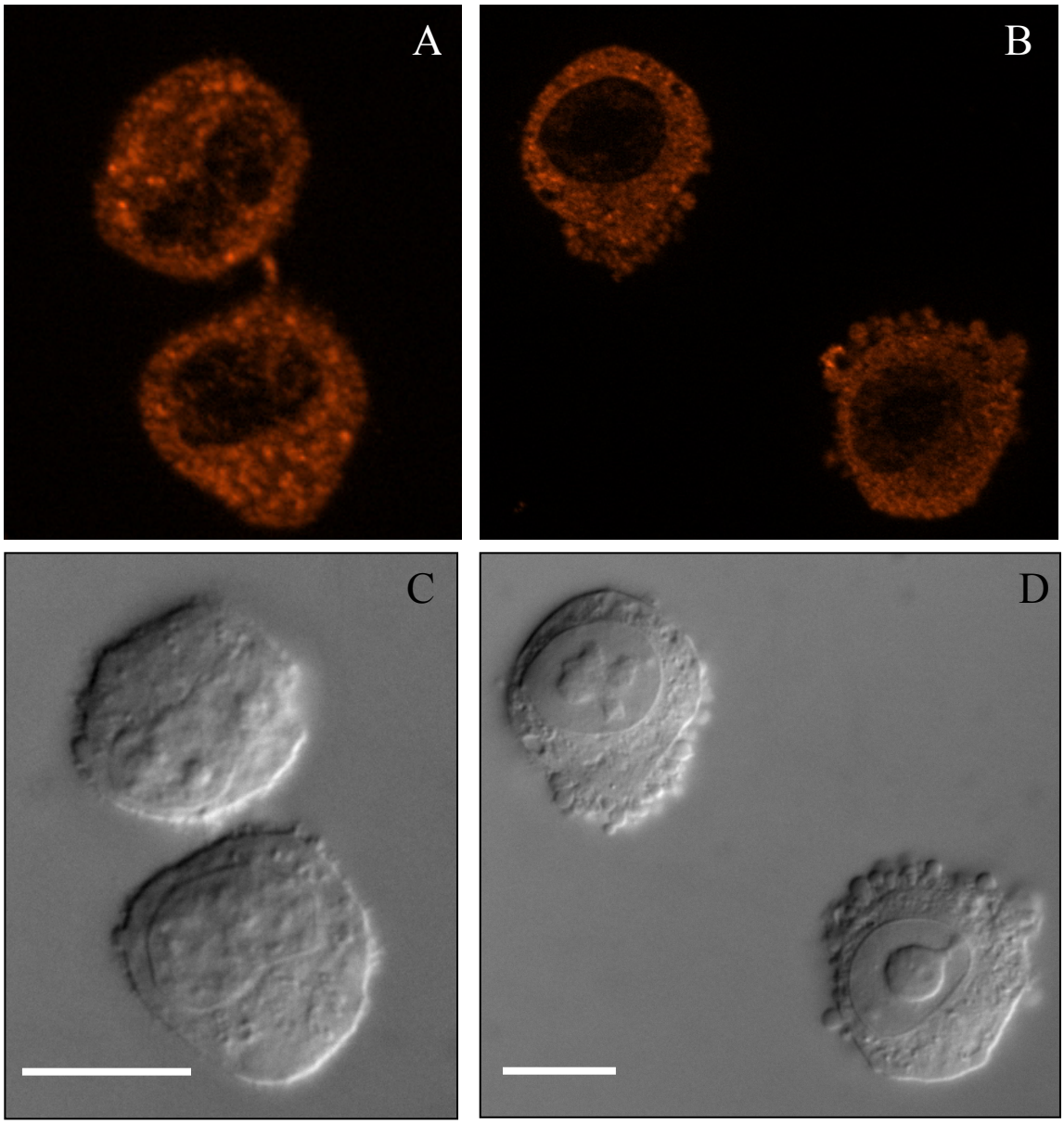

Figure 6.14: Cytosolic p53 localization in non-adapted (panel A) and low-temperature adapted (panel B) CHO cells under hypothermic conditions. Reference micrographs of relevant non- and cold-adapted cells are illustrated in panels C and C respectively. (Bar = 25 μm)

Chapter 6.3 – Discussion

The perceived sensitivity to mechanical agitation of the low temperature-adapted population discussed in Chapter 5 was further investigated in an effort to quantify the magnitude of the sensitivity in context of the parental non-adapted population.

Quantification was performed in two respects; a population-based assay which determined the overall response of the two populations to varying degrees of mechanical agitation; and on a cellular level, where individual cells were measured within each of the populations. Physiological causes for the increased fragility were also investigated; identifying cytoskeletal changes induced through the adaptation process likely resulted in the increased fragility.

6.3.1 – The Effect of Adaptation-induced Fragility on Populations of Recombinant CHO Cells

The inability of the low temperature-adapted cells to proliferate in an agitated environment demonstrated an inherent fragility which developed through the selection process. The relationship determined through exposing populations of cells to a series of increasing levels of mechanical stress demonstrated that cellular damage was proportional to the rate of agitation (using the presence of a cytosolic enzyme in the culture supernatant as a marker for compromised cell membranes). This indicates that the inhibited culture growth can be attributed to physical cell damage, rather than an induced cell cycle arrest or another regulated form of growth arrest; facilitating the entry of a non-secreted cytosolic enzyme (lactate dehydrogenase) into the culture supernatant.

The extent of membrane damage varied significantly between the two populations; with the low temperature adapted cells losing membrane integrity 10-fold faster than the non-adapted population in response to the same external stresses (Figure 6.1A and B). It was also immediately apparent that the culturing of cells within macroporous microcarriers decreased the cells susceptibility over 4-fold (Figures 6.1C and D), presumably by sequestering the cells within an environment sheltered from hydrodynamic forces.

This was confirmed through in situ viability determination of individual microcarrier-entrapped cells exposed high levels of hydrodynamic stress. Within the microcarrier structure, the rate of membrane failure was direction proportional to the proximity of the cell to the exterior of the carrier. This demonstrates that the carrier structure and the localization of the cell within it are responsible for the protective nature of microcarrier culturing; a phenomenon which has been presented previously in within our research group and others (128, 143, 144), although not to this resolution.

6.3.2 – Increased Cellular Fragility and Loss of Heterogeneity within the Adapted Population

The final stage of characterization which was performed was to determine the effect of the increased fragility on the physical properties of intact adapted cells. CHO cells (when cultured in suspension) are spherical(145), robust cells, capable of growth within agitated cultures without a significant loss of viability. As already discussed, the low temperature-adapted population was found to be incapable growth within this type of environment, leading to the presumption that they were significantly more fragile.

The strength of their mechanical structure was investigated at the resolution of an individual cell, subjecting populations to a fixed centrifugal force, following the method of Brown et al.(136), and monitoring for any structural deformation which occurred. A deformability index (DI) was calculated for each observed cell to allow relative comparisons within and between populations; a value which represents the ratio of the X or Y-axis diameter of the cell to its Z-axis height. This provides an intuitive system for recognizing the strength of a cell's structure; where a DI of 1.0 indicates no deformation occurred (the cell was spherical with a width equal to its diameter), 2.0 represents a cell which was compressed to half its initial height, and further increasing values signifying cells which were compressed to even greater extents. From this, cells were categorized more generally, being either resistant (DI < 2.0) or susceptible (DI > 2.0) to mechanical deformation.

The parental, non-adapted population was found to be heterogeneous in terms of the strength of its member's structures; containing both resistant and susceptible phenotypes. The size of the cell appeared to have an effect the strength of its structure, as all the cells classified as susceptible to deformation were larger than 15 μm in diameter. However within the population of cells smaller than this; a cell of a given size could be found to be either susceptible or resistant.

The cold-adapted population exhibited a significantly different profile, containing no cells resistant to deformation. The absence of smaller cells (which were the most resistance to deformation in the non-adapted population) could partially account for this

result, although the smaller cells within the non-adapted population demonstrated that this effect was not solely a function of cell size. Therefore it is likely that additional intracellular effects (other than the size of the cell) are responsible the fragility of the adapted population.

6.3.3 – Fragility within Adapted Population is a Result of a Compromised Intermediate Filament Network

The strength of the overall cellular structure is conferred through a combination of an intact cell membrane and an organized cytoskeleton. The cell membrane is a dynamic, fluid structure which must remain intact and pliable through many environmental conditions and cellular processes for the cell to remain viable(137). In this work, two strategies were attempted to determine whether deficiencies in the membrane itself were responsible for the fragility of the adapted population.

6.3.3.1 – Increased Fragility a Result of a Membrane-independent Cellular Event

The first approach involved the supplementation of the culture media with a complex concentrate of lipoproteins, cholesterol and fatty acids; which would compensate for any deficiencies in the culture media or the cell's synthetic pathways. Supplementing low temperature-adapted cultures with up to 5-fold greater than the manufacturer's recommended concentration had no restorative effect on the ability of the population to survive within agitated cultures.

Pluronic™ F-68, a non-ionic surfactant with known cellular protective properties against hydrodynamic stress(138), was also utilized to attempt facilitate growth in stirred-tank cultures. Concentrations were increased up to 5-fold greater than the experimentally determined ideal(139), however no protective effect was observed beyond the 0.2% concentration routinely used within the serum-free media developed for the growth of the parental population.

These procedures reduced the likelihood of the membrane as an adaptation-induced weak point in the cell structure by ensuring all membrane components were available in excess and coating to membrane with a surfactant to reduce in-culture shear forces.

6.3.3.2 – Truncated Vimentin Forms Result in a Disorganized, Irregular Intermediate Filament Network

The cytoskeleton is a network of three classes of filament proteins: actin filaments, intermediate filaments (IF) and microtubules; each with many functional roles within the cell. The intermediate filament network, and particularly the type III intermediate filament protein vimentin, is well characterized for its structural role in the cell(136, 140). However, the role of vimentin within the cell is complex; with additional roles in the intracellular activation of caspases(142, 146, 147), nuclear(148, 149) and Golgi organization(150), cell adhesion, migration and cell signaling(151).

Due to its well characterized role as a structural element within the cell(136) and reports of vimentin expression being modulated as a result of hypothermic (32°C)

exposure(141), the role of vimentin in the increased cell fragility was investigated. The continuous peripheral protective protein network in the parental population was absent from a subset of cells in the adapted population, and irregular in appearance in others. This is reminiscent of the results of Brown et al.(136), who observed the disruptive of effect of calyculin A on the vimentin IF network and a subsequent increase in cell fragility. The cold-adapted vimentin network also appeared in internalize itself to the perinuclear region of the cell. As it is known that there is a direct interaction between the vimentin IF network and the Golgi apparatus (through the Golgi-specific protein formiminotransferase)(150); it could be speculated that in addition to up-regulation of proteins involved in the secretory pathway(141), interactions between vimentin and the Golgi apparatus were increased to support increased cellular translation.

These results indicate that the mechanism behind the disruption of the vimentin IF network is likely induced site-specific proteolysis of the vimentin monomer. The smaller molecular weight vimentin peptides observed in the adapted cell population existed primarily in two forms; a 43 and 31 kDa form (compared to 57 kDa of an intact monomer). The cleavage of the vimentin monomer was necessarily specific as it resulted in only two molecular weight forms (minimal protein fragments were observed at other weight ranges). Proteolysis of vimentin has been previously reported(142, 146, 152-154), believed to be involved in the apoptosis signaling pathway; as both an inducer molecule and a substrate for executioner and initiator caspases. Caspases, a family of cysteine proteases, regulate and mediate the process of apoptosis through highly regulated proteolysis of intracellular proteins(155). Members of the caspase family

which have been observed to cleave vimentin include the initiator caspases 8 and 9, and the executioner caspases 3 and 6; cleaving at aspartic acid residues 85 or 259 and 429 respectively(146). Retroviral proteases (PRs); including those from human immunodeficiency virus type 1 (HIV-1) and type 2 (HIV-2), bovine leukemia virus (BLV), Mason-Pfizer monkey virus (M-PMV) and myeloblastosis-associated virus (MAV) have also been found to be involved in vimentin degradation(156), however this requires an active infection within the cell population which was not present in cultures described in this work.

Caspase or PR-induced proteolysis of vimentin results in a complex mixture of fragments of varying molecular weights. Caspase-proteolysis produces fragments of 47, 41, 28 and 22 kDa, and additional fragments which would not be detected by the anti-vimentin monoclonal antibody (clone V9) used throughout this thesis(146) due to its specificity to the carboxyl-terminal end of protein. These fragments fit within the range of fragments observed within the adapted population vimentin profile (43 and 31 kDa), considering that the SDS-PAGE method of molecular weight determination should be assumed to include an error of at least ± 5 to 10%(157).

6.3.3.3 – Caspase and Apoptosis-independent Vimentin Proteolysis

Vimentin proteolysis has been hypothesized to function as a regulatory mechanism involved in the restructuring of cellular intermediate filament networks; as the extreme insolubility of the vimentin monomers would inhibit polymerization and

depolymerization(158). To determine whether the vimentin degradation was caspase-mediated, the activity of executioner caspases 3 and 7 was assayed against the background level present in the non-adapted, robust cell population. From the lack of significant differences between the two populations, it can be inferred that the absence of executioner caspase activity (and the deduced lack of upstream initiator caspase activity which would have induced executioner activity) presents the adaptation-induced vimentin degradation as a caspase-independent phenomenon.

Further markers of apoptosis, specifically early-stage apoptotic p53 translocation(159) and late-stage caspase-activated DNAse activity(160) were investigated. Both wild-type and mutant forms of p53, a transcription factor involved in cell cycle regulation and the initiation of apoptosis, require nuclear accumulation to affect gene expression(159). The cytosolic sequestering of p53 under hypothermic conditions in the adapted and non-adapted populations, inhibiting its interacting with cellular genetic material, demonstrated that the hypothermic growth arrest exhibited by the non-adapted population and the degradation of vimentin monomers occurred independently of p53-induced growth arrest and in the absence of apoptotic initiation.

The lack of caspase-activated DNAse activity further confirms the absence of an apoptotic phenotype, compelling evidence that the dissociation of the vimentin IF network is mediated by a novel apoptosis- and retrovirus-independent mechanism. While this does not present a direct molecular mechanism for the increased cellular fragility, it

does describe an emergent correlation between the mechanical properties of the cold-adapted population and intra-cellular regulation of structural proteins.

6.3.4 – Increased Cellular Fragility an Emergent Trait of Low Temperature-Adaptation Process

In the context of the biopharmaceutical protein production and the success of the low temperature-adapted populations presented in this thesis, it is still unknown whether the enhanced shear sensitivity was a direct consequence of adaptation to low temperature growth or an independent, simultaneously isolated trait. However, it is important to note that in the cold-adapted (32°C) cell populations described by Yoon et al.(33), previously discussed in Chapter 1.5.6, the iterative subculturing throughout their adaptation process was performed in a series of stirred spinner flask vessels. The possibility that this process, inherently selective against fragile cells, played a role in the inability of their cultures to sustain high levels of specific heterologous protein expression throughout the adaptation process cannot be overlooked.

This thesis presents this significant reduction in cell robustness, induced through an active regulatory mechanism (rather than a limiting nutrient leading to a weakened membrane), as an adaptive trait which cannot be easily isolated from the beneficial effects of the low temperature adaptation process.

Chapter 7 – Conclusions and Future Work

Chapter 7.1 – Conclusions

This thesis presents a novel method of cell culture optimization which had not been successfully implemented in published literature. The induction of active hypothermic growth, allowing for increased cell proliferation under typically prohibitive sub-physiological temperatures, without the addition of exogenous growth factors or targeted genetic modification yielded significantly increased product titres of a therapeutic biologic.

The strength of this approach is that it approaches the development of a cold-adapted cell population by selecting for the desired phenotype, rather than attempting to induce the phenotype through predictive genetic modification. This circumvents the primary limitation of genetic modifications; the lack of a thorough understand of cellular metabolism, and in the case of the Chinese hamster ovary cell line CHO-K1, the lack of a publicly available genome sequence. Through the culturing of cells under a significant selective pressure (a prohibitive growth temperature), a sub-population of cells capable of active hypothermic growth was isolated without prior knowledge of the metabolic systems responsible its regulation. These isolates can also be used to gain knowledge of such regulatory systems, by retrospectively investigating the changes which were induced; in this case, the circumvention of temperature dependent cell cycle control and factors leading to a cell's mechanical integrity.

This thesis presents a process which has successfully isolated a population of cold-adapted cells which has not lost its ability to produce enhanced titres of heterologous protein under sub-physiological conditions. This is in contrast to the only other published account of cold-adaptation of a recombinant cell line, which failed to maintain an elevated specific productivity(111). Also described is a scalable bioprocess which has the potential to employ these cells in multi-litre stirred-tank bioreactor cultures, a criteria which is essential for an industrially relevant cell line.

Chapter 7.2 – Future Work

The work described in this dissertation could be furthered by carrying research forward in two distinct directions. Published literature on mild-hypothermic growth of CHO cells leads to the speculation that optimization of the low temperature culture conditions, specifically environmental (pH and dissolved oxygen) and nutrient conditions, would likely yield significantly enhanced protein production beyond what has been achieved in this project. Cells under mild hypothermic temperatures have been found to be increasingly sensitive to changes in pH(75), and require significantly different nutrient requirements(109); these variables, along with the inherent link between temperature and the capacity of culture media to absorb oxygen, have not yet been thoroughly explored. A comprehensive investigation of a low temperature environment, the cellular cold-shock metabolic response, and its effect on the protein production of the adapted cells would likely yield significant benefits in terms of protein expression.

Additionally, the population of cold-adapted cells offers an opportunity to identify novel regulatory mechanisms involved in cold-induced growth arrest and elevated recombinant protein expression. A more detailed understanding of these regulatory systems would provide targets for direct genetic manipulation, further improving already successful controlled proliferation strategies.

This thesis provides strong and convincing evidence that a recombinant Chinese hamster ovary cell line is capable of adaptation to sub-physiological temperatures, and that this adaptation can be used advantageously for the production of recombinant therapeutics. This allows the effects of cold-induced growth arrest, the most significant limitation to product yields under hypothermic conditions, to be minimized; increasing product yields several fold with only minimal additional input costs.

Chapter 8 - References

1. Puck TT. Growth and genetics in somatic mammalian cells in vitro. J. Cell Physiol. Suppl. 1958 Dec;52(Supp 1):287-302.

2. Fujita J. Cold shock response in mammalian cells. J. Mol. Microbiol. Biotechnol. 1999 Nov;1(2):243-55.

3. Karpusas M, Whitty A, Runkel L, Hochman P. The structure of human interferon-beta: implications for activity. Cell. Mol. Life Sci. 1998 Nov;54(11):1203-16.

4. Jayapal KP, Wlaschin KF, Hu W, Yap MGS. Recombinant Protein Therapeutics from CHO Cells - 20 Years and Counting. Chem. Eng. Prog. 2007;103(10):40.

5. Walsh G, Jefferis R. Post-translational modifications in the context of therapeutic proteins. Nat. Biotechnol. 2006 Oct;24(10):1241-52.

6. Sinclair AM, Elliott S. Glycoengineering: the effect of glycosylation on the properties of therapeutic proteins. J. Pharm. Sci. 2005 Aug;94(8):1626-35.

7. Wurm FM. Production of recombinant protein therapeutics in cultivated mammalian cells. Nat. Biotechnol. 2004 Nov;22(11):1393-8.

8. Lukas J, Lukas C, Bartek J. Mammalian cell cycle checkpoints: signalling pathways and their organization in space and time. DNA Repair. 2004 Aug-Sep;3(8-9):997-1007.

9. Kastan MB, Bartek J. Cell-cycle checkpoints and cancer. Nature. 2004 Nov 18;432(7015):316-23.

10. Afshari CA, Barrett JC. Disruption of G0-G1 arrest in quiescent and senescent cells treated with phosphatase inhibitors. Cancer Res. 1994 May 1;54(9):2317-21.

11. Kumar N, Gammell P, Clynes M. Proliferation control strategies to improve productivity and survival during CHO based production culture. Cytotechnology. 2007;53(1):33-46.

12. Bi JX, Shuttleworth J, Al-Rubeai M. Uncoupling of cell growth and proliferation results in enhancement of productivity in p21CIP1-arrested CHO cells. Biotechnol. Bioeng. 2004 Mar 30;85(7):741-9.

13. Carvalhal AV, Marcelino I, Carrondo MJ. Metabolic changes during cell growth inhibition by p27 overexpression. Appl. Microbiol. Biotechnol. 2003 Dec;63(2):164-73.

14. Dez C, Tollervey D. Ribosome synthesis meets the cell cycle. Curr. Opin. Microbiol. 2004 Dec;7(6):631-7.

15. Weinberg RA. The retinoblastoma protein and cell cycle control. Cell. 1995 May 5;81(3):323-30.

16. Magae J, Wu CL, Illenye S, Harlow E, Heintz NH. Nuclear localization of DP and E2F transcription factors by heterodimeric partners and retinoblastoma protein family members. J. Cell Sci. 1996 Jul;109 (Pt 7):1717-26.

17. Lagger G, O'Carroll D, Rembold M, Khier H, Tischler J, Weitzer G, et al. Essential function of histone deacetylase 1 in proliferation control and CDK inhibitor repression. EMBO J. 2002 Jun 3;21(11):2672-81.

18. Hendrick V, Winnepenninckx P, Abdelkafi C, Vandeputte O, Cherlet M, Marique T, et al. Increased productivity of recombinant tissular plasminogen activator (t-PA) by butyrate and shift of temperature: a cell cycle phases analysis. Cytotechnology. 2001 Jul;36(1-3):71-83.

19. Hunt L, Batard P, Jordan M, Wurm FM. Fluorescent proteins in animal cells for process development: optimization of sodium butyrate treatment as an example. Biotechnol Bioeng. 2002 Mar 5;77(5):528-37.

20. Hwa Chang K, Hwa Park J, Hyung Lee Y, Ho Kim J, Ok Chun H, Hak Kim J, et al. Dimethylsulfoxide and sodium butyrate enhance the production of recombinant cyclooxygenase 2 in stably transformed Drosophila melanogaster S2 cells. Biotechnol. Lett. 2002;24(16):1353-9.

21. Fiore M, Zanier R, Degrassi F. Reversible G(1) arrest by dimethyl sulfoxide as a new method to synchronize Chinese hamster cells. Mutagenesis. 2002 Sep;17(5):419-24.

22. Liu CH, Chu IM, Hwang SM. Enhanced expression of various exogenous genes in recombinant Chinese hamster ovary cells in presence of dimethyl sulfoxide. Biotechnol. Lett. 2001;23(20):1641-5.

23. Allen MJ, Boyce JP, Trentalange MT, Treiber DL, Rasmussen B, Tillotson B, et al. Identification of novel small molecule enhancers of protein production by cultured mammalian cells. Biotechnol. Bioeng. 2008 Aug 15;100(6):1193-204.

24. Wright JA. Morphology and growth rate changes in Chinese hamster cells cultured in presence of sodium butyrate. Exp. Cell Res. 1973 Apr;78(2):456-60.

25. Gorman CM, Howard BH, Reeves R. Expression of recombinant plasmids in mammalian cells is enhanced by sodium butyrate. Nucleic Acids Res. 1983 Nov 11;11(21):7631-48.

26. Dorner AJ, Wasley LC, Kaufman RJ. Increased synthesis of secreted proteins induces expression of glucose-regulated proteins in butyrate-treated Chinese hamster ovary cells. J. Biol. Chem. 1989 Dec 5;264(34):20602-7.

27. Vaziri C, Stice L, Faller DV. Butyrate-induced G1 arrest results from p21-independent disruption of retinoblastoma protein-mediated signals. Cell Growth Differ. 1998 Jun;9(6):465-74.

28. Xue S, Rao PN. Sodium butyrate blocks HeLa cells preferentially in early G1 phase of the cell cycle. J. Cell Sci. 1981 Oct;51:163-71.

29. D'Anna JA, Tobey RA, Gurley LR. Concentration-dependent effects of sodium butyrate in Chinese hamster cells: cell-cycle progression, inner-histone acetylation, histone H1 dephosphorylation, and induction of an H1-like protein. Biochemistry. 1980 Jun 10;19(12):2656-71.

30. Schwartz B, Avivi-Green C, Polak-Charcon S. Sodium butyrate induces retinoblastoma protein dephosphorylation, p16 expression and growth arrest of colon cancer cells. Mol. Cell. Biochem. 1998 Nov;188(1-2):21-30.

31. Buquet-Fagot C, Lallemand F, Charollais RH, Mester J. Sodium butyrate inhibits the phosphorylation of the retinoblastoma gene product in mouse fibroblasts by a transcription-dependent mechanism. J. Cell. Physiol. 1996 Mar;166(3):631-6.

32. Siavoshian S, Blottiere HM, Cherbut C, Galmiche JP. Butyrate stimulates cyclin D and p21 and inhibits cyclin-dependent kinase 2 expression in HT-29 colonic epithelial cells. Biochem. Biophys. Res. Commun. 1997 Mar 6;232(1):169-72.

33. Archer SY, Meng S, Shei A, Hodin RA. p21(WAF1) is required for butyrate-mediated growth inhibition of human colon cancer cells. Proc. Natl. Acad. Sci. USA. 1998 Jun 9;95(12):6791-6.

34. Göttlicher M, Minucci S, Zhu P, Kramer OH, Schimpf A, Giavara S, et al. Valproic acid defines a novel class of HDAC inhibitors inducing differentiation of transformed cells. EMBO J. 2001 Dec 17;20(24):6969-78.

35. Kramer OH, Gottlicher M, Heinzel T. Histone deacetylase as a therapeutic target. Trends Endocrinol. Metab. 2001 Sep;12(7):294-300.

36. Nolan L, Johnson PW, Ganesan A, Packham G, Crabb SJ. Will histone deacetylase inhibitors require combination with other agents to fulfil their therapeutic potential? Br. J. Cancer. 2008 Sep 2;99(5):689-94.

37. Dokmanovic M, Clarke C, Marks PA. Histone deacetylase inhibitors: overview and perspectives. Mol. Cancer Res. 2007 Oct;5(10):981-9.

38. Yee JC, de Leon Gatti M, Philp RJ, Yap M, Hu WS. Genomic and proteomic exploration of CHO and hybridoma cells under sodium butyrate treatment. Biotechnol. Bioeng. 2008 Apr 1;99(5):1186-204.

39. Jiang Z, Sharfstein ST. Sodium butyrate stimulates monoclonal antibody over-expression in CHO cells by improving gene accessibility. Biotechnol. Bioeng. 2008 May 1;100(1):189-94.

40. Mimura Y, Lund J, Church S, Dong S, Li J, Goodall M, et al. Butyrate increases production of human chimeric IgG in CHO-K1 cells whilst maintaining function and glycoform profile. J. Immunol. Methods. 2001 Jan 1;247(1-2):205-16.

41. Lamotte D, Buckberry L, Monaco L, Soria M, Jenkins N, Engasser JM, et al. Na-butyrate increases the production and alpha2,6-sialylation of recombinant interferon-gamma expressed by alpha2,6- sialyltransferase engineered CHO cells. Cytotechnology. 1999 Jan;29(1):55-64.

42. Jeon MK, Lee GM. Correlation between enhancing effect of sodium butyrate on specific productivity and mRNA transcription level in recombinant Chinese hamster ovary cells producing antibody. J. Microbiol. Biotechnol. 2007 Jun;17(6):1036-40.

43. Kuo MH, Allis CD. Roles of histone acetyltransferases and deacetylases in gene regulation. Bioessays. 1998 Aug;20(8):615-26.

44. Calabresse C, Venturini L, Ronco G, Villa P, Chomienne C, Belpomme D. Butyric acid and its monosaccharide ester induce apoptosis in the HL-60 cell line. Biochem. Biophys. Res. Commun. 1993 Aug 31;195(1):31-8.

45. Kim NS, Lee GM. Overexpression of bcl-2 inhibits sodium butyrate-induced apoptosis in Chinese hamster ovary cells resulting in enhanced humanized antibody production. Biotechnol. Bioeng. 2000;71(3):184-93.

46. Kim NS, Lee GM. Inhibition of sodium butyrate-induced apoptosis in recombinant Chinese hamster ovary cells by constitutively expressing antisense RNA of caspase-3. Biotechnol. Bioeng. 2002 Apr 20;78(2):217-28.

47. Fussenegger M, Moser S, Bailey JE. Regulated multicistronic expression technology for mammalian metabolic engineering. Cytotechnology. 1998 Nov;28(1-3):111-26.

48. Fussenegger M, Mazur X, Bailey JE. A novel cytostatic process enhances the productivity of Chinese hamster ovary cells. Biotechnol. Bioeng. 1997 Sep 20;55(6):927-39.

49. Mazur X, Fussenegger M, Renner WA, Bailey JE. Higher productivity of growth-arrested Chinese hamster ovary cells expressing the cyclin-dependent kinase inhibitor p27. Biotechnol. Prog. 1998 Sep-Oct;14(5):705-13.

50. Meents H, Enenkel B, Werner RG, Fussenegger M. p27Kip1-mediated controlled proliferation technology increases constitutive sICAM production in CHO-DUKX adapted for growth in suspension and serum-free media. Biotechnol. Bioeng. 2002 Sep 20;79(6):619-27.

51. Fussenegger M, Schlatter S, Daetwyler D, Mazur X, Bailey JE. Controlled proliferation by multigene metabolic engineering enhances the productivity of Chinese hamster ovary cells. Nat. Biotechnol. 1998;16(5):468-72.

52. Ekholm SV, Reed SI. Regulation of G1 cyclin-dependent kinases in the mammalian cell cycle. Curr. Opin. Cell Biol. 2000;12(6):676-84.

53. Reynisdottir I, Polyak K, Iavarone A, Massague J. Kip/Cip and Ink4 Cdk inhibitors cooperate to induce cell cycle arrest in response to TGF-beta. Genes Dev. 1995 Aug 1;9(15):1831-45.

54. Datto MB, Li Y, Panus JF, Howe DJ, Xiong Y, Wang XF. Transforming growth factor beta induces the cyclin-dependent kinase inhibitor p21 through a p53-independent mechanism. Proc. Natl. Acad. Sci. USA. 1995 Jun 6;92(12):5545-9.

55. Vazquez A, Bond EE, Levine AJ, Bond GL. The genetics of the p53 pathway, apoptosis and cancer therapy. Nat. Rev. Drug Discov. 2008 Dec;7(12):979-87.

56. Khoo SH, Al-Rubeai M. Detailed understanding of enhanced specific antibody productivity in NS0 myeloma cells. Biotechnol. Bioeng. 2009 Jan 1;102(1):188-99.

57. Zahn-Zabal M, Kobr M, Girod PA, Imhof M, Chatellard P, de Jesus M, et al. Development of stable cell lines for production or regulated expression using matrix attachment regions. J. Biotechnol. 2001 Apr 27;87(1):29-42.

58. Watanabe I, Okada S. Effects of temperature on growth rate of cultured mammalian cells (L5178Y). J. Cell Biol. 1967 Feb;32(2):309-23.

59. Lindquist S. The heat-shock response. Annu. Rev. Biochem. 1986;55:1151-91.

60. Kühl NM, Rensing L. Heat shock effects on cell cycle progression. Cell. Mol. Life Sci. 2000 Mar;57(3):450-63.

61. Phadtare S, Alsina J, Inouye M. Cold-shock response and cold-shock proteins. Curr. Opin. Microbiol. 1999 Apr;2(2):175-80.

62. Sonna LA, Fujita J, Gaffin SL, Lilly CM. Invited review: Effects of heat and cold stress on mammalian gene expression. J. Appl. Physiol. 2002 Apr;92(4):1725-42.

63. Rieder CL, Cole RW. Cold-shock and the Mammalian cell cycle. Cell Cycle. 2002 May-Jun;1(3):169-75.

64. Al-Fageeh MB, Smales CM. Control and regulation of the cellular responses to cold shock: the responses in yeast and mammalian systems. Journal of Biochemistry. 2006 Jul 15;397(2):247-59.

65. Underhill MF, Smales CM. The cold-shock response in mammalian cells: investigating the HeLa cell cold-shock proteome. Cytotechnology. 2007;53(1):47-53.

66. Gammell P, Barron N, Kumar N, Clynes M. Initial identification of low temperature and culture stage induction of miRNA expression in suspension CHO-K1 cells. J. Biotechnol. 2007 Jun 30;130(3):213-8.

67. Beer C, Buhr P, Hahn H, Laubner D, Wirth M. Gene expression analysis of murine cells producing amphotropic mouse leukaemia virus at a cultivation temperature of 32 and 37 degrees C. J. Gen. Virol. 2003 Jul;84(Pt 7):1677-86.

68. Baik JY, Lee MS, An SR, Yoon SK, Joo EJ, Kim YH, et al. Initial transcriptome and proteome analyses of low culture temperature-induced expression in CHO cells producing erythropoietin. Biotechnol. Bioeng. 2006 Feb 5;93(2):361-71.

69. Nishiyama H, Itoh K, Kaneko Y, Kishishita M, Yoshida O, Fujita J. A glycine-rich RNA-binding protein mediating cold-inducible suppression of mammalian cell growth. J. Cell Biol. 1997 May 19;137(4):899-908.

70. Dresios J, Aschrafi A, Owens GC, Vanderklish PW, Edelman GM, Mauro VP. Cold stress-induced protein Rbm3 binds 60S ribosomal subunits, alters microRNA levels, and enhances global protein synthesis. Proc. Natl. Acad. Sci. USA. 2005 Feb 8;102(6):1865-70.

71. Matijasevic Z, Snyder JE, Ludlum DB. Hypothermia causes a reversible, p53-mediated cell cycle arrest in cultured fibroblasts. Oncol. Res. 1998;10(11-12):605-10.

72. Yoon SK, Song JY, Lee GM. Effect of low culture temperature on specific productivity, transcription level, and heterogeneity of erythropoietin in Chinese hamster ovary cells. Biotechnol. Bioeng. 2003 May 5;82(3):289-98.

73. Jorjani P, Ozturk SS. Effects of cell density and temperature on oxygen consumption rate for different mammalian cell lines. Biotechnol. Bioeng. 1999 Aug 5;64(3):349-56.

74. Rodriguez J, Spearman M, Huzel N, Butler M. Enhanced production of monomeric interferon-beta by CHO cells through the control of culture conditions. Biotechnol. Prog. 2005 Jan-Feb;21(1):22-30.

75. Yoon SK, Choi SL, Song JY, Lee GM. Effect of culture pH on erythropoietin production by Chinese hamster ovary cells grown in suspension at 32.5 and 37.0 degrees C. Biotechnol. Bioeng. 2005 Feb 5;89(3):345-56.

76. Oguchi S, Saito H, Tsukahara M, Tsumura H. pH Condition in temperature shift cultivation enhances cell longevity and specific hMab productivity in CHO culture. Cytotechnology. 2006 Nov;52(3):199-207.

77. Sakurai T, Itoh K, Liu Y, Higashitsuji H, Sumitomo Y, Sakamaki K, et al. Low temperature protects mammalian cells from apoptosis initiated by various stimuli in vitro. Exp. Cell Res. 2005 Oct 1;309(2):264-72.

78. Moore A, Mercer J, Dutina G, Donahue CJ, Bauer KD, Mather JP, et al. Effects of temperature shift on cell cycle, apoptosis and nucleotide pools in CHO cell batch cultures. Cytotechnology. 1997;23(1):47-54.

79. Kaufmann H, Mazur X, Marone R, Bailey JE, Fussenegger M. Comparative analysis of two controlled proliferation strategies regarding product quality, influence on tetracycline-regulated gene expression, and productivity. Biotechnol. Bioeng. 2001 Mar 20;72(6):592-602.

80. Yoon SK, Kim SH, Lee GM. Effect of low culture temperature on specific productivity and transcription level of anti-4-1BB antibody in recombinant Chinese hamster ovary cells. Biotechnol. Prog. 2003 Jul-Aug;19(4):1383-6.

81. Yoon SK, Hwang SO, Lee GM. Enhancing effect of low culture temperature on specific antibody productivity of recombinant Chinese hamster ovary cells: clonal variation. Biotechnol. Prog. 2004 Nov-Dec;20(6):1683-8.

82. Nam JH, Zhang F, Ermonval M, Linhardt RJ, Sharfstein ST. The effects of culture conditions on the glycosylation of secreted human placental alkaline phosphatase produced in Chinese hamster ovary cells. Biotechnol. Bioeng. 2008 Aug 15;100(6):1178-92.

83. Tharmalingam T, Sunley K, Butler M. High yields of monomeric recombinant beta-interferon from macroporous microcarrier cultures under hypothermic conditions. Biotechnol. Prog. 2008 Jul-Aug;24(4):832-8.

84. Fox SR, Yap MX, Yap MG, Wang DI. Active hypothermic growth: a novel means for increasing total interferon-gamma production by Chinese-hamster ovary cells. Biotechnol. Appl. Biochem. 2005 Jun;41(Pt 3):265-72.

85. Schatz SM, Kerschbaumer RJ, Gerstenbauer G, Kral M, Dorner F, Scheiflinger F. Higher expression of Fab antibody fragments in a CHO cell line at reduced temperature. Biotechnol. Bioeng. 2003 Nov 20;84(4):433-8.

86. Chen ZL, Wu BC, Liu H, Liu XM, Huang PT. Temperature shift as a process optimization step for the production of pro-urokinase by a recombinant Chinese hamster ovary cell line in high-density perfusion culture. J. Biosci. Bioeng. 2004;97(4):239-43.

87. Thieringer HA, Jones PG, Inouye M. Cold shock and adaptation. Bioessays. 1998 Jan;20(1):49-57.

88. VanBogelen RA, Neidhardt FC. Ribosomes as sensors of heat and cold shock in Escherichia coli. Proc. Natl. Acad. Sci. USA. 1990 Aug;87(15):5589-93.

89. Burdon RH. Temperature and animal cell protein synthesis. Symposia of the Society for Experimental Biology. 1987;41:113-33.

90. Nishiyama H, Higashitsuji H, Yokoi H, Itoh K, Danno S, Matsuda T, et al. Cloning and characterization of human CIRP (cold-inducible RNA-binding protein) cDNA and chromosomal assignment of the gene. Gene. 1997 Dec 19;204(1-2):115-20.

91. Sheikh MS, Carrier F, Papathanasiou MA, Hollander MC, Zhan Q, Yu K, et al. Identification of several human homologs of hamster DNA damage-inducible transcripts. Cloning and characterization of a novel UV-inducible cDNA that codes for a putative RNA-binding protein. J. Biol. Chem. 1997 Oct 17;272(42):26720-6.

92. Derry JM, Kerns JA, Francke U. RBM3, a novel human gene in Xp11.23 with a putative RNA-binding domain. Hum. Mol. Genet. 1995 Dec;4(12):2307-11.

93. Chappell SA, Owens GC, Mauro VP. A 5' Leader of Rbm3, a Cold Stress-induced mRNA, Mediates Internal Initiation of Translation with Increased Efficiency under Conditions of Mild Hypothermia. J. Biol. Chem. 2001 Oct 5;276(40):36917-22.

94. Al-Fageeh MB, Marchant RJ, Carden MJ, Smales CM. The cold-shock response in cultured mammalian cells: harnessing the response for the improvement of recombinant protein production. Biotechnol. Bioeng. 2006 Apr 5;93(5):829-35.

95. Merrick WC. Cap-dependent and cap-independent translation in eukaryotic systems. Gene. 2004 May 12;332:1-11.

96. Ermolenko DN, Makhatadze GI. Bacterial cold-shock proteins. Cell. Mol. Life Sci. 2002 Nov;59(11):1902-13.

97. Underhill MF, Marchant RJ, Carden MJ, James DC, Smales CM. On the effect of transient expression of mutated eIF2alpha and eIF4E eukaryotic translation initiation factors on reporter gene expression in mammalian cells upon cold-shock. Mol. Biotechnol. 2006 Oct;34(2):141-9.

98. Wek RC, Jiang HY, Anthony TG. Coping with stress: eIF2 kinases and translational control. Biochem. Soc. Trans. 2006 Feb;34(Pt 1):7-11.

99. Fernandez J, Yaman I, Sarnow P, Snider MD, Hatzoglou M. Regulation of internal ribosomal entry site-mediated translation by phosphorylation of the translation initiation factor eIF2alpha. J. Biol. Chem. 2002 May 24;277(21):19198-205.

100. Sureban SM, Ramalingam S, Natarajan G, May R, Subramaniam D, Bishnupuri KS, et al. Translation regulatory factor RBM3 is a proto-oncogene that prevents mitotic catastrophe. Oncogene. 2008 Jul 31;27(33):4544-56.

101. Danno S, Nishiyama H, Higashitsuji H, Yokoi H, Xue JH, Itoh K, et al. Increased transcript level of RBM3, a member of the glycine-rich RNA-binding protein family, in human cells in response to cold stress. Biochem. Biophys. Res. Commun. 1997 Jul 30;236(3):804-7.

102. Xue JH, Nonoguchi K, Fukumoto M, Sato T, Nishiyama H, Higashitsuji H, et al. Effects of ischemia and H2O2 on the cold stress protein CIRP expression in rat neuronal cells. Free Radical Biology & Medicine. 1999 Dec;27(11-12):1238-44.

103. Yang C, Carrier F. The UV-inducible RNA-binding protein A18 (A18 hnRNP) plays a protective role in the genotoxic stress response. J. Biol. Chem. 2001 Dec 14;276(50):47277-84.

104. Hong JK, Kim YG, Yoon SK, Lee GM. Down-regulation of cold-inducible RNA-binding protein does not improve hypothermic growth of Chinese hamster ovary cells producing erythropoietin. Metab. Eng. 2007 Mar;9(2):208-16.

105. Tan HK, Lee MM, Yap MG, Wang DI. Overexpression of cold-inducible RNA-binding protein increases interferon-gamma production in Chinese-hamster ovary cells. Biotechnol. Appl. Biochem. 2008 Apr;49(Pt 4):247-57.

106. Ohnishi T, Wang X, Ohnishi K, Takahashi A. p53-dependent induction of WAF1 by cold shock in human glioblastoma cells. Oncogene. 1998 Mar;16(11):1507-11.

107. Dutton RL, Scharer JM, Moo-Young M. Descriptive parameter evaluation in mammalian cell culture. Cytotechnology. 1998;26(2):139-52.

108. Kaufmann H, Mazur X, Fussenegger M, Bailey JE. Influence of low temperature on productivity, proteome and protein phosphorylation of CHO cells. Biotechnol. Bioeng. 1999 Jun 5;63(5):573-82.

109. Fox SR, Patel UA, Yap MG, Wang DI. Maximizing interferon-gamma production by Chinese hamster ovary cells through temperature shift optimization: experimental and modeling. Biotechnol. Bioeng. 2004 Jan 20;85(2):177-84.

110. Sanfeliu A, Chung JD, Stephanopoulos G. Effect of insulin stimulation on the proliferation and death of Chinese hamster ovary cells. Biotechnol. Bioeng. 2000 Nov 20;70(4):421-7.

111. Yoon SK, Hong JK, Choo SH, Song JY, Park HW, Lee GM. Adaptation of Chinese hamster ovary cells to low culture temperature: cell growth and recombinant protein production. J. Biotechnol. 2006 Apr 20;122(4):463-72.

112. Li GC, Hahn GM. Adaptation to different growth temperatures modifies some mammalian cell survival responses. Exp. Cell Res. 1980 Aug;128(2):475-9.

113. Strober W. Trypan blue exclusion test of cell viability. Curr. Protoc. Immunol. 2001 May;Appendix 3:Appendix 3B.

114. Spearman M, Rodriguez J, Huzel N, Butler M. Production and glycosylation of recombinant beta-interferon in suspension and cytopore microcarrier cultures of CHO cells. Biotechnol. Prog. 2005 Jan-Feb;21(1):31-9.

115. Laemmli U. Cleavage of structural proteins during the assembly of the head of bacteriophage T4. Nature. 1970;277:680-5.

116. Basu A, Yang K, Wang M, Liu S, Chintala R, Palm T, et al. Structure-function engineering of interferon-beta-1b for improving stability, solubility, potency, immunogenicity, and pharmacokinetic properties by site-selective mono-PEGylation. Bioconj. Chem. 2006 May-Jun;17(3):618-30.

117. Pestka S, Krause CD, Walter MR. Interferons, interferon-like cytokines, and their receptors. Immunol. Rev. 2004 Dec;202:8-32.

118. Chuppa S, Tsai YS, Yoon S, Shackleford S, Rozales C, Bhat R, et al. Fermentor temperature as a tool for control of high-density perfusion cultures of mammalian cells. Biotechnol. Bioeng. 1997;55(2):328-38.

119. Attal J, Theron MC, Houdebine LM. The optimal use of IRES (internal ribosome entry site) in expression vectors. Genet. Anal.: Biomol. Eng. 1999 Nov;15(3-5):161-5.

120. Erenpreisa J, Cragg MS. Mitotic death: a mechanism of survival? A review. Cancer Cell Int. 2004;1(1).

121. Hayduk EJ, Choe LH, Lee KH. A two-dimensional electrophoresis map of Chinese hamster ovary cell proteins based on fluorescence staining. Electrophoresis. 2004 Aug;25(15):2545-56.

122. Nurminsky DI, Nurminskaya MV, Benevolenskaya EV, Shevelyov YY, Hartl DL, Gvozdev VA. Cytoplasmic dynein intermediate-chain isoforms with different targeting properties created by tissue-specific alternative splicing. Mol. Cell. Biol. 1998 Nov;18(11):6816-25.

123. Lane JD, Vergnolle MA, Woodman PG, Allan VJ. Apoptotic cleavage of cytoplasmic dynein intermediate chain and p150(Glued) stops dynein-dependent membrane motility. J. Cell Biol. 2001 Jun 25;153(7):1415-26.

124. Kim I, Ahn J, Liu C, Tanabe K, Apodaca J, Suzuki T, et al. The Png1-Rad23 complex regulates glycoprotein turnover. J. Cell Biol. 2006 Jan 16;172(2):211-9.

125. Jimenez A, Santos MA, Revuelta JL. Phosphoribosyl pyrophosphate synthetase activity affects growth and riboflavin production in Ashbya gossypii. BMC Biotechnol. 2008;8:67.

126. Firth JD, Ebert BL, Ratcliffe PJ. Hypoxic regulation of lactate dehydrogenase A. Interaction between hypoxia-inducible factor 1 and cAMP response elements. J. Biol. Chem. 1995 Sep 8;270(36):21021-7.

127. Sunley K, Tharmalingam T, Butler M. CHO Cells Adapted to Hypothermic Growth Produce High Yields of Recombinant beta-Interferon. Biotechnol. Prog. 2008;24:898-906.

128. Healthcare G. Microcarrier Cell Culture: Principles and Methods. 18-1140-62 AB ed.: Elanders Tofters; 2005.

129. Matthews BD, Overby DR, Mannix R, Ingber DE. Cellular adaptation to mechanical stress: role of integrins, Rho, cytoskeletal tension and mechanosensitive ion channels. J. Cell Sci. 2006 Feb 1;119(Pt 3):508-18.

130. Klevecz RR. Temporal order in mammalian cells. I. The periodic synthesis of lactate dehydrogenase in the cell cycle. J. Cell Biol. 1969 Nov;43(2):207-19.

131. Allen MJ, Rushton N. Use of the CytoTox 96 (TM) Assay in Routine Biocompatibility Testing In Vitro. Promega Notes Magazine. 1994;45:7-11.

132. Legrand C, Bour JM, Jacob C, Capiaumont J, Martial A, Marc A, et al. Lactate dehydrogenase (LDH) activity of the cultured eukaryotic cells as marker of the number of dead cells in the medium [corrected]. J. Biotechnol. 1992 Sep;25(3):231-43.

133. Hoskins JM, Meynell GG, Sanders FK. A comparison of methods for estimating the viable count of a suspension of tumour cells. Exp. Cell Res. 1956 Aug;11(2):297-305.

134. Jones KH, Senft JA. An improved method to determine cell viability by simultaneous staining with fluorescein diacetate-propidium iodide. J. Histochem. Cytochem. 1985 Jan;33(1):77-9.

135. Schaefer LH, Schuster D, Schaffer J. Structured illumination microscopy: artefact analysis and reduction utilizing a parameter optimization approach. J. Microsc. 2004 Nov;216(Pt 2):165-74.

136. Brown MJ, Hallam JA, Colucci-Guyon E, Shaw S. Rigidity of circulating lymphocytes is primarily conferred by vimentin intermediate filaments. J. Immunol. 2001 Jun 1;166(11):6640-6.

137. Savonniere S, Zeghari N, Miccoli L, Muller S, Maugras M, Donner M. Effects of lipid supplementation of culture media on cell growth, antibody production, membrane structure and dynamics in two hybridomas. J. Biotechnol. 1996 Jul 18;48(1-2):161-73.

138. Zhang Z, al-Rubeai M, Thomas CR. Effect of Pluronic F-68 on the mechanical properties of mammalian cells. Enzyme Microb. Technol. 1992 Dec;14(12):980-3.

139. Tharmalingam T, Ghebeh H, Wuerz T, Butler M. Pluronic enhances the robustness and reduces the cell attachment of mammalian cells. Mol. Biotechnol. 2008 Jun;39(2):167-77.

140. Eckes B, Dogic D, Colucci-Guyon E, Wang N, Maniotis A, Ingber D, et al. Impaired mechanical stability, migration and contractile capacity in vimentin-deficient fibroblasts. J. Cell Sci. 1998 Jul;111 (Pt 13):1897-907.

141. Kumar N, Gammell P, Meleady P, Henry M, Clynes M. Differential protein expression following low temperature culture of suspension CHO-K1 cells. BMC Biotechnol. 2008;8:42.

142. Byun Y, Chen F, Chang R, Trivedi M, Green KJ, Cryns VL. Caspase cleavage of vimentin disrupts intermediate filaments and promotes apoptosis. Cell Death Differ. 2001 May;8(5):443-50.

143. Ng YC, Berry JM, Butler M. Optimization of physical parameters for cell attachment and growth on macroporous microcarriers. Biotechnol. Bioeng. 1996 Jun 20;50(6):627-35.

144. Shiragami N, Honda H, Unno H. Anchorage-dependent animal cell culture by using a porous microcarrier. Bioprocess Biosystems Eng. 1993;8(5):295-9.

145. Takagi M, Kitabayashi T, Ito S, Fujiwara M, Tokuda A. Noninvasive measurement of three-dimensional morphology of adhered animal cells employing phase-shifting laser microscope. J. Biomed. Opt. 2007 Sep-Oct;12(5):054010.

146. Nakanishi K, Maruyama M, Shibata T, Morishima N. Identification of a caspase-9 substrate and detection of its cleavage in programmed cell death during mouse development. J. Biol. Chem. 2001 Nov 2;276(44):41237-44.

147. Dinsdale D, Lee JC, Dewson G, Cohen GM, Peter ME. Intermediate filaments control the intracellular distribution of caspases during apoptosis. Am. J. Pathol. 2004 Feb;164(2):395-407.

148. Morishima N. Changes in nuclear morphology during apoptosis correlate with vimentin cleavage by different caspases located either upstream or downstream of Bcl-2 action. Genes Cells. 1999;4(7):401-14.

149. Sarria AJ. The presence or absence of a vimentin-type intermediate filament network affects the shape of the nucleus in human SW-13 cells. J. Cell Sci. 1994;107(6):1593-607.

150. Gao Y, Sztul E. A novel interaction of the Golgi complex with the vimentin intermediate filament cytoskeleton. J. Cell Biol. 2001 Mar 5;152(5):877-94.

151. Ivaska J, Pallari HM, Nevo J, Eriksson JE. Novel functions of vimentin in cell adhesion, migration, and signaling. Exp. Cell Res. 2007;313(10):2050-62.

152. Nelson WJ, Traub P. Proteolysis of vimentin and desmin by the Ca2+-activated proteinase specific for these intermediate filament proteins. Mol. Cell. Biol. 1983 Jun;3(6):1146-56.

153. Prasad SC, Thraves PJ, Kuettel MR, Srinivasarao GY, Dritschilo A, Soldatenkov VA. Apoptosis-associated proteolysis of vimentin in human prostate epithelial tumor cells. Biochem. Biophys. Res. Commun. 1998 Aug 19;249(2):332-8.

154. Zhang MH, Lee JS, Kim HJ, Jin DI, Kim JI, Lee KJ, et al. HSP90 protects apoptotic cleavage of vimentin in geldanamycin-induced apoptosis. Mol. Cell. Biol. 2006 Jan;281(1-2):111-21.

155. Elmore S. Apoptosis: a review of programmed cell death. Toxicol. Pathol. 2007;35(4):495-516.

156. Snásel J, Shoeman R, Horejsi M, Hruskova-Heidingsfeldova O, Sedlacek J, Ruml T, et al. Cleavage of vimentin by different retroviral proteases. Arch. Biochem. Biophys. 2000 May 15;377(2):241-5.

157. Chait BT, Kent SB. Weighing naked proteins: practical, high-accuracy mass measurement of peptides and proteins. Science. 1992 Sep 25;257(5078):1885-94.

158. Ben-Ze'ev A, Babiss LE, Fisher PB. Cleavage of vimentin in dense cell cultures. Inhibition upon transformation by type 5 adenovirus. Exp. Cell Res. 1986 Sep;166(1):47-62.

159. Shaulsky G, Goldfinger N, Tosky MS, Levine AJ, Rotter V. Nuclear localization is essential for the activity of p53 protein. Oncogene. 1991 Nov;6(11):2055-65.

160. Enari M, Sakahira H, Yokoyama H, Okawa K, Iwamatsu A, Nagata S. A caspase-activated DNase that degrades DNA during apoptosis, and its inhibitor ICAD. Nature. 1998 Jan 1;391(6662):43-50.